UNIVERSIDADE FEDERAL DE MINAS GERAIS
PROGRAMA DE PÓS-GRADUAÇÃO EM SANEAMENTO, MEIO AMBIENTE E RECURSOS HÍDRICOS

TOWARD HIGH TEMPERATURE AND LOW pH GOLD MINING EFFLUENT RECLAMATION BY DIFFERENT MEMBRANE SEPARATION PROCESSES

Beatriz Gasparini Reis

Belo Horizonte
2018

TOWARD HIGH TEMPERATURE AND LOW pH GOLD MINING EFFLUENT RECLAMATION BY DIFFERENT MEMBRANE SEPARATION PROCESSES

Beatriz Gasparini Reis

Beatriz Gasparini Reis

TOWARD HIGH TEMPERATURE AND LOW pH GOLD MINING EFFLUENT RECLAMATION BY DIFFERENT MEMBRANE SEPARATION PROCESSES

Tese de doutorado apresentada ao Programa de Pós-graduação em Saneamento, Meio Ambiente e Recursos Hídricos da Universidade Federal de Minas Gerais, como requisito parcial à obtenção do título de Doutor em Saneamento, Meio Ambiente e Recursos Hídricos.

Área de concentração: Meio Ambiente

Linha de pesquisa: Caracterização, prevenção e controle da poluição

Orientador: Profa. Míriam Cristina Santos Amaral Moravia
Co-Orientador: Profa. Helen Conceição Ferraz (UFRJ)
Co-Orientador: Profa. Corinne Cabassud (INSA Toulouse – FR)

Belo Horizonte
Escola de Engenharia da UFMG
2018

Beatriz Gasparini Reis

TOWARD HIGH TEMPERATURE AND LOW pH GOLD MINING EFFLUENT RECLAMATION BY DIFFERENT MEMBRANE SEPARATION PROCESSES

PhD thesis presented to the Post-Graduate Program in Sanitation, Environment and Water Resources of the Federal University of Minas Gerais as a partial requirement to obtain the title of PhD in Sanitation, Environment and Water Resources.

Focus area: Environment

Research line: Characterization, prevention and control of pollution

Advisor: Profa. Míriam Cristina Santos Amaral Moravia
Co- Advisor: Profa. Profa. Helen Conceição Ferraz (UFRJ)
Co- Advisor: Profa. Corinne Cabassud (INSA Toulouse – FR)

Belo Horizonte
Escola de Engenharia da UFMG
2018

Reis, Beatriz Gasparini.
R375t Toward high temperature and low pH gold mining effluent reclamation by different membrane separation processes [manuscrito] / Beatriz Gasparini Reis.- 2018.
168 f, enc.: il.

Orientadora: Míriam Cristina Santos Amaral Moravia.
Coorientadoras: Helen Conceição Ferraz, Corinne Cabassud.

Tese (doutorado) - Universidade Federal de Minas Gerais, Escola de Engenharia.

Bibliografia: f. 157-168.

1. Engenharia sanitária - Teses. 2. Meio ambiente - Teses. 3. Água - Reutilização - Teses. 4. Extração por solventes - Teses. I. Moravia, Míriam Cristina Santos Amaral. II. Ferraz, Helen Conceição. III. Cabassud, Corinne. IV. Universidade Federal de Minas Gerais. Escola de Engenharia. V. Título.

CDU: 628(043)

UFMG

UNIVERSIDADE FEDERAL DE MINAS GERAIS
Escola de Engenharia
Programa de Pós-Graduação em Saneamento, Meio Ambiente e Recursos Hídricos
Avenida Antônio Carlos, 6627 - 4° andar - 31270-901 - Belo Horizonte – BRASIL
Telefax: 55 (31) 3409-1882 - posgrad@desa.ufmg.br
http://www.smarh.eng.ufmg.br

FOLHA DE APROVAÇÃO

Toward High Temperature and Low pH Gold Mining Effluent Reclamation by Different Membrane Separation Processes

BEATRIZ GASPARINI REIS

Tese defendida e aprovada pela banca examinadora constituída pelos Senhores:

Profa MIRIAM CRISTINA SANTOS AMARAL

Profa HELEN CONCEIÇÃO FERRY

Profa KÁTIA CECILIA DE SOUZA FIGUEIREDO

Prof. FABIO MERÇON

Prof. JOÃO PAULO CRESPO

Prof. FREDERICO DE ARAUJO KRONEMBERGER

Aprovada pelo Colegiado do PG SMARH

Prof. Antonio Teixeira de Matos
Coordenador

Subcoordenador do Programa de Pós-Graduação em Saneamento, Meio Ambiente e Recursos Hídricos/UFMG

Versão Final aprovada por

Profª. Miriam Cristina Santos Amaral Moravia
Orientadora

Belo Horizonte, 21 de agosto de 2018.

AGRADECIMENTOS

Agradeço a minha orientadora, profa. Miriam, pelo voto de confiança, por acreditar no meu potencial e ter estado ao meu lado durante toda essa caminhada. Por todos os ensinamentos, conselhos, confiança, amizade e por ser um grande exemplo para mim.

Às minha co-orientadora, profas. Helen, por todo apoio e auxílio, pelo carinho e por ter me recebido tão bem quando estive na COPPE/UFRJ cursando as diciplinas

À minha co-orientadora, profa. Corinne, por ter me recebido com tanto carinho e me proporcionado a experiência de fazer o doutorado sanduíche em um ambiente de trabalho tão agradável.

Às profas. Camila, Liséte, Mônica, Sílvia e Taciana, por também estarem sempre presente, pela colaboração, apoio, incentivo e também por serem grandes exemplos para mim.

À banca examinadora, pela prontidão com que aceitaram o convite e por terem se disponibilizado a avaliar essa tese.

Às queridas Luiza, Camila, Ana Lívia, Ginger, Marina e Marcela, que foram essenciais para a conclusão desse trabalho. Por toda a dedicação, boa vontade, perseverança, paciência, compreensão, esforço e amizade.

A todos os amigos do laboratório, por toda a ajuda, apoio, treinamentos, colaboração e amizade. Não tenho palavras para agradecer a presença de vocês ao longo de toda essa caminhada.

Ao Paul, Qiuming e Allan, por serem ótimos colegas e amigos e por terem me ajudado tanto durante o meu estágio no INSA. Agradecimento especial ao Paul, por toda a colaboração e ajuda com a parte de VMD.

Aos queridos amigos da pós, por toda a amizade e companheirismo. Em especial à Laura, Bárbara, Natalie, Eduardo, André, Cacá, Marília, Fê, Rafa, Eliz e Sandrine. A todo o grupo GEAPS e GRUPOA pela amizade, por compartilharem ricas discussões e desafios e por estarem sempre presentes durante a execução desse trabalho.

Ao meu amigo queridíssimo Heron e às meninas de Toulouse, especialmente Ana, por ter me apoiado tanto em épocas tão necessárias, sempre com muito carinho.

Ao DESA e aos professores do Programa, que contribuíram para minha formação, com tantos conselhos e por serem exemplos para mim, e a todos os funcionários do Departamento pelo auxílio e apoio.

Aos professores da COPPE/UFRJ, por terem me recebido com carinho e me apoiarem durante o curso das disciplinas.

Ao INSA de Toulouse, professores, funcionários e alunos, por terem me recebido tão bem, pela colaboração e convivência.

Às agência de fomento, CNPq, CAPES e FAPEMIG, pelo apoio financeiro aos projeto e concessão da bolsa de doutorado e bolsa de doutorado sanduíche.

À UFMG por me permitido trilhar essa carreira profissional, desde a graduação até o doutorado.

Aos meus pais, por todo o apoio, pelo amor incondicional, por acreditarem na minha capacidade e me incentivarem sempre a seguir os meus sonhos. Por serem companheiros e grandes exemplos para mim, sempre. À minha irmã Luiza, por estar sempre ao meu lado, por ser uma grande amiga e sempre me dar forças. Às nossas meninas Jude, Pipa, Marie, Filó e Amora por encherem meus dias de amor e alegria.

A todos os familiares e amigos, que são essenciais em todos os dias da minha vida.

RESUMO

Efluentes de mineração de ouro caracterizam-se por um pH baixo e concentrações elevadas de sulfato, metais e metalóides, especialmente o arsénio, que é um elemento tóxico que requer tratamento específico. O tratamento de efluentes mineração de ouro por nanofiltração (NF) e destilação assistida por membranas (DM) é um processo muito promissor uma vez que essas membranas podem reter íons bivalentes de forma eficiente para a produção de um permeado de alta qualidade que pode ser reutilizado na indústria. Esse estudo teve como objetivo avaliar as principais condições operacionais do tratamento de efluentes da mineração de ouro por NF, MD a vácuo (VMD) e DM por contato direto (DCMD) conjgado ou não com a extração de arsênio por solvente (SX) e conduzir um estimativa preliminar de custos operacionais. Os resultados mostraram que todos os processos avaliados foram eficientes no tratamento de efluente de mineração de ouro, permitindo o fluxo de permeado elevado e eficiências satisfatórias de retenção de solutos até uma taxa de recuperação de 30% (para sistemas de DM) e 40% (para NF), sendo que o pH do efluente afetou tanto a eficiência de retenção de solutos quanto a tendência de incrustação da membrana. Para NF, maiores fluxos de permeado foram obtidos e o sistema pode operar até uma maior taxa de recuperação, porém apresenta custos de resfriamento do efluente. A retenção de 85% de arsênio III e 75% de arsênio V foi alcançada e permeado obtido pode ser reutilizado na indústria. Já os sistemas de MD (VMD e DCMD) apresentaram eficiências bastante elevadas (acima de 96%), fluxo de permeado relativamente alto, se comparado à NF. No entanto, possuem baixo custo operacional por permitirem o aproveitamento do calor residual do efluente como força motriz do processo e permeado de alta qualidade, sem restrições para reuso industrial. SX apresentou elevada eficiência de remoção de arsênio (80%) para extratante Aliquat 336, com remoção de arsenito e arsenato. A concentração de sulfato em solução deve ser controlada para garantir a eficiência da extração. A aplicação desses processos de separação por membranas reduz os custos com a precipitação química, o volume de lodo gerado e permite o reúso de água, enquanto a SX permite remoção e recuperação de arsênio. Sendo assim, o uso e/ ou conjugação das as tecnologias testadas representando assim uma grande economia para a indústria ao mesmo tempo em que contribui para a ecoeficiência da mineração.

Palavras-chave: Efluente de mineração de ouro; Nanofiltração; Destilação assistida por membranas; Extração por solvente; Condições operacionais; Incrustação; Reúso de água.

ABSTRACT

Gold mining effluents are characterized by low pH and high concentrations of sulfate, metals and metalloids, especially arsenic, which is a toxic element that requires specific treatment. The treatment of gold mining effluents by nanofiltration (NF) and membrane distillation (MD) is a very promising alternative since these membranes can retain bivalent ions efficiently for the production of a high quality permeate that can be reused on industry. The objective of this study was to evaluate the main operational conditions for treatment of gold mining effluents by NF, vacuum MD (VMD) and direct contact MD (DCMD) conjugated or not to arsenic solvent extraction (SX) and to conduct a preliminary estimation of operating costs. The results showed that all technologies were efficient in the treatment of gold mining effluent, allowed the high permeate flux and satisfactory solids retention efficiencies up to a recovery rate of 30% (for MD systems) and 40% (for NF), and the pH of the effluent affected both the solute retention efficiency and the membrane fouling trend. For NF, higher permeate fluxes were obtained and the system can operate up to a higher recovery rate, but presents costs of effluent cooling. The retention of 85% of arsenic III and 75% of arsenic V was achieved and the permeate obtained can be reused in the industry. On the other hand, the MD systems (both VMD and DCMD) presented fairly high rejection (above 96%), relatively high permeate flux, compared to NF. However, they have a low operating cost as they allow for the recovery of the residual heat of the effluent as a driving force of MD process and produce a permeate of high quality, without restrictions for industrial reuse. Solvent extraction (SX) showed high arsenic removal efficiency (80%) for Aliquat 336, extraction bot arsenite and arsenate. The concentration of sulfate in solution must be controlled for guarantee the extraction efficiency. The application of the membrane separation processes reduces the costs with chemical precipitation, the volume of sludge generated and allows the reuse of water, while SX can allow for arsenic recovery. Thus, the use and / or conjugation the these processes represent a great economic advantage for the industry while contributing to the mining eco-efficiency.

Key-words: Gold mining wastewater; Nanofiltration; Membrane distillation; Solvent extraction; Operating conditions; Fouling; Water Reuse.

TABLE OF CONTENTS

LIST OF FIGURES

LIST OF TABLES

CHAPTER 1:
INTRODUCTION

1.1 BACKGROUND AND JUSTIFICATION

Gold is a metal that presents several applications and has a great demand on the international market, making gold ores mining and processing an activity of great economic importance for the countries that owe gold deposits. However, despite being profitable, this activity cause several environmental impacts (GETANEH and ALEMAYEHU, 2006) that includes the destruction of natural habitats, biodiversity loss, disposal of large amounts of waste and contamination of water bodies.

The production of large volumes of contaminated effluents is an environmental impact that stands out and it is being intensified each day. The intense mining activity has resulted in the intensive use of the ores high content of metals of interest, so that the industry is increasingly turning to lower quality ores that requires high volume of water, per ton of metal produced, for their processing. In this way, the lower quality of available ores together with the intensive mining activity highly increase the mining sector dependency on water (KESIEME, 2015).

The composition of mining waters is much diversified and depends on factors such as type of ore and mineral extracted, the chemical additives used, the extraction process and the processing done. In general, among the characteristics of some inorganic mining waters, it can be cited the presence of ions as Al^{3+}, Ca^{2+}, Mg^{2+}, Na^{+}, K^{+}, Cl^{-}, CO_3^{2-}, HCO_3^{-} and SO_4^{2-} (KESIEME, 2015) and strongly acid pH. Also, this waters often contain high concentrations of heavy metals, such as As, Hg, Cd, Cr and Hg (CHAN AND DUDENEY (2008) and LANGSCH et al. (2012)), which represents an aggravating factor as those are toxic, require proper treatment and restrict any water use.

Among toxic metals that can be found in mining waters, the arsenic is highlighted. Arsenic can occur naturally in the environment (MANDAL; SUZUKI, 2002) as its mobilization can occur through natural processes, such as erosion and biological activity, and anthropic activity, such as agriculture, mining, etc (SMITH et al., 2008). However, due to the intense anthropic activities, high levels of arsenic have been found in the environment, especially around gold mining areas (BORBA; FIGUEIREDO; MATSCHULLAT, 2003). This fact is of great worry since this metal is highly toxic, has a carcinogenic potential and causes several other health damages.

The contamination of soils and water bodies by arsenic is a major global problem (ZAW; EMETT, 2002). It is estimated that tens of millions of people are at risk of exposure to excessive levels of arsenic (NG; WANG; SHRAIM, 2003). Thus, it is mandatory to eliminate it from water bodies (BEY et al., 2010) and its main sources of contamination, such as industrial effluents.

The metallurgical industry is among the largest producers of effluents containing metals such as arsenic. Their generation occurs in the processing of different types of ores, including copper, gold, nickel and zinc (IBERHAN; WINIEWSKI, 2002) and they represent a hazardous and undesirable waste.

Besides the necessity of a proper treatment for these contaminated effluents, mining industry also faces a complex context. With the imposition of increasingly restrictive release standards, there is a worldwide trend towards charging not only for water collection, but also for the discharge of effluents. The situation becomes more critical since the very supply of water of appropriate quality for industry plants has gradually diminished, generating conflicts over the use of water. In this way, the reuse of effluents has become an environmentally and economically viable option for the industries (KESIEME; ARAL, 2015). Mining effluents are very promising for reuse, but the presence of metals and ions such as sulfate represent a barrier to such use and should be removed.

Classic removal techniques such as chemical precipitation, adsorption, ion exchange and electrochemical removal are often used by metallurgical industry to remove arsenic from their effluents. However, several disadvantages lead to a reduced efficiency in the elimination of these metals, especially against complex aqueous matrices (AGREDA et al., 2011). Arsenic removal is usually more efficient when it is at low concentrations (LEIST et al., 2000), which makes the excessive presence of this pollutant in industrial effluents also difficult to treat. Conventional processes, in addition to incomplete removal, also have high energy requirements and toxic sludge production (ECCLES, 1999), which also represents a hazardous waste.

Furthermore, the valence state presented by the arsenic in the effluent is of extreme importance for its removal. Most of the processes present higher arsenate [As (V)] removal efficiency compared to arsenite [As (III)]. Thus, when the concentration of arsenite is high, an

oxidation step can be required in order to achieve satisfactory removal results in the treatment that is performed later (DRIOLI et al., 2006).

Sulfate is also an important component usually present on mining waters, especially on sites where sulfide ores are processed, that although is not toxic, must also be controlled in mining waters. A regulation for the maximum permissible concentration for this ion in water bodies exists in Brazil (BRASIL, 2005; MINAS GERAIS, 2008; BRASIL, 2011) as its presence in the water supply can have laxative and dehydration effects on the population. In the industry, the control of sulfate in reuse waters is of extreme importance, since it presents corrosive and high scaling potential, factors that make sulfate one of the major water quality problems in long-term mining and processing operations (BOWELL, 2004).

Sulfate can be removed by several processes, especially precipitation with calcium, lime or hydrated lime. Although it is less efficient than barium precipitation (BOWELL, 2004), it allows for lowers associated costs, avoids problems handling reagents and still enables the recovery of calcium as $CaCO_3$ (GELDENHUYS et al., 2003). Deng et al. (2013) showed that mining acid effluent can be efficiently treated by the addition of lime in two stages, generating precipitates of calcium sulfate.

However, this classic treatment does not allow for water reuse and produces high amounts of waste. As already stated by other authors (AGRAWAL; MISHRA; SAHU, 2016), the mining industry has been intensively forced, both by economic pressure and / or environmental regulation, to review the quantity and types of all wastewater and residues they produce. Increasingly stringent legislation regarding the discharge of acidic effluents and increasing attention to the recycling / reuse of these effluents after adequate treatment poses strong challenges and high economic motivation for the development of new treatment technologies (KESIEME, 2015). The new approach considers all waste and by-product disposal as secondary resources for a new value-added product (AGRAWAL; MISHRA; SAHU, 2016).

In this context, membrane separation processes are highlighted, either for the control of the arsenic and sulfate concentrations of these effluents, or for the concentration of contaminated streams and production of water for reuse. Nanofiltration and membrane distillation are techniques that stand out for their high capacity of retaining dissolved salts and molecules, presenting great application in the treatment of effluents and reuse water generation (ACERO et al., 2010; FU; WANG, 2011; GOODMAN et al., 2013; ZHANG et al., 2011).

The application of a two-stage nanofiltration for the treatment of the gold mining effluent studied in this work, an acid water with high temperature and high concentration os sulfate and arsenic, mixed with water from the calcined dam (1:1), a water with a lower temperature (room temperature) and low concentration of those contaminants, was investigated by other authors (ANDRADE et al., 2018). The permeate recovery rate used was 40% for the first stage and 85% for the second stage, resulting in a global recovery rate of 67%, and the intermediate precipitation of arsenic and calcium was performed in order to increase the recovery rate. A very promising result was achieved as 187 m^3/h of reuse water was produced and the waste production (as sludge) was reduced, an important practice as this presents a hazardous waste because of the presence of arsenic. However, the concentrate production on the first stage that was sent to precipitation have a flow rate greater than that of the contaminated gold mining effluent alone, what increase the volume of contaminated stream to be treated and dilute the arsenic present. Thus, it is important to test the potential treatment of the contaminated gold effluent alone by nanofiltration, evaluation the best operational conditions that allow for a higher permeate flux and low membrane fouling.

This research is justified since most of the studies in the literature regarding the removal of arsenic aim at the removal of this metal from drinking water (AKBARI; MEHRABADI; TORABIAN, 2010; HARISHA et al., 2010), surface water (AHMED et al., 2010), underground water (SAITUA; GIL; PADILLA, 2011), and electrolytic solutions from the copper production process (GUPTA; BEGUM, 2008; GUPTA; BEGUM, 2008; IBERHAN; WINIEWSKI, 2002; IBERHAN; WIŚNIEWSKI, 2003). Few studies on the removal of arsenic from industrial effluents and the studies that deal with these waters often use synthetic effluents and / or low concentrations of arsenic. Mining effluents, which represent the largest sources of arsenic, present high concentrations of this metal together of other pollutants, making its treatment a great challenge.

In general, As (V) is the most studied species, since most of the processes present high arsenic removal efficiency in this valence state. However, in many effluents, such as mining, arsenic may be present in the form of As (III). In conventional processes this is usually oxidized to As (V), resulting in additional costs.

Nanofiltration (NF) is a suitable technology for the treatment of gold mining effluent in general, showing high permeate fluxes and high removal efficiency with low energy

consumption, besides being a well-established technology. A limited number of studies evaluating the removal of arsenic of mining wastewater by NF membranes have been reported so far and its efficiency on removing this contaminant will depend largely on the type of membrane used, as well as the characteristics of the wastewater to be treated and operating conditions. Thus, it is of utmost importance that the NF technology be tested individually for each wastewaters that is desired to treat, like the gold mining effluent contaminated with arsenic, taking into account all its physicochemical characteristics.

Without mixing it with other effluents, the gold mining effluent presents high concentration of sulfate and arsenic, acid pH and also high temperature, which represents a great opportunity to the use of techniques such as membrane distillation (MD), never tested for this effluent before. MD is a process that has an even higher efficiency in the removal of pollutants, being able to concentrate solutions until their saturation without a significant decline of permeate flux (CABASSUD; WIRTH, 2003; DRIOLI; CURCIO; DI PROFIO, 2005; LUO et al., 2014). This technique is mostly used in desalination plants, but also showed good results in acid production/concentration (TOMASZEWSKA; GRYTA; MORAWSKI, 1995) and in the treatment of a mining solution containing sulfuric acid and several metals (KESIEME; ARAL, 2015), showing a great potential to the treatment of gold mining effluent.

Despite NF and MD present high efficiency on the removal of contaminants, both process produce a permeate which corresponds to the water for reuse and a concentrate, that still need to be treated. The presence of arsenic in the concentrate lead to the production of a hazardous waste. A promising technology for the removal and recovery of arsenic from mining effluents and prevent the hazardous waste production is the solvent extraction (SX). Removal of arsenic by SX is interesting from an environmental / health point of view, as it represents a toxic contaminant. However, if recovered with sufficient purity, this metal can be reused in the industry, representing no more a waste but a valueable by-product. SX can also be performed in membrane contactors, reducing the possible drawback presented by the dispersive process (BEY et al., 2010; DRIOLI; CURCIO; DI PROFIO, 2005).

It is important to note that the SX process is economically feasible when the solute concentration to be withdrawn is high. In this context, the use of alternative technologies, such as membrane distillation (KESIEME; ARAL, 2015) and nanofiltration, can represent a good strategy to concentrate the solution for acid or metal recovery, and still allow obtaining

water for reuse. Thus, the present work aims to investigate the reclamation of a high temperature, low pH and high salinity gold mining effluent contaminated with arsenic by nanofiltration and membrane distillation systems integrated or not to arsenic solvent extraction.

This study contributes to the development and expansion of the use of more advanced technologies for the effuents reclamation. The investigation of fouling in the membranes systems and the definition of the best operational conditions still contribute to the optimization of the performance of these processes, which directly implies the reduction of the operational costs and the increase of the viability of its application. In addition, the technical economical evaluation allow for a realistic estimation of the costs and savings associated with the treatment together with an environmental approach.

The originality of this work is the proposition of an advanced treatment for a real gold mining effluent, of strongly acid pH, high salinity, containing high concentrations of arsenic and high temperature. This treatment aims at the production of water for reuse and reduction of generated waste, which may have low energy demand and may also allow the recovery of by-products. The use of MD for mining effluent was proposed for the first time only in 2015, for a synthetic sulfuric acid solution containing sulfate metals (Fe, Ni, Zn, Mg, Co and Cu), aiming at the recovery of sulfuric acid. The present work proposes the evaluation of NF for the treatment of this effluent alone, as well as two MD processes, by direct contact and vacuum, the latter being a technology never proposed before for the treatment of mining effluents, conjugated or not to arsenic solvent extraction. These processes allow different configurations, always aiming at the zero discharge of effluent and allowing by-products recovery. The use of this process also has a significant environmental contribution, allowing a drastic reduction of the impact caused by both the discharge of effluents and the disposal of hazardous waste in the environment and extraction of raw material, contributing to the eco-efficiency of mining.

The hypotheses of this work are that: (I) the use of NF allows adequate treatment of the gold mining effluent, producing a permeate of sufficient quality for industrial reuse and retaining the main contaminants present in this effluent, mainly sulfate, sulfuric acid and arsenic , the latter two of which may be destined for recovery procedures; (II) the use of MD can be even more promising because it allows the production of a permeate of a quality that is even higher

than the permeate of NF, and can be used for industrial reuse of more noble purposes, and also concentrates with greater efficiency the contaminants present in the effluent of mining, mainly sulfate, sulfuric acid and arsenic, the latter two of which may be destined to recovery processes at a concentration even greater than that obtained in the NF streams; (III) the MD process can be used at even lower costs than usual by taking advantage of the high temperature of the studied effluent and thus presenting low energy demand, which can be supplied by solar energy, (IV) the SX process can be used both in the raw effluent and in the NF or MD concentrate for the removal and recovery of high purity arsenic, as well as to allow the recovery of sulfuric acid. In general, the use of membrane separation processes is technically and economically advantageous for wastewater treatment of gold processing.

1.2 OBJECTIVES

1.2.1 General objective

The objective of this work is to evaluate the feasibily of Nanofiltration, Vacuum Membrane Distillation, Direct Contact Membrane Distillation and Solvent Extraction in the reclamation of a gold mining effluent that presents high temperature, low pH, high salinity and arsenic contamination.

1.3 Specific objectives

The specific objectives are:

I. Evaluate the influence of pH and feed temperature, operating transmembrane pressure, feed temperature and permeate recovery rate in the performance (retention and fouling mechanism) of nanofiltration (NF) applied to gold mining effluent.

II. Evaluate the influence of pH and feed temperature, vacuum pressure and permeate recovery rate in the performance (retention and fouling mechanism) of vacuum membrane distillation (VMD) applied to gold mining effluent.;

III. Evaluate the influence of pH and feed temperature, temperature difference between feed and distillate, flow velocity of the streams and degree of permeate recovery in the

performance (retention and fouling mechanism) of direct contact membrane distillation (DCMD) applied to gold mining effluent.;

IV. Compare the technical and economical applicability of nanofiltration (NF) and membrane assisted distillation (MD) technologies to the treatment of the gold mining effluent, taking into account environmental valuation.

V. Evaluate the feasibility of arsenic removal by solvent extraction (SX) from the gold mining effluent and / or the concentrates from nanofiltration (NF) and membrane assisted distillation (MD) technologies and influence of the type of extractant, aqueous phase pH, operational temperature, aqueous phase sulfate concentration and reaction time

1.3 DOCUMENT STRUCTURE

This thesis is divided into 7 Chapters. The first, "Chapter 1: Introduction" aims at presenting the background and justificative of this work, with the objectives of the study.

The second chapter, "Chapter 2: The feasibility of nanofiltration process for sulfuric acid plant wastewater reclamation", refers to specific objective I.

The third, "Chapter 3: Comparison of nanofiltration (NF) and direct contact membrane distillation (DCMD) as an alternative for gold mining effluent reclamation", compares the application of those two techniques (NF and DCMD) on the real gold mining effluent and presents a technical-economical evaluation of both, as indicated by specific objectives III and IV.

The fourth chapter, "Chapter 4: the feasibility of vacuum membrane distillation (VMD) for sulfuric acid plant wastewater reclamation", presents the results found for VMD application to a synthetic solution with characteristics similar to that of the gold mining effluents, as described on specific objective II. The results presented here were obtained during the sandwich PhD in Toulouse (France).

The fifth chapter, “Chapter 5: The feasibility of direct contact membrane distillation (DCMD) for sulfuric acid plant wastewater reclamation”, refers to the results obtained for DCMD application on the treatment of the same solution used for VMD application in Chapter 4. This chapter aims to attend to the specific objective III.

The sixth chapter, “Chapter 6: The feasibility of solvent extraction (SX) to remove arsenic from the gold mining effluent”, aims to attend to the last specific objective (V), presenting the results found for different extractans and extraction operational conditions.

Finally, the seventh chapter, “Chapter 7: Final Considerations”, summarize the conclusions found in this work, and chapter 8 contains all references used in the thesis.

CHAPTER 2:

THE FEASIBILITY OF NANOFILTRATION PROCESS FOR SULFURIC ACID PLANT WASTEWATER RECLAMATION

2.1 INTRODUCTION

Sulfuric acid is one of the largest-volume industrial chemicals produced in the world. World production of sulfuric acid was about 230 million tons in 2017 ("The Essencial Chemical Industry - Online," 2016) and about 60% of this production was used in fertilizer production ("IHS MARKIT", 2017). Sulfuric acid is used with phosphate rock in the manufacture of phosphate fertilizers. Smaller amounts are used in the production of ammonium and potassium sulfate; and also used as an acidic dehydrating agent in organic chemical and petrochemical processes, as well as in oil refining. In the metal processing industry, sulfuric acid is used for pickling and descaling steel; for the extraction of copper, uranium and vanadium from ores; and in non-ferrous metal purification and plating. In the inorganic chemical industry, it is used most notably in the production of titanium dioxide. Many processes of sulfuric acid production have been developed according to the large number of sources of raw materials (SO_2), and their specific characteristics. The sulfuric acid production draw in two fundamental steps, (1) Conversion of SO_2 into SO_3 and (2) Absorption of SO_3, developed via either of three methods: contact process, wet process and lead chamber method.

SO_2 can be produced by the roasting of sulfide ores, like pyrite (FeS_2) and copper, lead and zinc sulfides (ASHAR; GOLWALKAR, 2013; HIJI; NTALIKWA; VUAI, 2014). To extract the valuable metals from this ores, metallurgical process involving roasting are applied, generating gases containing SO_2 with variable concentrations (ASHAR; GOLWALKAR, 2013). Pyrite is the most common sulfide mineral, it can contains up to 50% of sulfur and present a great correlation with gold, as geological properties indicates that the presence of gold is more likely to happen when the more iron is present in the seam (HIJI; NTALIKWA; VUAI, 2014). Thus, the gold ore processing also generates large amounts of SO_2 rich gases. The large supply of SO_2 has led the mining industry to integrate its ore beneficiation plants with sulfuric acid production plants, producing tons of this acid per year.

All acid plants produce some form of wastewater either from the process such as weak acid from a gas cleaning system, wash down water, accidental spills, boiler blow down, cooling water blow down, precipitation collected in a containment area, etc. Some wastewaters are not treated prior to release to the environment while others must be treat extensively to remove contaminants before it can be safely discharged.

Wastewaters from sulfuric acid plant integrate to gold ore processing are characterized by low pH and high concentration of sulfate and metals, like arsenic (Andrade et al., 2017a). Although sulfate is not toxic its removal from wastewaters is of utmost importance to allow the water reuse in mining operations, as it has a great potential of corrosion and fouling of equipment and pipelines (BOWELL, 2004). On the other hand, arsenic is a persistent, bio-accumulative, carcinogenic and toxic element. Arsenic is derived from extraction of metals by oxidation and acid dissolution of the arsenic-containing minerals such as arsenopyrite or Ni–Co–Fe arsenides and sulfarsenides presented in many gold and uranium ores (JIA; DEMOPOULOS, 2008).

For wastewater treatment, metallurgical industries usually adopt classical processes such as chemical precipitation, adsorption, ion exchange and electrochemical, being chemical precipitation more commonly used due to their low cost and operation simplicity (BARAKAT, 2011; CHOONG et al., 2007). These processes, however, have some drawbacks such as poor selectivity, high operating costs and production of a wastewater with improper quality for reuse at the end of treatment, due to a high sulfate concentration. Another issue is the accumulation of an arsenic contaminated sludge which must be disposed as a waste and still offers an enormous risk to the environment (BARAKAT, 2011; MOHAN; PITTMAN, 2007; WANG et al., 2007). In addition, the imposition of increasingly restrictive disposal and discharge standards as well as charges for water catchment and wastewater discharge have propelled the search for more efficient treatment technologies. As pointed out (JOHNSON; HALLBERG, 2005), the choice of a treatment system for mining waters should take into account not only the current legislation and established standards, but the treated water as a resource, seeking the removal and recycling of by-products presents in these wastewaters.

In this context, membrane separation processes, especially nanofiltration (NF) and reverse osmosis (RO), stand out as an alternative to conventional processes. These techniques have high efficiency in retention of metals and salts from aqueous media (AL-RASHDI; JOHNSON; HILAL, 2013), allowing not only the removal of potentially toxic elements, thereby matching the discharge standards, but also the obtaining of a permeate suitable for reuse. Further, it is possible to recover by-products such as acid and metals from concentrated streams (MULLETT; FORNARELLI; RALPH, 2014; RICCI et al., 2015a), thus contributing to mining ecological efficiency.

The use of NF and RO has been investigated for the treatment of metals-rich synthetic solutions, with characteristic similar to mining wastewaters (AL-ZOUBI et al., 2010), and real mining wastewaters themselves (AGUIAR et al., 2016; ANDRADE et al., 2017b, 2017c, 2017a, 2017d, 2018; RICCI et al., 2015b). NF has been considered the most appropriate technology as it results in larger fluxes with less energy consumption. NF is a promising technology to treat mining wastewater as it presents a high rejection of divalent anions as sulfate.

NF has also been investigated by several authors to remove arsenic from contaminated drinking water (AKBARI; MEHRABADI; TORABIAN, 2010; HARISHA et al., 2010), groundwater (XIA et al., 2007), natural waters (AHMED et al., 2010) and synthetic solutions (FIGOLI et al., 2010; NGUYEN et al., 2009a) and high removal rates were observed, particularly for As (V). However, most studies involve relatively low concentrations of arsenic (up to 2 mg L^{-1}) and the effect of interfering ions has not been properly investigated. A limited number of studies evaluating the removal of arsenic of mining wastewater by NF membranes have been reported. NF was used for treating acid mine drainage wastewater of an abandoned mercury mine in a region rich in arsenic pyrites (SIERRA; ÁLVAREZ SAIZ; GALLEGO, 2013). These authors observed over 99% of removal for metals such as iron, aluminum and arsenic, and over 97% to sulfate ions.

Different NF and RO membranes were tested in the treatment of a combined gold mining wastewater containing arsenic (ANDRADE et al., 2017c). After optimization of operating conditions, the results showed that although metals such as magnesium and calcium and sulfate ions were efficiently removed (95%, 94% and 94%, respectively), the highest removal efficiency found for arsenic was 58%. It is important to highlight that those authors studied a mining wastewater which was a result of the mixture of two wastewaters of different nature. One from the sulfuric acid production plant, the same wastewater evaluated in this work, characterized by acid pH and high arsenic and sulfate content, and other, from the calcined dam, characterized by alkaline pH. In this way, the arsenic and sulfate concentrations were diluted and acid pH was neutralized at some extent.

These results demonstrate that, although NF is a promising technology for arsenic and sulfate removal, the efficiency will depend largely on the type of membrane used, as well as the characteristics of the wastewater to be treated and operating conditions. Industrial

wastewaters are complex multicomponent aqueous matrices whose behavior under filtration is not straightforward from synthetic solutions. Mining wastewaters also have peculiar characteristics related both to the type of ore processed and to the process to which it is subjected, which can hamper the choice of treatment. Thus, it is of utmost importance that the NF technology be tested individually for each wastewaters that is desired to treat, taking into account all its physicochemical characteristics.

Furthermore, to treat a wastewater containing a specific pollutant such as arsenic, which requires appropriate treatment, it is desirable that this wastewater is treated separately, without undergoing mixing and dilution with other wastewaters. This enables smaller volumes of contaminated wastewaters to be intended to treatment by advanced techniques, lowering costs, and further allows the generation of a more concentrated stream of that pollutant which can be directed to a recovery process. Treatment of a wastewater directly from the stage where it is produced and undiluted requires greater attention to the fluctuations of wastewater characteristics such as pH, temperature and chemical composition, and the effect of these on the chosen treatment process.

Thus, the objective of this study was to evaluate the use of NF of a real sulfuric acid plant wastewater treatment aimed at removing arsenic and sulfate as well as production of water for industrial reuse.

2.2 MATERIALS AND METHODS

2.2.1 Sulfuric acid plant wastewater

The wastewater used in this study comes from sulfuric acid production plant integrated to a gold mining company located in the state of Minas Gerais (Brazil), specifically from the gas scrubber used to clean the SO_2 gas. Table 2.2 1 presents the physicochemical characterization of the sulfuric acid plant wastewater, obtained from three years of monitoring. As can be seen, it is an acid wastewater with a small content of suspended solids and low organic load. Arsenic (toxic), calcium, magnesium and sulfate represent the most relevant metals and pollutants present in this wastewater, and they are found in high concentrations.

Table 2.2-1: Physical-chemical characterization of the gas scrubber wastewater.

Parameter	Unit	Values	Parameter	Unit	Values
pH	-	1.7 ± 0.2	Total Aluminum	mg Al L^{-1}	100.7 ± 14.9
Conductivity	mS/cm	11.5 ± 2.3	Total Boron	mg B L^{-1}	0.6 ± 0.2
Color	uH	105.3 ± 65.9	Total Cadmium	mg Cd L^{-1}	0.28 ± 0.02
Turbidity	NTU	108.4 ± 75.4	Total Calcium	mg Ca L^{-1}	518 ± 213
TS	mg L^{-1}	8384 ± 999	Total Lead	mg Pb L^{-1}	2.3 ± 0.6
TFS	mg L^{-1}	5099 ± 1049	Total Cobalt	mg Co L^{-1}	1.4 ± 0.3
TVS	mg L^{-1}	3284 ± 1160	Total Copper	mg Cu L^{-1}	14.1 ± 1.5
TSS	mg L^{-1}	82.9 ± 45.1	Total Chrome	mg Cr L^{-1}	0.1 ± 0.1
FSS	mg L^{-1}	76.1 ± 46.4	Total Strontium	mg Sr L^{-1}	1.4 ± 0.2
VSS	mg L^{-1}	6.8 ± 4.6	Total Iron	mg Fe L^{-1}	102.9 ± 20.9
TOC	mg L^{-1}	4.4 ± 2.2	Total Phosphorus	mg P L^{-1}	8.5 ± 0.0
IC	mg L^{-1}	0.21 ± 0.04	Total Magnesium	mg Mg L^{-1}	274.0 ± 134.1
Chloride	mg Cl^-/L	62.5 ± 84.6	Total Manganese	mg Mn L^{-1}	25.3 ± 2.2
Nitrite	mg NO_2^- L^{-1}	0.7 ± 0.3	Total Nickel	mg Ni L^{-1}	1.4 ± 0.0
Nitrate	mg NO_3^- L^{-1}	1.9 ± 0.5	Total Potassium	mg K L^{-1}	40.9 ± 6.6
Fluoride	mg F^- L^{-1}	8.1 ± 5.0	Total Silver	mg Ag L^{-1}	0.1 ± 0.0
Phosphate	mg PO_4^{3-} L^{-1}	13.8 ± 1.2	Total Selenium	mg Se L^{-1}	0.1 ± 0.0
Sulfate	mg SO_4^{-2} L^{-1}	4919 ± 1179	Total Sodium	mg Na L^{-1}	32.5 ± 13.2
Total Arsenic	mg As L^{-1}	668 ± 209	Total Tungsten	mg W L^{-1}	0.5 ± 0.0
Arsenic III	*mg AsIII L^{-1}*	*613 ± 232*	Total Vanadium	mg V L^{-1}	0.3 ± 0.1
Arsenic V	*mg AsV L^{-1}*	*104 ± 44*	Total Zinc	mg Zn L^{-1}	73.7 ± 30.7

TS: total solids; TFS: total fixed solids; TVS: total volatile solids; TSS: total suspended solids; FSS: fixed suspended solids; VSS: volatile suspended solids; TOC: total organic carbon; IC: inorganic carbon.

2.2.2 Pretreatment procedure

Prior to NF test, the sulfuric acid plant wastewater was pre-treated by filtration to remove suspended solids using a 2.5 μm pore size cellulose filter (Whatman® quantitative filter paper, ashless, grade 42).

2.2.3 Nanofiltration experimental setup

Nanofiltration tests were conducted on a laboratory scale in a system (depicted in Figure 3.2-1) that consisted in a feed tank, a centrifugal pump connected to a speed controller, a flowmeter, a needle valve for pressure adjustment, a pressure gauge, a temperature gauge and

a stainless steel flat sheet membrane module. This module has a diameter of 9 cm, providing a 63.60 cm^2 filtration area. The radial inlet radius of the cell was 64 mm, and the channel height, 1 mm. A circular sample of the membrane was placed in the cell and a feed spacer of 28 mil (25.4 µm) was placed on its top to assure a proper flow distribution.

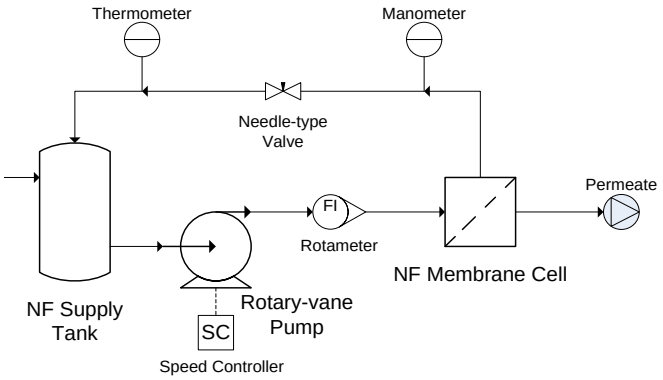

Figure 2.2-1: Schematic diagram of the NF unit used in the tests

The membrane used was NF90 (Dow Filmtec). It has a molecular weight cut-off of 100 Da (ZULAIKHA et al., 2014), average membrane hydraulic resistance of 5.8 x 10^{13} m^{-1}, and salt rejection of 85-95% to NaCl (2,000 mg L^{-1}) and 97% to $MgSO_4$ (2,000 mg L^{-1}) (DOWFilmec^{TM}).

2.2.4 Nanofiltration experimental procedure

The nanofltration experiments were carried out with the previously filtered sulfuric acid plant wastewater under different pH, pressure, temperature and recovery rate. Feed pH was adjusted at 1.0, 1.6 (raw wastewater pH), 2.9, 4.3, 5.3 and 6.0 using 5 N NaOH and 98% H_2SO_4 solutions. The transmembrane pressure (TMP) was controlled at 4, 6, 8 and 10 bar. It was not possible to evaluate TMP higher than 10 bar due to the constraints of the experimental unit. The temperature was kept at 25 ± 2°C, 30 ± 2°C, 35 ± 2°C and 40 ± 2°C by heating up the wastewater on a hotplate and it was maintained by an immersed coil. This temperature range was selected considering the following limits: the room temperature (25°C) and the natural temperature of the wastewater (40°C), so that in a full-scale application there is no need for wastewater cooling other than cooling that may occur in the equalization tank. In each operating condition, the following procedure was adopted: (1) filtration of de-ionized water under four different TMP (10, 8, 6 and 4 bar) until a constant flux was obtained to each pressure, to calculate the membrane hydraulic permeability; (2) filtration of wastewater under the selected condition and feed flow of 2.4 $L.min^{-1}$ (3) wash of the fouled membrane module

by flowing de-ionized water for 2 minutes with feed flow rate of 1.2 L min^{-1} to remove loosely deposited foulants at the membrane surface; (4) filtration of de-ionized water for 20 minutes under the TMP of 10 bar; (5) chemical cleaning of membrane (pH 2 HNO_3 solution followed by 0.4% (m/m) NaOH); (6) filtration of de-ionized water under three different TMP (10, 8, 6 and 4 bar) until a constant flux was obtained to each pressure to re-evaluate the hydraulic permeability. All tests were conduct in duplicates. The permeate flow rate was measured at every 10 minutes.

The previously filtered wastewater (feed), and the permeate obtained at the end of test were analyzed for pH, conductivity, concentration of arsenic (total, III and V), sulfate, calcium and magnesium, and the values found were used to evaluate the process efficiency.

To determine the ideal permeate recovery rate (RR), 6 liters of pre-filtered sulfuric acid plant wastewater were submitted to NF system. Feed solution pH was previously adjusted to the optimal value as determined from previous tests. The test was conducted with concentrate recirculation and continuous removal of permeate. To every 100 ml of permeate collected, flux and temperature were measured and to every 300 ml, conductivity, arsenic (III, V and total) sulfate, calcium and magnesium analysis were performed. At the end of this test, the membrane used was removed from the cell, divided into two pieces. One of them was submitted to chemical cleaning in a separated vassel. Both fragments were dried at room temperature and then analyzed with respect to membrane surface characterization and chemical properties. As comparison, a virgin NF90 membrane was also analyzed. Samples of raw wastewater and NF concentrate and permeate from the considered ideal recovery rate were also subjected to analysis of metals by ICP.

2.2.5 Analytical methods

The sulfuric acid plant wastewater and aqueous samples collected in different stages of the treatment were analyzed for pH (pHmeter Qualxtron QX 1500); conductivity (Hanna conductivity meter HI 9835); ions sulfate, calcium, chloride and sodium (Dionex ICS-1000 ion chromatography, equipped with column type IonPac AS-22 and IonPac ICS 12-A); total arsenic, As (III) and As (V) (DHAR et al., 2004); suspended solids (APHA, 2005); and metals (inductively coupled plasma optical emission spectrometry (ICP-OES) Varian, 720-ES).

For the characterization of surface and chemical properties of the membrane analysis of scanning electron microscopy (SEM) (Scanning Electron Microscope - Quanta 200 EIF),

energy dispersive X-ray spectroscopy (EDS) (Pioneer Si (Li) with a resolution of 134 eV, coupled to SEM) and atomic force microsocopy (AFM) (microscope Asylum Research MFP-3D-AS, with Olympus AC 160TS probe in intermittent contact mode) were performed. The samples were coated with a 4nm thick gold layer for SEM analysis. For AFM, a silicon probe (AC240TS-R3, Olympus) was used and tapping mode was performed over a 5 × 5 μm² membrane area. A minimum of three different areas of each membrane were visualized and AFM software was used to determine the mean value of the root-mean-squared roughness (RMS).

2.2.6 Preliminary Investment and Cost Estimation

In order to estimate the capital and operational expenses (CapEx and OpEx) of the optimized NF system studied in this work, a preliminary study was conducted. It considered the costs associated with the membrane unit, membrane replacement, alkalizing agents (for permeate pH adjustment, necessary for its reuse), chemical cleaning agents, energy consumption, and also system maintenance.

For the NF membrane unit a capital cost of 8,750.00 U$ m^{-3} h^{-1} of wastewater volumetric flow was considered as this price was provided by a major supplier of commercial membranes in Brazil. The wastewater volumetric flow was 140 m^3 h^{-1}, which is the real flow rate of this wastewater in the mining company and also the capacity of the designed system (Q_{des}). One filtration stage was considered for NF.

The investment rate i_c (equal to 14% in Brazil, in 2017), and the design life of the plant (DL), considered to be 15 years for the NF system, were used on Equation 1 (SETHI; WIESNER, 2000) to annualize the capital cost by means of the amortization factor (A/P) in order to estimate the capital cost per cubic meter of wastewater.

$$A/P = \frac{i_c \cdot (1 + i_c)^{DL}}{(1 + i_c)^{DL} - 1} \quad (1)$$

Equation 2 could then be applied to calculate the capital cost per cubic meter (C_{cap/m^2}), using the system capital cost (C_{cap}) and the capacity of the designed system (Q_{des}), which were both described before.

$$C_{cap/m^2} = \frac{C_{cap} \cdot A/P}{Q_{des}} \quad (2)$$

In the previous study (Andrade et al., 2017d), the results suggest a minimum membrane lifetime of 536 days for NF treating mining wastewater with similar characteristics. Then, the OpEx was calculated for a membrane lifespan of 1, 2, 3, 4 and 5 years. The required NF membrane area was determined considering a 45% recovery rate and an average permeate flux of 25 L h^{-1} m^{-2}. NF membranes costs were 50.00 US$ per square meter, price provided by a large commercial membrane supplier.

The alkalizing agent cost (NaOH) was also calculated based on the volume of NaOH solution used to adjust the pH of the NF 45% RR permeate. In this estimate, it was considered a price of 425.00 US$ ton^{-1} of NaOH[1]. Despite NaOH be more expensive than $CaCO_3$ it generates less sludge since calcium present in $CaCO_3$ can reacts with sulfate ions resulting in $CaSO_4$ precipitation.

For the cost estimation of the chemical cleaning agent, only the use of citric acid ($C_6H_8O_7$) solution at pH = 2 was considered since the use of NaOH as cleaning agent did not bring any benefit (Andrade et al., 2017d). The approximate price of 62.5 US$ kg^{-1} of $C_6H_8O_7$[2] for the citric acid was used and the cleaning frequency was assumed to be of once a week for one hour (AGUIAR et al., 2016). In order to calculate the volume of the cleaning solution required, the volume of the NF modules and an estimated volume of the feed and return pipes were considered.

For the energy cost estimation, equations 3 and 4 were used to calculate the NF feed pump energy requirement (E_f). For this, it was used values of NF feed flow (Q_f), NF average permeate flux (J, considered 25 L.h^{-1}.m^{-2}), the total area of the NF membrane (A), the recovery rate (RR, 45%), the applied pressure (ΔP,10 bar), and the efficiency of the feed pump (η, assumed to be 70%).

[1] Value available at: < http://www.icis.com/resources/news/2006/05/06/2013928/chemical-profile-caustic-soda/>. Accessed on: 2 March 2017

[2] Value available at: < https://www.spectrumchemical.com>. Accessed on: 2 March 2017.

$$Q_f = \frac{J \cdot \mathrm{A}}{RR} \quad (3)$$

$$E_f = \frac{\Delta P \cdot \mathrm{Q_f}}{\eta} \quad (4)$$

The mining company studied pays an energy tariff of 0.04 US$ kWh^{-1} (considering an exchange rate of US$1 = R$0.25) in Brazil, which was also considered in the calculations. Maintenance costs were estimated at 5% per year of the initial investment cost (SHEN et al., 2014).

2.2.7 Calculations

In order to calculate the flux at the permeation temperature [J(T)], equation 5 was used. It considered the permeate volume collected (ΔV), the collection time (Δt) and effective membrane area (A):

$$J(T) = \frac{\Delta V}{A \Delta t} \quad (5)$$

J(T) was normalized to 25°C [J(25°C)] using a correction factor calculated by the ratio of the water viscosity at the permeation temperature [$\mu(\mathrm{T})$] and at 25°C [$\mu(25°\mathrm{C})$], as show in equation 6:

$$J(25°C) = \frac{\mu(T)}{\mu(25°C)} * J(T) \quad (6)$$

Van't Hoff equation (equation 7) was used to estimate the osmotic pressure difference at different permeate recovery rates. For this, the universal gas constant (R, in L Pa $K^{-1}mol^{-1}$), the temperature of permeation (T, in K), and the sum of the difference in concentrations of the main dissolved species in the concentrate and permeate solutions ($\Sigma \Delta C$, in mol/L) were used.

$$\Delta\pi = RT\Sigma\Delta\mathrm{C} \quad (7)$$

In this calculation, it was used the concentrations of sulfate and calcium analyzed for RR 5, 10, 15, 20, 25, 30, 35, 40, 45, 50 and 60% and mathematically adjusted for other RR values.

Pollutants and conductivity rejection [R(%)] were calculated using Equation 8, that considered the conductivity or pollutant concentration of the feed (C_f) and permeate (C_p) streams:

$$R(\%) = \frac{C_f - C_p}{C_f} \times 100 \quad (8)$$

The wastewater recovery rate (RR) was defined considering the accumulated permeate volume (V_p) and initial feed volume (V_f) as shown by equation 9:

$$RR = \frac{V_p}{V_f} * 100 \quad (9)$$

The specific energy consumption (SEC) was defined by the relation between the rate of work done by the pump (W_{pump}) and permeate flow rate (Q_p) (Zhu et al., 2009), as follows:

$$SEC = \frac{W_{pump}}{Q_p} \quad (10)$$

W_{pump} was calculated by multiplying the volumetric feed flow rate (Q_f) by ΔP, which is assumed to be equivalent to the permeate pressure

$$W_{pump} = \Delta P \times Q_f \quad (11)$$

By combining Equations 9, 10 and 11, the equation to determine SEC can be rewritten as follows:

$$SEC = \frac{\Delta P}{RR} \quad (12)$$

To investigate the process of membrane fouling and flow decrease as a function of operating time the Hermia's model was applied, as used by other authors (BENÍTEZ; ACERO; LEAL, 2006; KAYA et al., 2010; MOHAMMADI; ESMAEELIFAR, 2005). This model consists in applying the experimental data on four different filtration models equations, listed in Table 2.2 2. Graphs of $\ln(J^{-1})$, $J^{-\frac{1}{2}}$, J^{-1} and J^{-2} as a function of time were made. Assuming a linear correlation, the slope of each curve provides a coefficient depending on the flow rate

and solution properties (k) (SHIM et al., 2015). The regression coefficient (R^2) and the original permeate flux (J_0) were also determined by the equations of that model (Kaya et al., 2010).

Table 2.2-2: Filtration models and their equations

Model	Equation
Complete blocking filtration	$\ln(J^{-1}) - \ln(J0)^{-1} + k.t$
Standard blocking filtration	$J^{-\frac{1}{2}} - J0^{-\frac{1}{2}} + k.t$
Intermediate blocking filtration	$J^{-1} - J0^{-1} + k.t$
Cake filtration	$J^{-2} - J0^{-2} + k.t$

2.3 RESULTS AND DISCUSSION

2.3.1 pH influence on NF performance

pH has a major influence on the charge equilibrium both of the membrane surface groups and of ionic species in solution. The analysis of the effect of the feed stream pH is extremely important to predict the treatment efficiency in face of eventual wastewater physicochemical characteristics fluctuations, very common in the industry. In addition, it helps the decision of when to perform the adjustment of the wastewater pH, before or after treatment, since the wastewater studied in this work, as well as other mining wastewaters, has acidic pH.

The sulfuric acid plant wastewater studied has a natural pH around 2.0. As can be observed in Table 2.3 1, as the wastewater pH was increased, it was observed a reduction of the conductivity and also reduction of sulfate, calcium and magnesium ions concentration in the filtration pretreatment step, due to precipitate formation. The precipitate formation was measured in terms of suspended solids. As it can be seen, suspended solids concentration increases when pH is increased, showing the higher value for pH 6. Results suggest this precipitation is comprised mainly by calcium sulfate salt. The drastic reduction of sulfate ions at pH 5 and 6, not followed by calcium and magnesium cations, indicate precipitation of some other metal with sulfate. The sharp reduction in the concentration of arsenic in pH 6, mainly present in its neutral form, indicates its possible adsorption to the precipitate formed, being removed in the filtration process before the NF. The presence of arsenic in the formed sludge is not attractive from an environmental point of view, since it features a hazardous waste and presents risks to the environment, neither economical, since part of the arsenic and also sulfate that is desired to recover would be lost.

Table 2.3-1: Physicochemical characterization of the sulfuric acid plant wastewater at pHs 1, 2, 3, 4, 5, and 6 and respective permeates flux, water permeability, fouling and chemical irreversible resistance and osmotic pressure obtained for each test (T= 25°C; P= 10 bar; RR= 2%).

pH		Conductivity (mS cm^{-1})	Sulfate (mg L^{-1})	Total As (mg L^{-1})	As 3 (mg L^{-1})	As 5 (mg L^{-1})	Mg (mg L^{-1})	Ca (mg L^{-1})	Suspended solids after pH adjustment (mg/L)[a]		Jf/Jw[d]	Jf/Ji[e]	Kp/Kw[f]	Rf (m^{-1})	Rci (m^{-1})	Osmotic pressure (bar)
									TSS[b]	FSS[c]						
1.01	Feed	34.80	11399	430	354	76	301	594	0.04	0.02	0.28	0.76	0.57	6.44E+13	6.44E+13	5.142
	Perm.	*7.79*	*1111*	*1845*	*170*	*15*	*8*	*27*								
1.60[g]	Feed	12.27	6309	493	404	89	358	631	0.48	0.40	0.63	0.96	0.86	8.73E+12	1.36E+13	2.737
	Perm.	*0.86*	*202*	*173*	*159*	*14*	*14*	*25*								
2.93	Feed	7.72	6041	481	411	70	313	489	0.99	0.82	0.64	0.84	0.80	2.85E+13	2.41E+13	1.962
	Perm.	*0.54*	*284*	*183*	*165*	*18*	*12*	*18*								
4.28	Feed	6.92	6033	517	466	51	337	483	1.55	1.25	0.63	0.89	0.78	1.76E+13	2.86E+13	1.893
	Perm.	*0.49*	*321*	*261*	*241*	*20*	*6*	*12*								
5.33	Feed	7.77	6272	503	440	63	340	490	1.98	1.68	0.60	0.82	0.74	1.71E+13	3.16E+13	1.892
	Perm.	*0.71*	*337*	*273*	*246*	*27*	*16*	*20*								
6.01	Feed	7.74	5461	353	314	39	358	537	2.54	2.09	0.57	0.77	0.70	3.45E+13	3.8E+13	1.815
	Perm.	*0.78*	*362*	*273*	*261*	*12*	*13*	*18*								

Perm.: permeate; [a]: estimate of mud production; [b]TSS: total suspended solids; [c]FSS: fixed suspended solids; [d]final permeate flux(Jf) and water flux (Ji) ratio; [e]final permeate flux(Jf) and initial permeate flux (Ji) ratio; [f]permeate permeability (Kp) and water permeability (Kw); [g]raw wastewater (no pH adjustment); (Rf) fouling resistance; (Rci) chemically irreversible resistance.

The lower permeate flux was observed at pH 1, which can be due to the increase in the concentration of ions hydrogen and sulfate in the feed caused by the addition of sulfuric acid to the wastewater, in order to decrease its pH. The addition of sulfuric acid also lead to an increase of the osmotic pressure of the wastewater, which increased from 2.7 to 5.14 bar.

A decrease in the permeate flux was also observed at feed pH 5 and 6. At those pH the permeate flux decline was also higher, as final permeate flux represents 82% (pH 5) and 77% (pH 6) of the initial flux. These results suggest that at feed pH of 5 and 6 fouling has a more pronounced effect, which can be due to higher concentration polarization or even the precipitation of salts at the membrane surface observed on membrane surface at the end of the test. This represents an operational disadvantage, since physical and chemical cleanings are required more frequently. This causes more frequent interruptions in the system and decrease the membranes lifespan.

It is known that pH adjustment has several consequences both for the feed, changing its quality and enhancing phenomena like concentration polarization and salt precipitation, and for membranes, which can have its functional groups protonated/deprotonated, changing membrane surface charge/potential, also modifying its adsorption capacity and strength of attraction/repulsion of ions (CHILDRESS; ELIMELECH, 2000). The high retention efficiencies of sulfate, calcium and magnesium can be explained by the small ratio between NF90 membrane pores size and the hydrated radius of these ions and also by their divalent charge. As sulfate, calcium and magnesium showed little removal variation along the different feed pH, it is suggested that charge effect is not the most important factor for their removal, as reported elsewhere for NF90 (NICOLINI; BORGES; FERRAZ, 2016).

It is highlighted that for all evaluated pH the high retention observed for sulfate was not followed by for arsenic, which was retained with less efficiency. Furthermore, the arsenic retention was strongly influenced by feed pH. It is known that the pH of the medium strongly influence arsenic speciation. In aqueous medium, arsenite and arsenate are found in basically two species each. Arsenite [As (III)] is usually found in its neutral H_3AsO_3 form at pH lower than 9.2 and at higher pHs the anion $H_2AsO_3^-$ is the predominant form. By the other hand, arsenate [As (V)] is commonly found in their monovalent $H_2AsO_4^-$ anionic form in pH lower that 6.9 while at pH higher than 6.9 the divalent $HAsO_4^{2-}$ form is the commonest (YAN; KERRICH; HENDRY, 2000). Besides, according to some authors (NGUYEN et al., 2009b)

three mechanisms govern arsenic retention by NF membranes: exclusion by size, by charge and ionic preferential permeation.

As can be observed, increasing the pH decrease the arsenic retention due to electrostatic repulsion phenomenon decrease. When pH is increased to 6, arsenic retention strongly reduces. These results suggest that the IEP value for NF90 membrane is between 5.5 and 5.7 as indicated (CARVALHO et al., 2011; DO et al., 2012). At pH values above the IEP of NF90, its surface functional groups become deprotonated and a negative membrane charge is observed. The negative charge increases its capacity of retention of anions, such as $H_2AsO_4^-$ [As (V)]. However since the arsenic in this wastewater is found predominantly in the form of H_3AsO_3 [As (III)], the increase in As (V) retention dos not result in the increase of total arsenic retention.

According to authors (WANG et al., 2009), arsenic removal efficiency by NF membrane also decreases when the feed concentrations of arsenic, sulfate and calcium increases. Furthermore, the rejection observed for As (III) (17-61%) is much lower than that observed for As (V) (57-85%). As the wastewater investigated in this study contains high concentrations of sulfate, calcium and arsenic, in both forms arsenite and arsenate, the low arsenic removal is also justified.

The evaluation of nanofiltration retention mechanisms when treating real wastewaters, multicomponent aqueous matrices, are more complex than those observed when studying mono- or bicomponent solutions. Further, also for the treatment of sulfuric acid plant wastewater studied here, the retention of higher valency counter ions in order to achieve electroneutrality was the most important retention mechanism, more than Donnan effect or retention by size.

The results shows that NF of the raw wastewater in its original pH (around 2) showed the best results with respect to the removal of pollutants, especially arsenic. Also, the use the wastewater with its original pH is more advantageous in economic and environmental point of view as it would reduce the consumption of consumables for pH adjustment and avoid mud production, allowing more efficient by-products recovery.

2.3.2 TMP influence on NF performance

Figure 2.3-1 shows the influence of the transmembrane pressure (TMP) on the performance of the NF90 nanofiltration membrane for real sulfuric acid plant wastewater treatment.

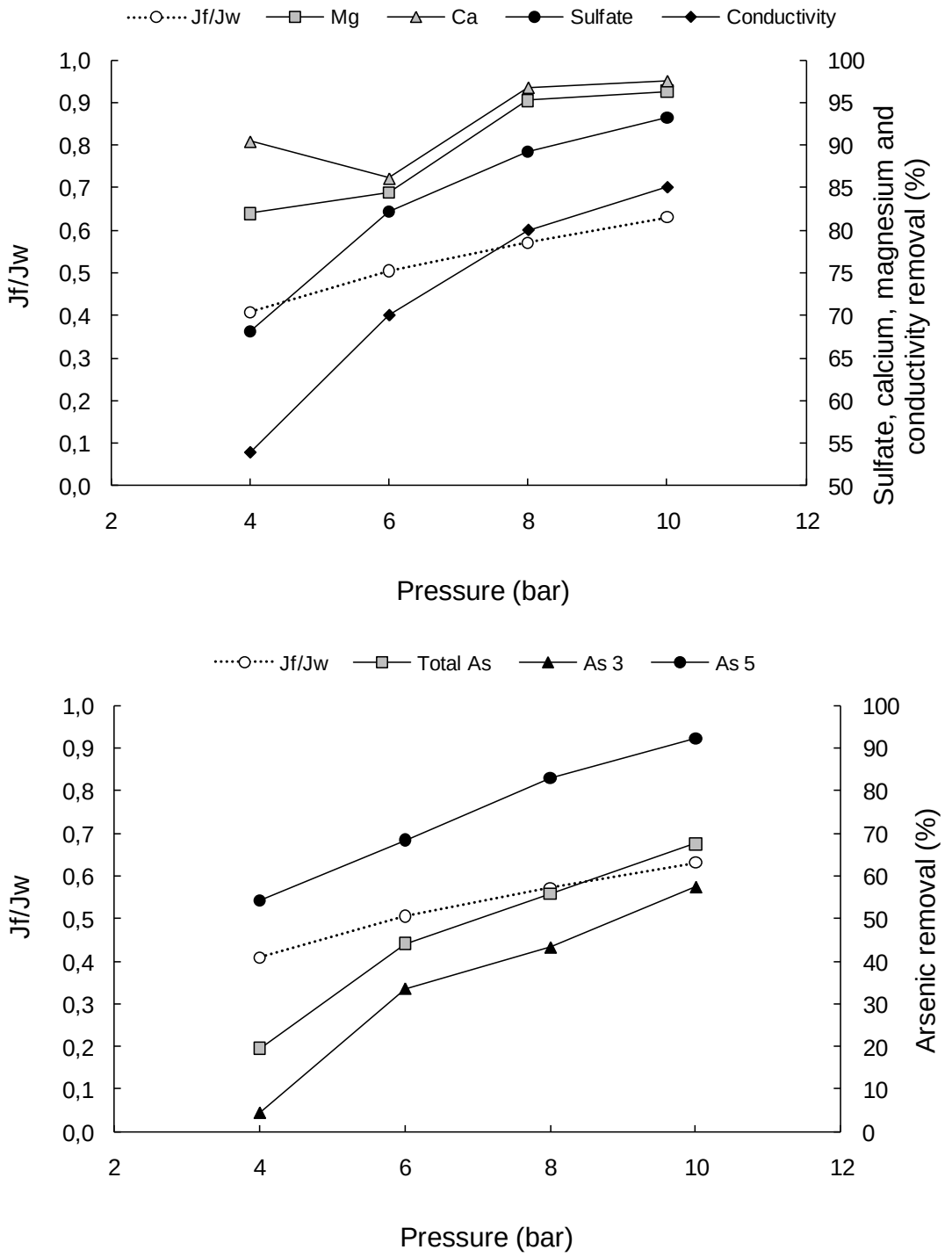

Figure 2.3-1: Effect of the operating TMP in the permeate flux and sulfate, calcium, magnesium, arsenic and conductivity rejection (T= 25°C; pH= 2; RR= 2%).

As can be seen, the removal of conductivity, sulfate, calcium and magnesium increases as pressure increases. This result is expected, being explained by the dilution phenomenon. As pressure increases, solvent flux also increases while solute flux remains constant. These results corroborate with those obtained by different authors that have also studied the effect of

pressure applied in nanofiltration systems to the rejection of As (III) and As (V) (AHMED et al., 2010; AKBARI; MEHRABADI; TORABIAN, 2010; SATO et al., 2002).

Regarding the energy consumption, the operation of NF at TMP of 4, 6, 8 and 10 bar involves the SEC of 0.75±0.01, 0.73±0.03, 0.60±0.07 and 0.57±0.05 kWh m^{-3} respectively. As can be seen decreasing values of SEC was obtained as operating pressure increases indicating that despite the operation at high pressure having a higher energy requirements, production of a larger volume of permeate obtained at higher pressures compensates the energy consumption.

As noted (KAYA et al., 2010), the operating pressure is one of the most critical parameters when employing membrane systems and is closely related to the phenomena of fouling and concentration polarization, which should be investigated. To explain the fouling mechanisms, the Hermia's model was used. The values of k, R^2, and J_0 found for each model for evaluated pressures are listed in Table 2.3-2. The higher the value of R^2, the higher the fit of the experimental data to the model.

Table 2.3-2: Evaluation of fouling mechanisms using Hermia's model for pressures of (a) 4 bar, (b) 6 bar, (c) 8 bar e (d) 10 bar.

Applied pressure (bar)	Jf/Ji	Model											
		Complete blocking filtration			Standard blocking filtration			Intermediate blocking filtration			Cake filtration		
		Jo ($L\ m^{-2}h^{-1}$)	k	R^2	Jo ($L\ m^{-2}h^{-1}$)	k	R^2	Jo ($L\ m^{-2}h^{-1}$)	k	R^2	Jo ($L\ m^{-2}h^{-1}$)	k	R^2
10	0.77	33,0	0.0031	0.85	33.0	0.00030	0.87	33.1	0.000111878	0.89	33.2	8.09391E-06	0.93
8	0.81	25,1	0.0026	0.90	25.2	0.00028	0.91	25.2	0.000122886	0.92	25.4	1.15161E-05	0.94
6	0.73	14,0	0.0014	0.77	14.0	0.00019	0.79	14.0	0.000105267	0.80	14.0	1.61873E-05	0.82
4	0.72	10,2	0.0020	0.82	10.2	0.00033	0.83	10.2	0.000222881	0.83	10.3	4.98238E-05	0.83

In general, for all TMP values evaluated the best fit was obtained for the cake filtration model, except for the pressure of 4 bar, which showed a similar adjustment for the intermediate blocking filtration, standard blocking filtration e complete blocking filtration. Those results are consistent with flux decay profile for all pressures, mainly for TMP of 10 and 8 bar. As can be seen (Figure 2.3-2), permeate flux on these pressures showed sharp decay especially in the first 25 minutes of permeation. As discussed above, as TMP increases initial flux values also increases, based on Darcy's law. However, sharp flux decline can also occur due to increase of concentration polarization and fouling, caused by the driving force enhanced at higher pressures, that makes both solvent and solutes to be more convected

towards the membrane surface, contributing to the accumulation of more molecules on it (MUKHERJEE et al., 2016).

Thus, cake formation on membrane surface is enhanced by TMP increase. In this way, it is consistent that cake filtration model plays a major role to describe the fouling phenomenon. For TMP 4 and 6 bar, flux remained almost constant during the whole test. This results shows that fouling did not have much influence in permeate flux during filtration test, explaining why lower value of R^2 was obtained in Hermia's model.

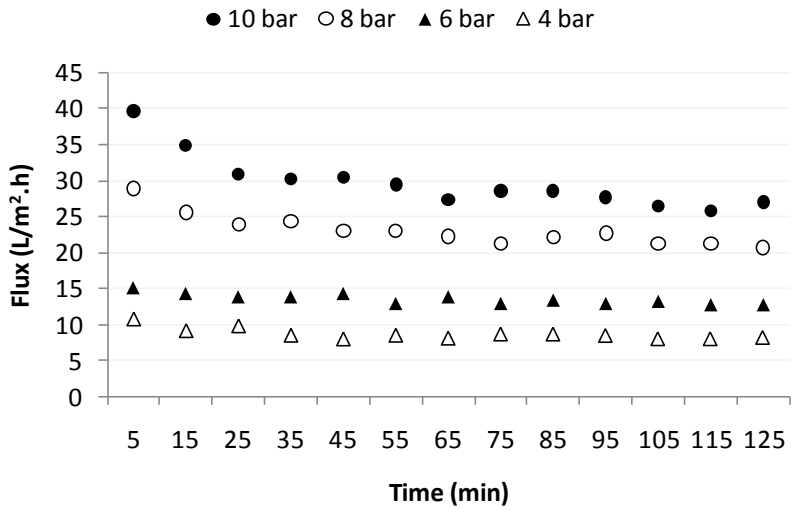

Figure 2.3-2: Permeate flux in a function of the filtration time for NF tests using 10, 8, 6 and 4 bar (pH = 2; T= 25^{o}C; RR= 2%).

Thus, considering the operational conditions, the flux decline presented by each TMP, energy consumption, permeate production and permeate characteristics, was select the TMP of 10 bar.

2.3.3 Temperature influence on NF performance

It is known that the temperature has a great influence in both permeate flux and in the passage of solutes through the membrane (BAKER, 2004). The Figure 2.3-3 shows the influence of temperature on the NF membrane performance for real sulfuric acid plant wastewater. It is important to highlight the importance of this evaluation since the wastewater studied is an wastewater of a gas scrubber and it has temperatures ranging from 30 to 40^{o}C. Assessing the impact of these fluctuations in the performance of the treatment is imperative to optimize the operational conditions.

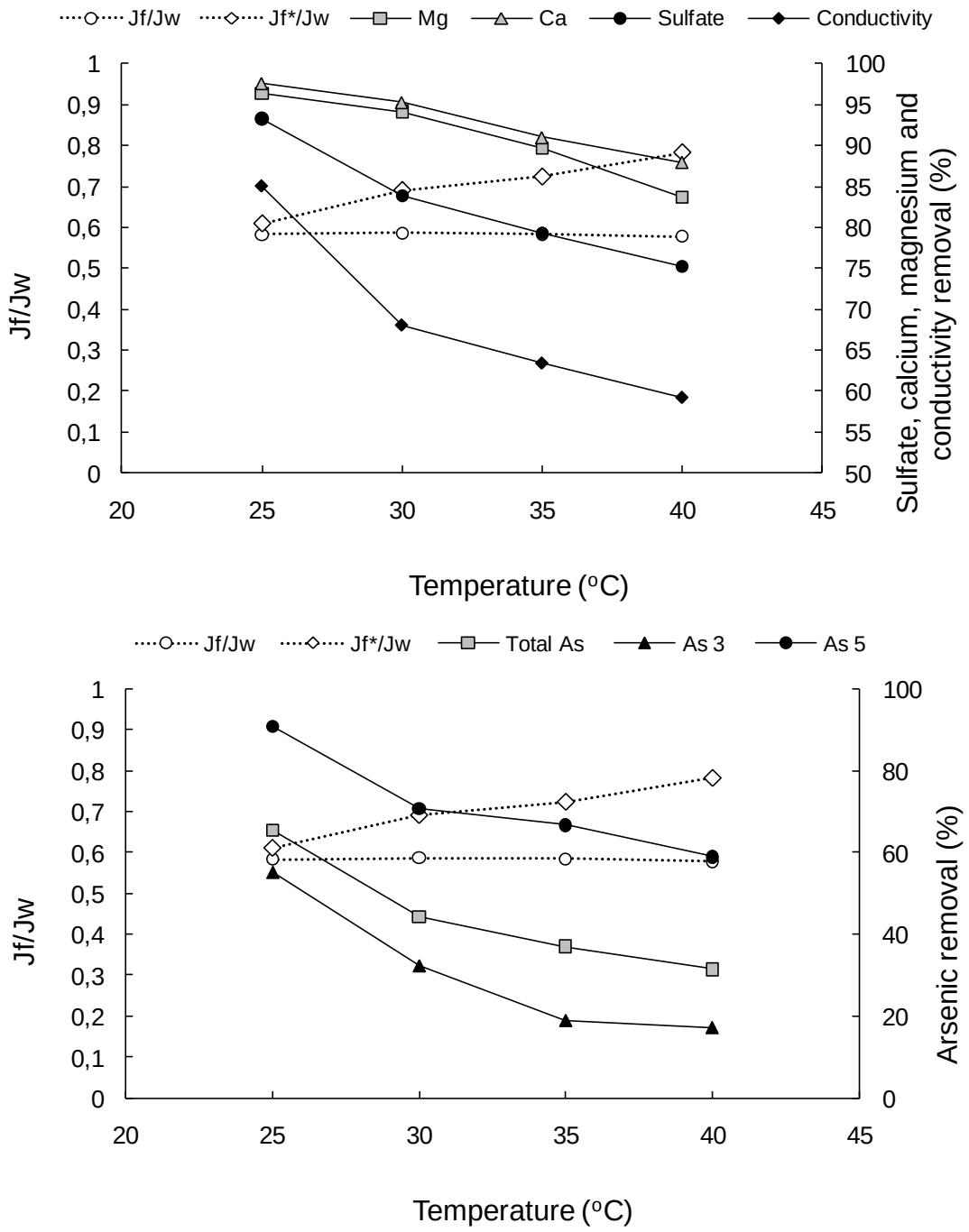

Figure 4

Figure 2.3-3: Effect of the operating temperature in the permeate flux and sulfate, calcium, magnesium, arsenic and conductivity rejection (P= 10 bar; pH= 2; RR= 2%).

As Figure 2.3-3 shows, a decrease in retention efficiency was observed as temperature increases. Increasing temperature can cause reduction of the removal efficiency by increasing diffusivity of the solutes. This phenomenon was observed (FIGOLI et al., 2010) as a decrease on arsenic rejection by NF membrane with temperature increase was found and attributed this

to the increase of arsenic diffusivity and therefore its diffusive transport through the membrane. These authors also observed that this phenomenon is valid for other contaminants present in the wastewater and that sulfate suffers less change on its removal than arsenic ions. The results found in this work corroborate those found previously (FIGOLI et al., 2010) and, as mentioned before, is explained by sulfate's larger valence and hydrated radius.

The increasing of temperature from 25 to 40°C can drastically changes the quality of permeate, which can compromise its industrial reuse, thus attention should be given to permeate quality when NF is performed at higher temperatures. The hardness and higher sulfate concentration observed on permeate stream can increase the risk of salts precipitation on pipes. On the other hand, arsenic concentration in the product may not compromise permeate reuse for activities in which there is no human contact with it, but it represents a loss of a byproduct that could be recovered. Thus, in case where the permeate quality influenced by high temperature restrict the permeate reuse, it is strongly recommended that cooling is performed before NF in order to ensure maximum removal efficiency of the system.

As observed in figure 4, the temperature increase consequently increased the permeate flux due to feed viscosity reduction, since the permeate flux at 25°C values for all temperature evaluated were similar.

Hermia's model was also used for evaluating the membrane fouling mechanism at different temperature with the values of k, R^2, and J_0 found for each model evaluated for each temperature listed in Table 2.3-3.

Table 2.3-3: Evaluation of fouling mechanisms using Hermia's model for temperatures of (a) 25°C, (b) 30°C, (c) 35°C e (d) 40°C.

Temperature (°C)	Jf/Ji	Model											
		Complete blocking filtration			Standard blocking filtration			Intermediate blocking filtration			Cake filtration		
		Jo ($L\ m^{-2}h^{-1}$)	k	R^2	Jo ($L\ m^{-2}h^{-1}$)	k	R^2	Jo ($L\ m^{-2}h^{-1}$)	k	R^2	Jo ($L\ m^{-2}h^{-1}$)	k	R^2
25	0.72	32.4	0.0025	0.80	32.4	0.00024	0.81	32.4	8.90066E-05	0.82	32.5	6.40949E-06	0.84
30	0.78	37.1	0.0024	0.89	37.1	0.00021	0.90	37.2	7.12333E-05	0.91	37.3	4.29027E-06	0.92
35	0.80	39.8	0.0015	0.89	39.7	0.00012	0.89	39.8	4.00273E-05	0.90	39.8	2.19174E-06	0.91
40	0.80	40.0	0.0020	0.91	40.1	0.00017	0.92	40.2	5.68292E-05	0.92	40.5	3.22711E-06	0.93

As can be seen, for all evaluated temperatures the best suited model was the filtration cake, showing that even increasing temperature, the filtration cake still plays a major role to describe the fouling phenomenon, as was observed for TMP.

2.3.4 Determination of the optimal NF recovery rate

For systems that operate by pressure difference like NF systems, the evaluation of the recovery rate is not only of great importance but it is one of the its main design parameters (GREENLEE et al., 2009). As membrane permeability to water is higher than for solutes, the increase of the recovery rate causes an increase of solutes in the concentrate, which therefore increases osmolality and fouling. This can lead to a reduction of the permeate flux and hence the overall process efficiency, making it necessary to evaluate the optimal recovery rate.

With regard to the removal of pollutants, removal rates were high and remained practically constant until the 45% RR (Figure 2.3-4). From this value, a reduction of arsenic species removal was observed, which can be attributed to the increase of their concentration in feed caused by increasing the recovery rate. This phenomenon is observed mainly to the As (III), which in the case of a neutral species, its diffusion is proportional to its concentration (SEIDEL; WAYPA; ELIMELECH, 2001), moving more freely through the membrane. These results corroborate those found in the literature (AKBARI; MEHRABADI; TORABIAN, 2010; BRANDHUBER; AMY, 2001; SEIDEL; WAYPA; ELIMELECH, 2001). A small decay can be observed for As (V) removal from 40% to 45% RR, but since this specie is present in a concentration almost 6 times lower than As (III) and removal rate was still high, this decay was not considered limiting for NF operation.

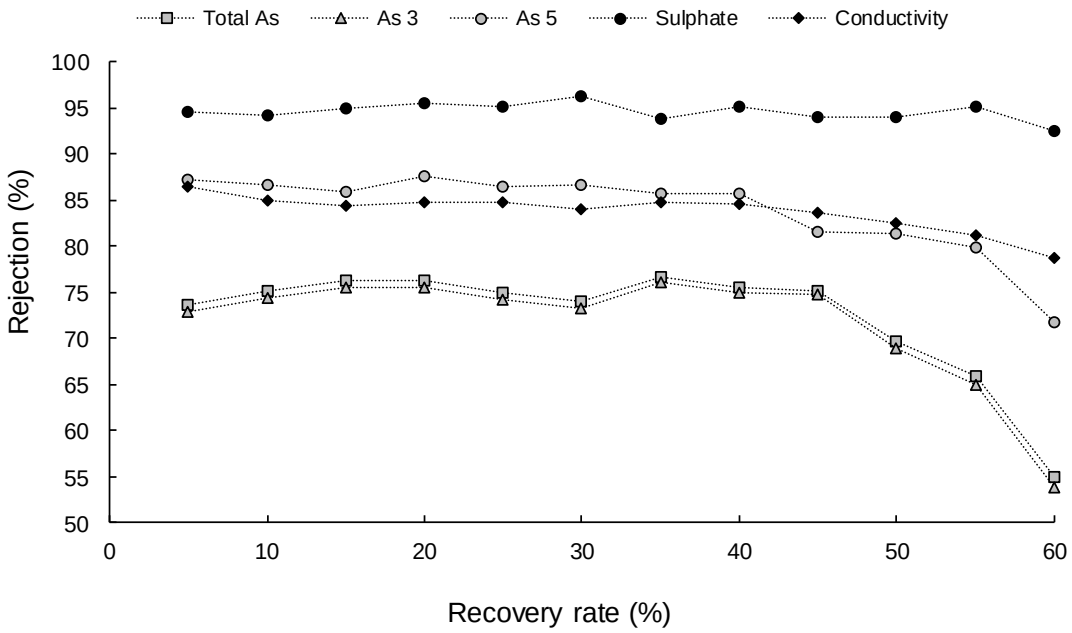

Figure 2.3-4: Effect of the recovery rate in the rejection of sulfate, calcium, magnesium, arsenic and conductivity (P= 10 bar; pH= 2; T = 25^{o}C).

There were no pronounced variation in the rejection of the calcium, magnesium and sulfate ions, even when the recovery rate was 60%, but due to the changes observed for arsenic, 45% RR was considered as the maximum and optimal recovery rate to operate NF system treating raw sulfuric acid production plant wastewater.

The phenomenon concentration polarization is a factor that intensely affects recovery rate and becomes more pronounced as higher recovery rates are employed. As RR increases, the salt concentration at the membrane surface increases and it can affect membrane selectivity. Regarding this phenomenon, the salt rejection of the NF membrane was also evaluated by calculating the salt concentration at the membrane surface and its real rejection.

Equation 13 (NOBLE; STERN, 1995) enables to calculate the salt concentration at the membrane surface (C_m) using the molar concentrations in the retentate (C_r) and permeate (C_p), the permeate flux (J, in $m^3\ h^{-1}\ m^{-2}$) and the mass transfer coefficient (k), which was calculated as demonstrated by other authors (RICCI et al., 2015a).

$$\frac{C_m - C_p}{C_r - C_p} = \exp\left(\frac{J}{k}\right) \tag{13}$$

Considering the set of conditions of this study, the numerical value obtained for sulfate (SO_4^{-2}) was 6.56×10^{-5} m s^{-1} and for calcium (Ca^{+2}), 5.46×10^{-5} m s^{-1}. The real rejection (R_{real}) can be calculated, as shown in equation 14:

$$R_{real} = \left(1 - \frac{C_p}{C_m}\right) \cdot 100\% \tag{14}$$

Figure 2.3-5 shows the calculated membrane concentration and real rejection for calcium and sulfate ions as a function of the RR. It can be observed that besides RR and C_m increased, R_{real} remained almost constant, suggesting that the membrane selectivity was preserved during sulfuric acid plant wastewater treatment by NF. The the sharpest increase of the sulfate C_m, in relation to the calcium C_m, was probably due to the positive charge of membrane surface at pH 2 that has an attractive interaction with anions.

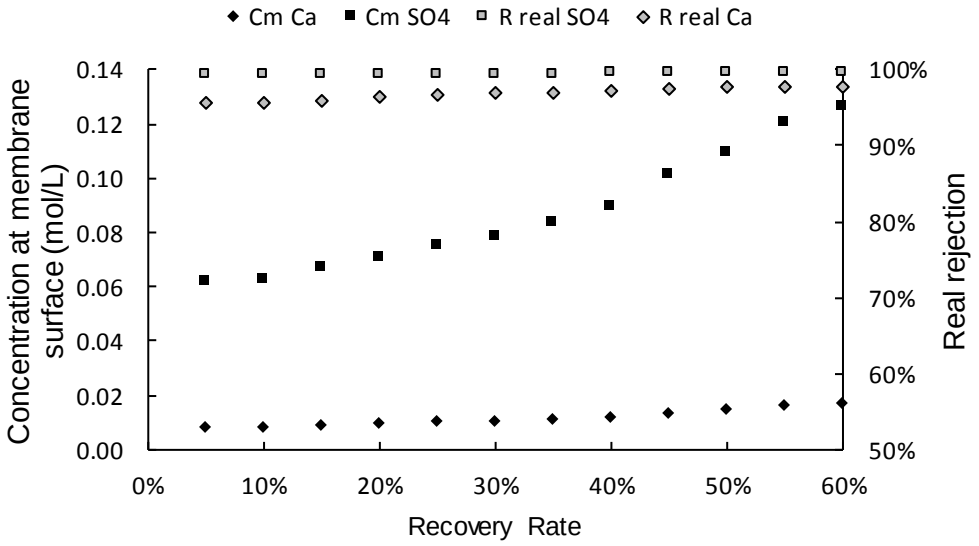

Figure 2.3-5: Membrane concentration (Cm) and real rejection (Rreal) for calcium and sulfate ions in a function of recovery rate.

As concentration polarization causes a difference between salt concentrations at the bulk of the solution (C_f or C_r) and at the membrane surface (C_m), supersaturation degree also needs to be evaluated separately for these two conditions as a function of RR. For this, the product of the molar concentration of calcium and sulfate ions (IP) and the solubility product under operational conditions (K'_{sp}) can be used to calculate $CaSO_4$ supersaturation degree, as shown in equation 15 (RICCI et al., 2015a):

$$S = \left[\frac{IP}{K_{sp}{}'}\right]^{\frac{1}{2}} \quad (15)1$$

The calculation of K'_{sp} is possible using the calcium sulfate solubility product at 25 °C and at ionic strength equal to zero (K_{sp}), and the activity coefficients of the ions calcium ($\gamma_{Ca^{2+}}$) and sulfate ($\gamma_{SO_4{}^{2-}}$), predicted by Davies equation.

$$K'_{sp} = \frac{K_{sp}}{\gamma_{Ca^{2+}}\gamma_{SO_4{}^{2-}}} \quad (16)$$

The calculated supersaturation degrees for $CaSO_4$ in the bulk of the solution (S_b) and at the membrane surface (S_m) for RR rates up to 60% are shown in Table 2.3-4. Supersaturation degree higher than unity (S > 1) indicates that the solution is supersaturated. It can be

observed that the feed solution was already supersaturated (S_b = 1.21) before the test begin (at RR = 0%), which is plausible due to the high concentration of calcium and sulfate ions in the wastewater.

Table 2.3-4: Supersaturation degree in the bulk of the solution (Sb) and at the membrane surface (Sm) at different recovery rates

Recovery Rate	**0%**	**5%**	**10%**	**15%**	**20%**	**25%**	**30%**	**35%**	**40%**	**45%**	**50%**	**55%**	**60%**
Sb	1.21	1.25	1.30	1.35	1.40	1.47	1.54	1.62	1.71	1.82	1.94	2.11	2.30
Sm	-	1.51	1.52	1.59	1.64	1.71	1.87	1.95	2.04	2.40	2.54	2.74	2.97

As can be seen, S_b continuously increase with RR increase due to the increased ionic concentration in the solution. Moreover, because of the concentration polarization phenomenon, S_m was higher than S_b for all RR values.

Because the presence of some minerals in supersaturation in the feed solution can indicates that potential membrane scaling problems can occur, the use of antiscaling is recommended in this situations (BADER, 2007; GABELICH et al., 2007). According to industry guidelines, for $CaSO_4$ an upper operating limit of supersaturation below 2.3 is recommend (HYDRANAUTICS, 2013). As can be seen, S_m reaches the value of 2.3 at about 45% RR. Thus, 45% RR is not only the limit of RR operation in order to obtain a permeate of better quality but also to prevent membrane scaling. For presenting a S_m higher then 2.3, the use of antiscaling could be appropriate if a RR of 45% is adopted as it can increase maximum water recovery and decrease the fouling tendency, extending membrane lifespan.

Besides membrane scaling, RR is highly restricted by osmotic pressure increase as well (BI et al., 2014). As described before, the increase of RR provokes an increase in the ionic concentration of the feed solution and consequently in the osmotic pressure (π_f) and osmotic pressure differential ($\Delta\pi$) as well. Thus, as RR increases continuously, the process effective pressure decreases. Figure 2.3-6 shows the permeate flux (Jf/Jw), process effective pressure ($P - \sigma\Delta\pi$) and fouling resistance (R_f) in a function of RR.

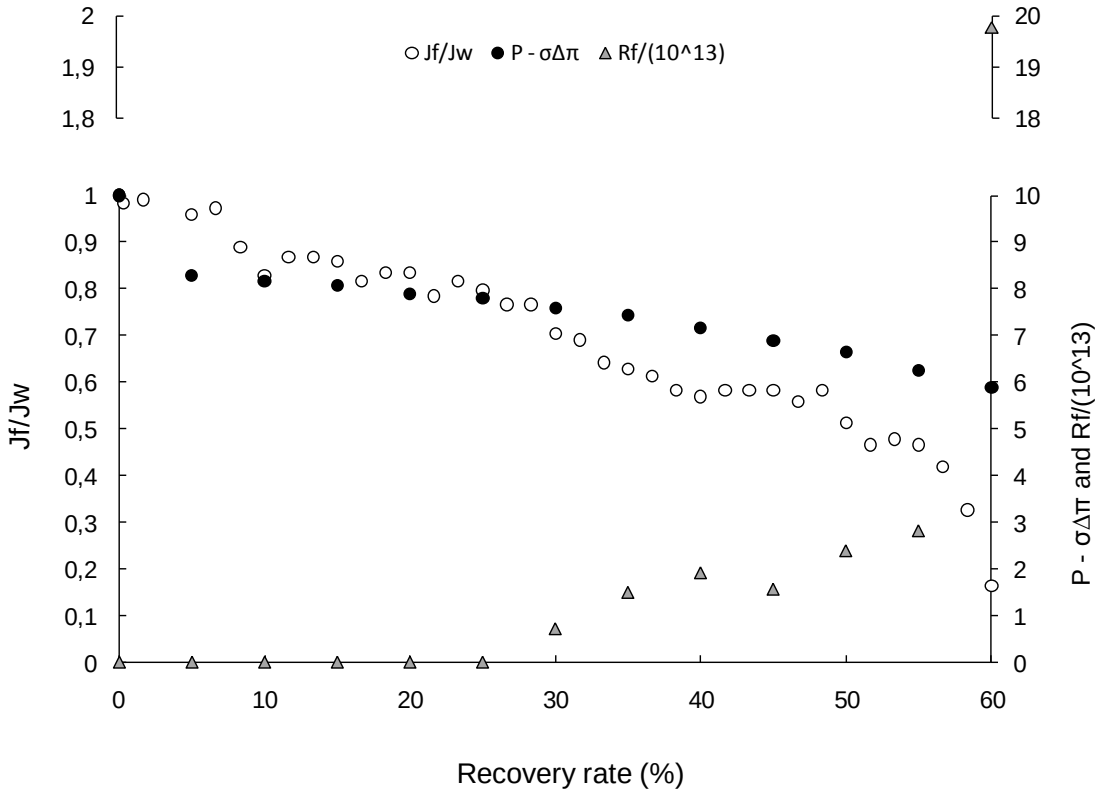

Figure 2.3-6: Effect of the recovery rate in the permeate flux and effective pressure (P= 10 bar; pH= 2; T = 25°C).

As can be observed, as the RR increases a progressive reduction of the permeate flux is obtained. Importantly, the flux increase from 40% to 45% was due to test interruption at 40% for continuing in the next day. The initial normalized permeate flux was 61.5 L/h.m^2, it decreased to 36.1 L h^{-1} m^{-2} at 55% RR, and reached 12.9 L h^{-1} m^{-2} at the end of the experiment (RR = 60%).

It is clear from Figure 2.3-6 that up to 55% RR, the permeate flux decay followed the effective pressure decay, suggesting the absence of severe membrane scaling. On the contrary, after 55% RR a strong decay of the permeate flux can be observed, which was did not follow the effective pressure decay, showing that membrane fouling has to be considered as the decrease in the driving force alone did not explain the variation in permeate flux. The initial normalized permeate flux was 61.5 L h^{-1} m^{-2}, it decreased continuously to 36.1 L h^{-1} m^{-2} at 55% RR, after which a pronounced decay occurred and the permeate flux reached 12.9 L h^{-1} m^{-2} at the end of the experiment, at a RR of 60%.

In conclusion, 45% was the maximum RR obtained for a single NF step in the treatment of sulfuric acid plant wastewater with the NF90 membrane. Above this rate, the permeate flux decay is be more pronounced, membrane fouling can be more severe, which declines the quality of the permeate.

Membrane used in recovery rate test was analyzed in order to check for possible changes in its surface as well as identifying the type of fouled material (Figure 2.3-7). SEM micrographs of membrane surface were obtained from random areas of the samples. The observed contrasts are the result of the topography of the membrane samples. As can be seen in the SEM micrographs of the virgin membrane after chemical cleaning (M1), the morphology is typical of the membrane NF90 already reported by other authors (ANDRADE et al., 2017d; BOUSSU et al., 2006; MONDAL; WICKRAMASINGHE, 2008). It is a dense selective layer membrane, being possible to observe amorphous phase presenting crosslinked morphology as an intermingled. EDS qualitative analysis shows that the chemical elements present were carbon, oxygen and sulfur, characteristic of the polymeric material that the NF90 membrane is made of. Other authors (MONDAL; WICKRAMASINGHE, 2008) has analyzed NF90 membrane by XPS technique and found the same elements and also nitrogen, sodium and chlorine.

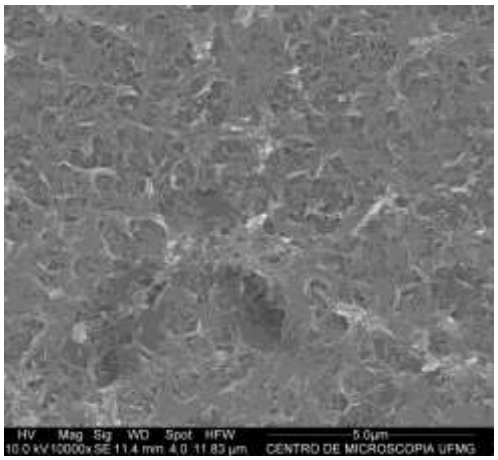

(10000x)

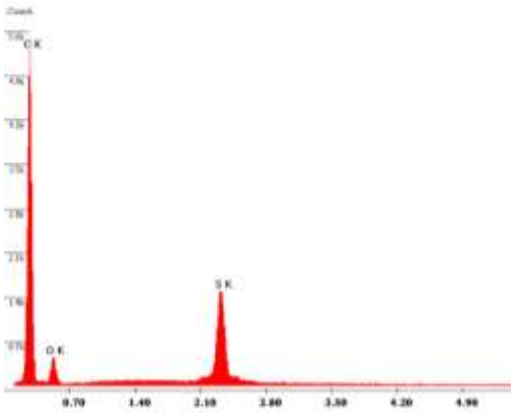

(a)

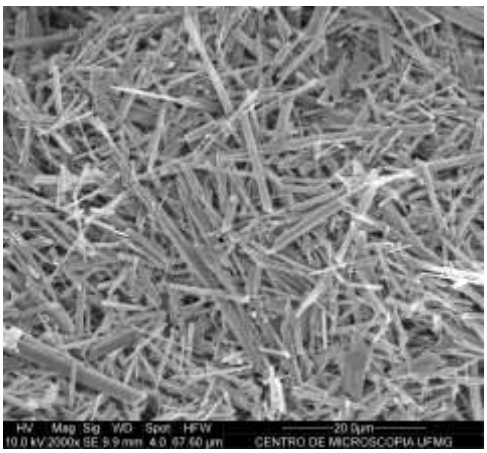

(2000x)

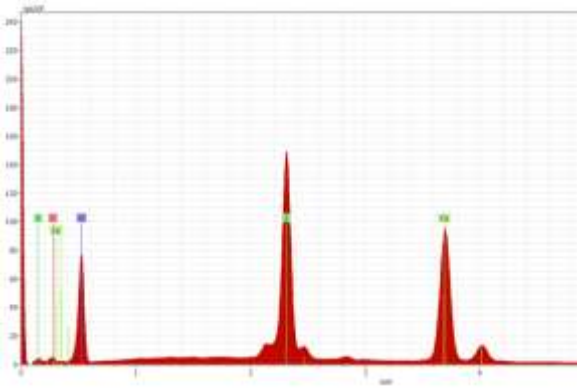

(b)

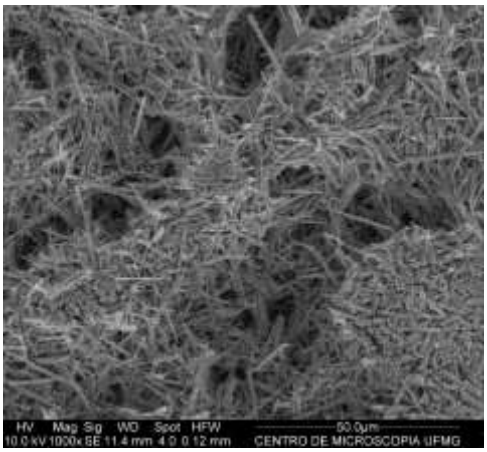

(1000x)

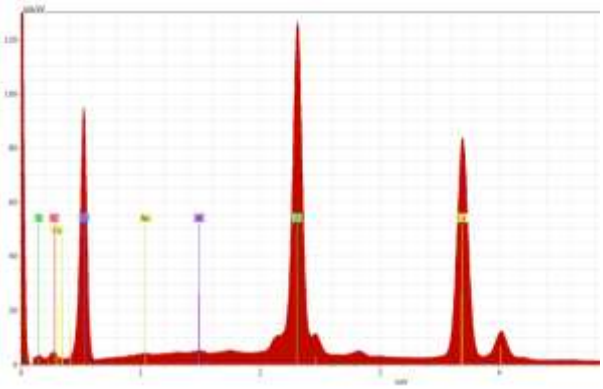

(c)

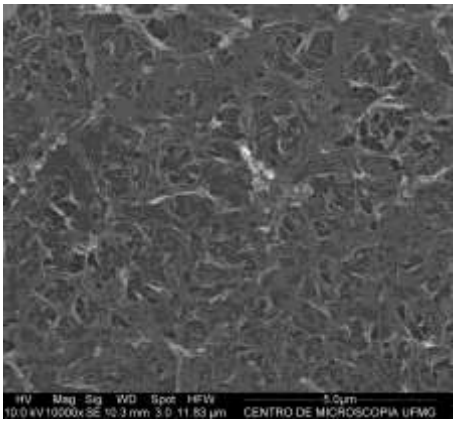

(10000x)

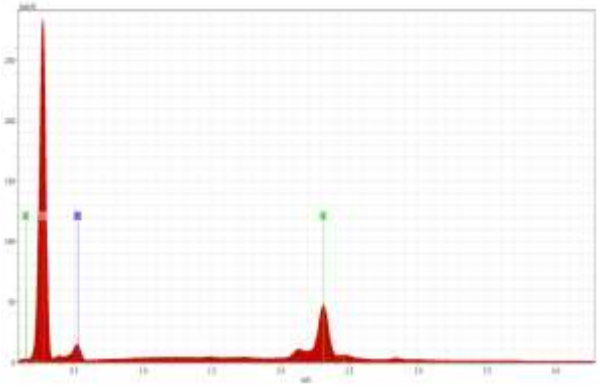

(d)

Figure 2.3-7: SEM micrographs and graphs obtained from the EDS analysis of the surface of (a) M1: virgin NF90 membrane after chemical cleaning; (B) M2: NF90 membrane after 60% RR test; (C) material deposited on the NF90 membrane surface after 60% RR test, removed from the membrane manually; (D) M3: NF90 membrane after 60% RR test and after chemical cleaning.

In the membrane used in the recovery rate test without further chemical cleaning (M2), it can be observed a main crystalline phase, a cluster of crystals covering the entire surface of the membrane. The EDS analysis showed the presence of carbon, sulfur, oxygen and calcium elements. The results indicated the membrane fouling by calcium precipitation. It is important to highlight that the membrane (M2) was removed from the NF cell after the 60% RR, an amount higher than the considered optimal recovery rate. At this recovery rate, the value of S_m for $CaSO_4$ at 60% RR (2.97), much higher than the upper operation limit of supersaturation recommended by industry guidelines (2.3).

The precipitate deposited on the surface of the membrane was removed mechanically and also analyzed in powder form (Figure 8.c). As expected, the observed morphology is very similar to that observed on the membrane surface, however the EDS analysis indicates the presence of carbon, sulfur, oxygen, calcium, aluminum and sodium as well. Comparing to M2 fragment, it is possible to see that the elements present in M2 were also observed in the precipitate (powder), indicating that indeed these elements refer to the crystalline phase deposited on the membrane after the test, not the polymeric material of the membrane.

The micrographs of the membrane after NF test and after further chemical cleaning shows a particular aspect. It is possible to observe that some fragments presented the morphology similar to that of virgin membrane, while others show two distinct phases, one similar to the reticular arrangement of the virgin membrane and another corresponding to some precipitated material (inorganic deposit).

It is known that chemical cleaning, although allowing membrane permeability recovery is not 100% efficient process, since some residual material can remain adhered to the membrane surface. According to the micrographs, there is a resilient material attached to the membrane surface in some regions. Besides, it is important to highlight that the cleaning procedure has not yet been optimized. In this context, it is important to highlight the importance of operating with an optimal RR in order to avoid this irreversible fouling, not removed by chemical cleaning.

The raw wastewater and concentrate and permeate obtained were evaluated with regard to their quality. The following table (Table 2.3-5) shows these samples characterization.

Table 2.3-5: Physicochemical characterization of raw wastewater, permeate and concentrate wastewater (45%RR), concentration factor and removal rate for each parameter

		Raw wastewater	**Concentrate (45% RR)**	*Concentration factor*	**Permeate (45% RR)**	*Removal rate*	Water quality standards for cooling water[a]
pH	-			-		-	6,9 - 9
Conductivity		11500	15500	*1.3*	1871	*84%*	
Sulfate	mg L^{-1}	4814	8465	1.8	354	*94%*	200
Total Aluminum	mg L^{-1}	86.6	156.0	*1.8*	1.8	*98%*	0,1
Total Antimony	mg L^{-1}	< 0.05	< 0.05	-	< 0.05	-	
Total Arsenic	mg L^{-1}	596.0	968.3	1.6	141.0	77%	
As 3	mg L^{-1}	516.9	831.5	1.6	132.5	74%	
As 5	mg L^{-1}	79.1	136.8	1.7	8.5	89%	
Total Barium	mg L^{-1}	< 0.18	< 0.18	-	< 0.18	-	
Total Beryllium	mg L^{-1}	< 0.036	< 0.036	-	< 0.036	-	
Total Boron	mg L^{-1}	< 0.90	1.1	-	0.3	-	
Total Cadmium	mg L^{-1}	0.26	0.7	*2.6*	0.01	*97%*	
Total Calcium	mg L^{-1}	405.5	539.2	*1.3*	9.7	*98%*	50
Total Lead	mg L^{-1}	2.5	3.3	*1.3*	0.3	*89%*	
Total Copper	mg L^{-1}	15.9	25.2	1.6	4.5	*72%*	-[b]
Total Cobalt	mg L^{-1}	1.42	3.0	*2.1*	0.03	*98%*	
Total Chrome	mg L^{-1}	0.13	0.7	*5.1*	0.02	*83%*	
Total Strontium	mg L^{-1}	1.62	3.2	*2.0*	0.05	*97%*	
Total Iron	mg L^{-1}	108.7	237.7	*2.2*	2.6	*98%*	0.5
Total Phosphorus	mg L^{-1}	8.5	15.1	1.8	0.4	*95%*	
Total Lithium	mg L^{-1}	< 0.51	< 0.51	-	< 0.51	-	
Total Magnesium	mg L^{-1}	159.9	287.2	1.8	4.3	*97%*	0.5
Total Manganese	mg L^{-1}	24.8	55.0	*2.2*	0.6	*98%*	
Total Molybdenum	mg L^{-1}	< 0.090	< 0.090	-	< 0.090	-	
Total Nickel	mg L^{-1}	1.4	2.5	1.8	0.1	*95%*	
Total Potassium	mg L^{-1}	40.2	65.4	*1.6*	1.9	*95%*	
Total Silver	mg L^{-1}	0.1	0.1	*1.1*	< 0.005	-	
Total Selenium	mg L^{-1}	< 0.1	< 0.1	-	< 0.1	-	
Total Sodium	mg L^{-1}	38.5	76.7	*2.0*	2.5	*94%*	
Total Titanium	mg L^{-1}	< 0.1	< 0.1	-	< 0.1	-	
Total Uranium	mg L^{-1}	< 0.15	< 0.15	-	< 0.15	-	
Total Vanadium	mg L^{-1}	0.2	0.6	*2.5*	< 0.010	-	
Total Zinc	mg L^{-1}	64.1	111.5	1.7	6.2	*90%*	-[b]

[a]- (Asano et al., 2007); [b]- accepeted as received if other standards have been met.

It is possible to observe that, in general, NF (RR = 45%) presented a high rejection rate for metals, from 72% to 98%, concentrating the elements around 1.6 to 2 times their initial concentration. If the quality of the NF permeate is compared with the required water quality

for industrial heating and cooling systems (ASANO et al., 2007), it is observed that after adjusting the pH the NF permeate would meet practically all the requirements to be reused in low pressure boilers.

The concentrate could be treated by chemical precipitation already used on industry, as now this steam is more concentrated and had its volume reduced to almost half (55%).

2.3.5 Preliminary Investment and Cost Estimate

Regarding the investment and costs associated to the NF system, the total capital cost (CapEx) was estimated at 551,250.00 US dollars. The description of the variables and its associated values are shown in Table 2.3 6. The values obtained in this work are in accordance to other indicated in the literature.

Table 2.3-6: Cost estimation of the NF treatment system for sulfuric acid plant wastewater

	Description	**Values**	**Units**
System Characteristics	Annual System Capacity	1.226.400	$m^3\ year^{-1}$
	Average Permeate Flux	0.025	$m^3\ h^{-1}\ m^{-2}$
	Required NF Membrane Area	2520.00	m^2
	Design Plant Life	15	Years
	Membrane Lifespan	1-5	Years
	Brazil Investment Rate	14%	
	Energy Price	0.04	US$ kWh^{-1}
CapEx	NF System	551,250.00	US$

The total operational cost (OpEx) was estimated for different membrane lifespan values (Table 2.3 7). Results ranged from 0.364 to 0.446 US dollars per cubic meter of wastewater for the highest and lowest membrane lifespan, respectively. Different membrane lifespan values give different costs for membrane replacement.

Table 2.3-7: Opex cost estimation of the NF system for sulfuric acid plant wastewater in a function of membrane lifespan

	Cost (US$) based on membrane Lifespan (years)									
Description	**1**		**2**		**3**		**4**		**5**	
NF Membrane Replacement	0.103	*(23%)*	0.051	*(13%)*	0.034	*(9%)*	0.026	*(7%)*	0.021	*(6%)*
Capital Cost Amortization	0.073	*(16%)*	0.073	*(19%)*	0.073	*(19%)*	0.073	*(20%)*	0.073	*(20%)*
Alkalizing Agent (pH = 7)[a]	0.250	*(56%)*	0.250	*(63%)*	0.250	*(66%)*	0.250	*(68%)*	0.250	*(69%)*
Cleaning Agent	0.001	*(0%)*	0.001	*(0%)*	0.001	*(0%)*	0.001	*(0%)*	0.001	*(0%)*
NF Energy Requirement	0.016	*(4%)*	0.016	*(4%)*	0.016	*(4%)*	0,016	*(4%)*	0,016	*(4%)*
Maintenance	0.004	*(1%)*	0.004	*(1%)*	0.004	*(1%)*	0,004	*(1%)*	0,004	*(1%)*
Total cost (US$)	**0.446**		**0.395**		**0.378**		**0.369**		**0.364**	

[a]- required for permeate pH neutralization depending on the use of the water.

As can be seen, irrespectively of membrane lifespan, the costs with alkalizing agent are the most representative portion within the total OpEx value, due to the high acidy of this wastewater. It is important to highlight that the neutralization of the permeate pH might not be necessary depending on the use of the water. For example, the permeate acid stream may be recirculated to the acid pretreatment stage of ores that precedes the pressure oxidation process. The carbonates and other gangue minerals present in the ore consume acid, causing the inhibition of the pressure oxidation of metal sulfates. In this way, sulfuric acid is used to promote the decomposition of those species. In this case, OpEx would drop to less than half as alkalizing agents represents 56% (1 year) to 69% (5 years lifespan) of the total value.

Following the alkalizing agent, membrane replacement is the second more representative portion (23%) for a lifespan of 1 year, which is expected for a short membrane lifespan, followed by the capital cost amortization (16%). As pointed by Andrade et al. (Andrade et al., 2017a), the current cost of fresh water is US$ 0.18 m^{-3} and for wastewater treatment US$ 1.60 m^{-3}, in the system currently installed the gold mining factory. In this way, since the high quality of the NF permeate, its industrial reuse could reduce the water consumption by approximately 551,880 m^3 per year (considering RR of 45% for NF), which represents savings of more than US$ 99,000 per year.

2.4 CONCLUSION

NF proved to be a suitable technology for the treatment of the sulfuric acid plant wastewater contaminated with arsenic. It allowed the generation of a permeate of sufficient quality for industrial reuse. The best operating conditions observed were the original wastewater feed pH (pH ~ 2), feed temperature of 25^{o}C, transmembrane pressure of 10 bar and recovery rate of 45%, above which the quality of the permeate became much lower.

Regarding the retention mechanisms, for the NF90 membrane and the studied sulfuric acid plant wastewater, the retention of higher valence counterions to balance the retained co-ion loads was the most important, more than the Donnan effect or the retention by size. No drastic changes were observed in the removal of pollutants or in the permeate flux in NF even when the feed pH was close to the membrane IEP.

The main mechanism responsible for the linear decay of the permeate flux with the increase of the recovery rate was the increase of the filtration resistance, caused by the increase of the

concentration of solutes near the surface of the membrane and development of incrustation. Osmotic pressure increasing reduces the driving force for permeation.

Finally, regarding investments and costs, the NF system had an estimated CapEx of 551,250.00 US dollars and OpEx of 0.364 to 0.446 US dollars per cubic meter of wastewater, for 5 to 1 year of membrane lifespan. The industrial reuse of the wastewater would reduce the water consumption by approximately 551,880 m^3 per year. This represents savings of more than US$ 99,000 per year.

Despite of the efficiency of NF on the treatment of the gold mining effluent, it is important to consider that this effluent presents high temperature and as it is treated alone, this temperature is not lowered by any mixture with other wastewater as tested by other authors . As showed in this Chapter, the best temperature for NF treatment was 25^oC. In this way, the high temperature of the feed can be a limitation for NF application. By the other hand, it represents a potential application for processes such as membrane distillation that requires a hot feed to guarantee its performance. Thus, the application of membrane distillation should also be tested for the gold mining effluent treatment.

2.5 ACKNOWLEDGMENTS

The authors thank the Coordination of Improvement of Higher Education Personnel (CAPES), the National Council for Scientific and Technological Development (CNPq) and Foundation for Research Support of Minas Gerais (FAPEMIG) for the scholarships and financial resources provided. We also thank microscopy center of the Federal University of Minas Gerais for AFM and SEM analysis.

CHAPTER 3:

COMPARISON OF NANOFILTRATION (NF) AND DIRECT CONTACT MEMBRANE DISTILLATION (DCMD) AS AN ALTERNATIVE FOR GOLD MINING EFFLUENT RECLAMATION

3.1 INTRODUCTION

Despite of the great economic importance of gold-based ores mining, this activity generates several environmental impacts. The production of contaminated effluents is a drawback that has been intensified because of the lower quality of the available ores, requiring more water for its processing, and mining activity intensification.

The composition of the mining wastewaters is very varied, being dependent of the type of ore/metal mined, local geochemical characteristics, the processes that are used, etc. But in general, regardless of their specificities, mine waters present important constituents such as Al^{3+}, Si^{+4}, Ca^{2+}, Mg^{2+}, Na^{+}, K^{+}, Cl^{-}, CO_3^{2-}, HCO_3^{-} and SO_4^{2-} ions and may also present heavy metals/metalloids such as Hg, Cd, Cr, Hg and As (CHAN; DUDENEY, 2008; LANGSCH et al., 2012). This is an aggravating factor and make mine waters require a proper treatment.

The environmental and legislative pressure that the industry has been suffering in addition to the high costs of water supply and effluents discharge has led to the reuse of effluents which is becoming an environmentally and economically viable option for industries. Mining effluents are promising for reuse, but the presence of metals, especially hazardous ones, and ions such as sulfate (corrosive potential and high fouling potential) represent a barrier to such use and must be removed.

In this context, membrane separation processes such as nanofiltration (NF) and membrane distillation (MD) stand out. Both NF and MD are systems able to retain salts and dissolved molecules, presenting a great application in the treatment of effluents and reuse water generation (ACERO et al., 2010; FU; WANG, 2011; GOODMAN et al., 2013).

The NF has already been applied to remove arsenic and sulfate from contaminated water and synthetic solutions (AHMED et al., 2010; AKBARI; MEHRABADI; TORABIAN, 2010; HARISHA et al., 2010; NGUYEN et al., 2009a; XIA et al., 2007) and also for the treatment of mining effluents (AGUIAR et al., 2016; ANDRADE et al., 2017c, 2017d, 2017b, 2017e; RICCI et al., 2015a; SIERRA; ÁLVAREZ SAIZ; GALLEGO, 2013), showing good results. Despite its removal efficiency, NF membranes are sensitive to high temperatures (FIGOLI et al., 2010), which represents a limitation for the treatment of certain wastewaters, like gas scrubber effluents (60°C). The strategy of reducing the temperature before membrane filtration requires expenditure on cooling (SNOW et al., 1996), making the use of MD a promising alternative.

MD is a process that has an even higher efficiency in the removal of pollutants, being able to concentrate solutions until their saturation without a significant decline of permeate flux (CABASSUD; WIRTH, 2003; DRIOLI; CURCIO; DI PROFIO, 2005; LUO et al., 2014). Direct contact membrane distillation (DMCD) is the most used and operationally simplified configuration, being much used in desalination plants, but also showed good results in acid production/concentration (TOMASZEWSKA; GRYTA; MORAWSKI, 1995) and in the treatment of a mining solution containing sulfuric acid and several metals (KESIEME; ARAL, 2015). Besides this effectiveness and minimum cost of operating capital, this process requires a low heat supply, which can be supplied by industrial residual heat or solar energy, resulting in a low fossil energy requirement (DRIOLI; CURCIO; DI PROFIO, 2005; LUO et al., 2014; MERICQ; LABORIE; CABASSUD, 2011).

Therefore, the objective of this work was to compare the use of NF and DCMD in the treatment of a real gold mining effluent. The processes effectiveness was characterized in terms of permeate flux and rejection of arsenic, sulfate, calcium, and magnesium. Moreover, the fouling behavior of NF and DCMD were assessed and compared. This study is timely and appropriate in light of the technical and economical comparison between two well-known effective technologies for the removal of pollutants and wastewater reclamation in the mining industry. It allows for a better understanding and orientation of decision making in industry exploring a case of a real effluent with its specifications.

3.2 MATERIALS AND METHODS

3.2.1 Gold mining effluent

The effluent used in this study comes from the sulfuric acid production plant of a gold mining company located in the state of Minas Gerais (Brazil). This effluent is generated in the gas scrubber used to remove impurities from the gas generated after the ore, which is rich in sulfur and arsenic, is boiled. The gas is composed mostly of sulfur dioxide, which is processed and used in the manufacture of sulfuric acid.

The effluent generated in the gas scrubber is acid, contains high concentrations of ions such as calcium, magnesium and mainly sulfate, and also presents arsenic contamination, both arsenite [As(III)] and arsenate [As(V)], in high concentrations Table 3.2-1).

Table 3.2-1: Physicochemical characterization of the gold mining effluent

Parameter	Unit	Mean and standard deviation
pH		1.80 ± 0.23
Conductivity	(µS/cm)	12420 ± 1010
Sulfate	(mg/L)	5501 ± 614
Calcium	(mg/L)	444 ± 263
Magnesium	(mg/L)	288 ± 129
Arsenic	(mg/L)	580 ± 94
As (V)	(mg/L)	*88 ± 51*
As (III)	(mg/L)	*440 ± 126*

Before being subjected to NF and MD, the mining effluent underwent previous filtration to remove the suspended solids. Filtration was performed in a vacuum pump using a commercial cellulose filter containing 2.5 µm pores (Whatman® quantitative filter paper, ashless, grade 42). No pH adjustment was performed.

3.2.2 Experimental setup

NF assays were performed on a laboratory scale in the filtration unit shown in Figure 3.2-1. It consisted of a feed tank, followed by a rotary-vane pump, which is connected to a speed controller, a rotameter and a stainless steel membrane module for a flat sheet membrane. After the cell, there is a manometer, thermometer and between those, a needle valve for pressure adjustment. Before being recirculated to the feed tank, the concentrate passed through a chiller in order to maintain the effluent at the temperature of the test (25°C).

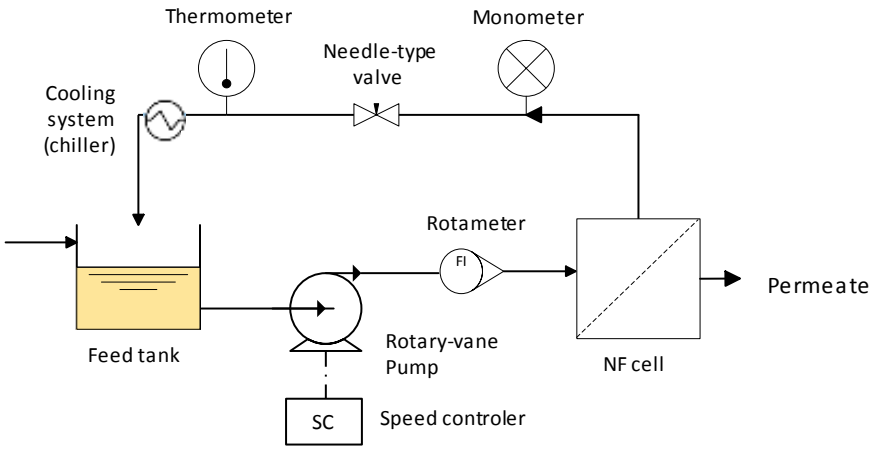

Figure 3.2-1: Schematic diagram of the NF system

In the stainless steel cell, a new 9 cm diameter flat membrane (0.0064 m^2 filtration area) was placed along with a 28 mil (25.4 µm) feed spacer at the top to ensure flow distribution. The membrane used was polyamide NF90 membrane (Dow Filmtech) with a molecular weight cut-off between 100-200 Da (DOLAR et al., 2011). The measurement of the permeate flux was done by collecting the volume of permeate in a measuring cylinder over a period of 60 seconds.

MD assays were also performed on a laboratory scale in the filtration unit shown in Figure 3.2-2. MD module is composed of two compartments between which the membrane was disposed. In one of the compartments, the effluent was circulated and in the other, cooled water. The feed tank is followed by a thermometer, a peristaltic pump, and a rotameter before the membrane module. Before being recirculated to the feed tank, the concentrate passed through a heating system in order to maintain the effluent at the temperature of the test (60^oC). The cold water reservoir (distillate tank) is placed on a digital balance and it is also followed by a thermometer, peristaltic pump, and a rotameter before the membrane module. The distillate passes through a cooling system (chiller) before being recirculated to the distillate tank.

The temperature differential is needed so that the permeate flux can be established. This flux was measured using the data collected in the digital balance as the increase in the distillate mass is provided by permeate production.

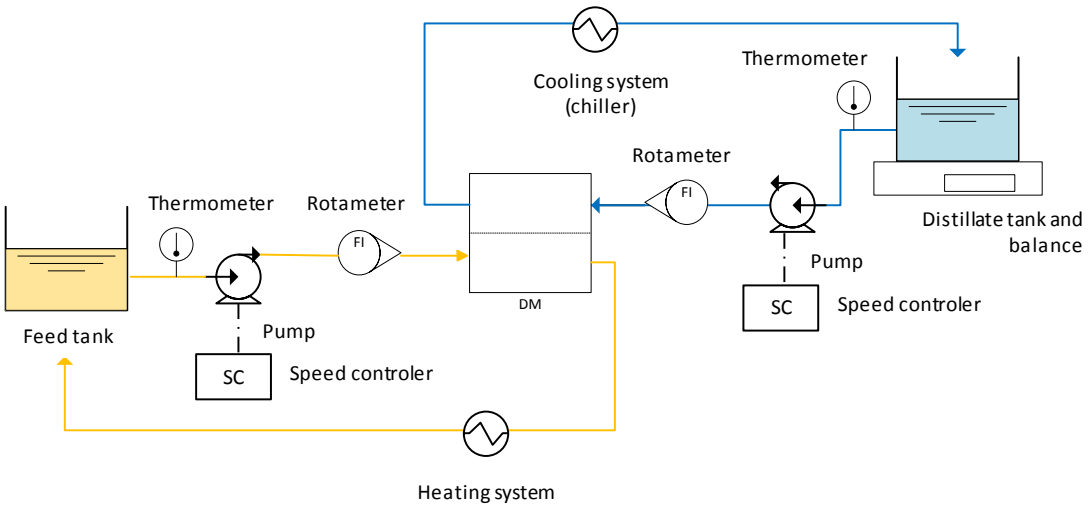

Figure 3.2-2: Schematic diagram of the MD system

For the membrane cell, a Sterlitech® (CF042D Crossflow Cell) cell was used, in which was positioned a new Sterlitech® PTFE microfiltration membrane. This membrane has an average pore size of 0.2 µm, liquid entry pressure <14.5 psi and for the experiment, the filtration area was 0.0042 m^2.

3.2.3 Experimental procedure

Before the tests, the membranes passed through a cleaning procedure in which they were submerged in a hydrochloric acid (HCl) 0.2% w/w solution for 20 minutes and then washed with distillate water. After chemical cleaning, water permeability was measured.

Before the systems were applied using the real effluent, distilled water was used as feed in both NF and DCMD systems and permeation occurred until reaching a steady permeate flux.

NF and DCMD tests were performed using real mining effluent and adopting the following operational conditions: feed velocities were maintained at 1.9 m/s (Re = 839) and 0.1 m/s (Re = 581) for NF and DCMD respectively. In NF, the applied transmembrane pressure was 10 bar and the temperature was maintained at 25±2^{o}C. Tests were performed in batch mode with recirculation of the concentrate. In DCMD, temperatures were maintained at 60^{o}C for the feed and 20^{o}C for the distillate. Both NF and DCMD were performed for at least the recovery rate of 45%. The permeate flux and conductivity were continuously measured and permeate samples were taken out at different times for physicochemical analysis.

3.2.4 Analytical Methods

The mining effluent and permeates were characterized in terms of the following physicochemical parameters: pH (pHmeter Qualxtron QX 1500); conductivity (Hanna conductivity meter HI 9835); calcium and magnesium cations (Dionex ICS-1000 ion chromatograph equipped with AS-22 and ICS 12-A columns); total arsenic, As (III) and As (V) (DHAR et al.; 2004); and total dissolved solids, sulfate and chloride (APHA, 2017).

3.2.5 Calculations

The NF permeate flux [$J_{P(NF)}$] can be calculated by Equation (1):

$$J_{P(NF)} = \frac{\Delta V_p}{A_m . \Delta t} \quad (1)$$

where ΔV_p is the volume of permeate collected, Δt is the collection time, and A_m is the effective membrane area. The permeate recovery ratio (RR_{NF}) can be defined by Equation (2):

$$RR_{NF} = \frac{V_p}{V_f} . 100 \quad (2)$$

where V_p corresponds to the accumulated volume of permeate and V_f to the initial volume of the feed.

The rejection [R(%)] of pollutants and conductivity was calculated using Equation 3, considering the conductivity/pollutant concentration of the feed (C_f) and permeate (C_p) streams.

$$R(\%) = \frac{C_f - C_p}{C_f} . 100 \quad (3)$$

In the DCMD system, the permeate flux [$J_{P(MD)}$] is calculated according to Equation (4):

$$J_{P(MD)} = \frac{m_{di} - m_{df}}{A_m . (t_i - t_f)} \quad (4)$$

Where m_{di} and m_{df} correspond to the mass (kg) of the initial and final distillate, respectively. A_m is the area of the membrane (in m^2), t_i and t_f correspond to the initial and final time, respectively.

The recovery rate [RR_{MD}] is calculated by Equation (5):

$$RR_{MD} = \frac{m_{df} - m_{di}}{m_{fi}} . 100 \quad (5)$$

Where m_{fi} corresponds to the mass (kg) of the initial feed.

It is important to note that since the DCMD process is initiated with a determined volume of cold water and over time the permeate volume that is produced is added to the initial water volume, the calculation of the concentration of a species in the permeate is made from Equation (6):

$$c_{p(MD)} = \frac{c_d . v_{td,y}}{v_{p,y}} . 100 \quad (6)$$

Where $c_{p(MD)}$ and c_d the concentration of the species in the permeate and the distillate, respectively. The $v_{td,y}$ is the total volume of distillate in time y and $v_{p,y}$ is the volume of permeate at the same time (y).

The rejection $[R(\%)]$ of a species is calculated on the basis of its concentration in the permeate, not the distillate.

The differences in osmotic pressure ($\Delta\pi$) between the concentrates and permeates of both NF and DCMD for different permeate recovery rates were estimated by the Equation of Van't Hoff, described in Equation (7).

$$\Delta\pi = RT\Delta\Sigma(C_c - C_p) \quad (7)$$

For this, it is used the universal gas constant (R), temperature of permeation (T) and the sum of the difference of the molar concentration of the main dissolved species that are present in the concentrate (C_c) and permeate (C_p) at each RR. In this study, data of pH and concentration of sulfate, calcium and magnesium were used to calculate the osmotic pressure.

Membrane resistance (R_m), feed boundary layer resistance (R_{fb}) and permeate boundary layer resistance (R_{pb}) were calculated as shown by Equations (8), (9) and (10) (SRISURICHAN; JIRARATANANON; FANE, 2006).

$$R_m = \frac{P_1 - P_2}{J_{p(MD)}} \quad (8)$$

$$R_{fb} = \frac{P_f - P_1}{J_{p(MD)}} \quad (9)$$

$$R_{pb} = \frac{P_2 - P_p}{J_{p(MD)}} \quad (10)$$

Those calculations were made considering values of vapor pressure at the feed (P_1) and permeate (P_2) membrane surface and at the bulk feed (P_f) and permeate (P_p), and $J_{p(MD)}$, the permeate flux.

Equation 11 was used to calculate the pressures and Equation 12 and 13 to estimate the temperatures at the membrane surface (SRISURICHAN; JIRARATANANON; FANE, 2006).

$$P = EXP\left(23.238 - \frac{3841}{T-45}\right) \tag{11}$$

$$T_{w,f} = \frac{h_m\left(T_p + \left(\frac{h_f}{h_p}\right)T_f\right) + h_f T_f - J_{p(MD)}\Delta H_v}{h_m + h_f(1 + \frac{h_m}{h_p})} \tag{12}$$

$$T_{w,p} = \frac{h_m\left(T_f + \left(\frac{h_p}{h_f}\right)T_p\right) + h_p T_p - J_{p(MD)}\Delta H_v}{h_m + h_p(1 + \frac{h_m}{h_f})} \tag{13}$$

Where $T_{w,f}$ and $T_{w,p}$ are the temperatures at interface for feed and permeate, respectively, calculated from the temperatures at the bulk for feed (T_f) and permeate (T_p), the convective heat transfer coefficient of the membrane (h_m), feed (h_f) and permeate (h_p), the vaporization heat (ΔH_v) and permeate flux ($J_{p(MD)}$).

As a mean to elucidate the fouling phenomenon Hermia's model was used (BENÍTEZ; ACERO; LEAL, 2006; CHANG et al., 2011; KAYA et al., 2010; MOHAMMADI; ESMAEELIFAR, 2005; SRISURICHAN; JIRARATANANON; FANE, 2006). Experimental data were tested for four different filtration models (Complete blocking filtration, Standard blocking filtration, Intermediate blocking filtration and Cake filtration) and their respective equations (Table 3.2-2). Graphs of the flux at a certain time (J) in a function of time were plotted. A coefficient depending on the flow rate and solution properties (k) (SHIM et al., 2015) was obtained by the slope of each curve and the equations of the models were used to calculate the regression coefficient (R^2) and the original permeate flux (J_0) (KAYA et al., 2010).

Table 3.2-2: Filtration models, their equations, and type of graphs plotted

Filtration Models	Equation	Graphs
Complete blocking filtration	$\ln(J^{-1}) - \ln(J_0)^{-1} + k.t$	$\ln(J^{-1})\ x\ time$
Standard blocking filtration	$J^{-\frac{1}{2}} - {J_0}^{-\frac{1}{2}} + k.t$	$J^{-\frac{1}{2}}\ x\ time$
Intermediate blocking filtration	$J^{-1} - {J_0}^{-1} + k.t$	$J^{-1}\ x\ time$
Cake filtration	$J^{-2} - {J_0}^{-2} + k.t$	$J^{-2}\ x\ time$

Energy consumption for the DCMD system is estimated both for heat/cooling energy and for circulation of the streams. Thermic energy (E_T) was estimated according to (QTAISHAT; BANAT, 2013) (Equation 14).

$$E_T = m_f . c_f . (T_{f,in} - T_{f,out}) \quad (14)$$

Where m_f is the feed flow rate, c_f is the specific heat of the feed, T_f is the temperature of the feed in ($T_{f,in}$) and out ($T_{f,out}$) of the module.

Thermal efficiency (ε_T) (Equation 15) can be calculated by the relation between permeate flux, membrane area and water evaporation enthalpy ($\Delta H_{v,w}$) and thermic energy (KHAYET, 2013).

$$\varepsilon_T = \frac{J_{p(MD)} . A_m . \Delta H_{v,w}}{E_T} \quad (15)$$

In the MD system, electric energy (E_E) can be calculated by equation (16):

$$E_E = \frac{m_f . \Delta P}{\eta} \quad (16)$$

Where m_f is the feed flow rate, ΔP is the pressure experienced by the membrane and η is the efficiency of the pump, which was considered equal to 0.95. ΔP was considered equal to 10 bar for the NF system and 0.0001752 for MD system (experimental data).

The efficiency of the MD system (ε_E), also known as gain output ratio (GOR), can also be calculated considering all the energy input in the system (both thermal and electric energy). as shown by equation (17) (KHAYET, 2013):

$$\varepsilon_E = GOR = \frac{J_{p(MD)}.A_m.\Delta H_{v,w}}{E_T + E_E} \quad (17)$$

3.2.6 Preliminary economic evaluation

A preliminary economic evaluation was performed for both NF and DCMD system to estimate their capital and operational expenses (Capex and Opex). All calculations were made considering the real feed flow rate (140 m^3/h), one filtration stage and the permeate flux relative to the optimized RR of each system.

For the NF, the membrane unit capital cost was based on a price provided by a major supplier of commercial membranes in Brazil, of 8750.00 U$/$m^3$/h of effluent (AGUIAR et al., 2016). To this value was added the cost of a heat exchanger as the effluent must be cooled before entering the NF system. The heat exchanger cost was calculated according to HITSOV et al. (2018).

For the DCMD, the Capex was calculated as shown by HITSOV et al. (2018), considering a membrane area of 24 m^2 per module and using the DCMD system capacity required.

The capital cost (C_{cap}) was calculated per cubic meter of effluent ($C_{cap/m3}$), from Equation 18:

$$C_{cap/m3} = \frac{C_{cap}.AF}{Q_{sys}} \quad (18)$$

Where Q_{sys} is the capacity of the designed system and AF is the amortization factor. AF is calculated by annualizing the capital cost, as shown in Equation 19 (SETHI; WIESNER, 2000):

$$\mathrm{AF} = \frac{i_c \cdot (1+i_c)^{DL}}{(1+i_c)^{DL} - 1} \quad (19)$$

Where i_c is the investment rate (equal to 14% in 2018 in Brazil) and DL is the design life of the plant, which was considered to be 15 years for both NF and MD systems.

To calculate Opex the variables alkalizing agent, capital cost amortization, membrane replacement, cleaning agent, energy requirement, and maintenance were considered for both NF and DCMD system. The alkalizing agent cost (NaOH) was calculated based on the

volume of NaOH solution used to adjust the pH of the NF and DCMD permeate to pH = 7.0. It was considered a price of 425.00 US$/ton of NaOH.

Maintenance costs were estimated at 5% per year of the initial investment cost (SHEN et al., 2014) for both of the systems. Due to the acidic nature of the studied effluent, membrane replacement was calculated considering a membrane lifespan of 1, 2,3, 4 and 5 years. NF and MD membrane costs were considered as 50 US$/$m^2$, price provided by a large commercial membrane supplier in Brazil) and 60 US$/$m^2$ (HITSOV et al., 2018), respectively.

To calculate the costs with cleaning agents, a cleaning frequency of once a week (4 times a month) with HCl was assumed. The approximate price of the HCl (37%) was 7.10 US$/L of HCl.

Energy requirement calculation was explained in the previous session for each system (NF and DCMD). Energy requirement cost was estimated considering the energy tariff currently paid by the mining company in Brazil, which is 0.04 US$/kW h (considering an exchange rate of US$1 = R$0.25).

3.3 RESULTS AND DISCUSSION

3.3.1 Changes in permeate flux and fouling

NF and DCMD were operated at typical temperatures (25 and 60°C, respectively) and pressure (10 bar for NF membrane) and fed with gold mining effluent. Figure 3.3-1 shows the normalized permeate flux (J_f/J_i) and feed osmotic pressure obtained throughout the NF and DCMD test up to permeate recovery rate of 45%. The initial flux values were 30.8 and 29.9 L $m^{-2}h^{-1}$ for NF and DCMD, respectively.

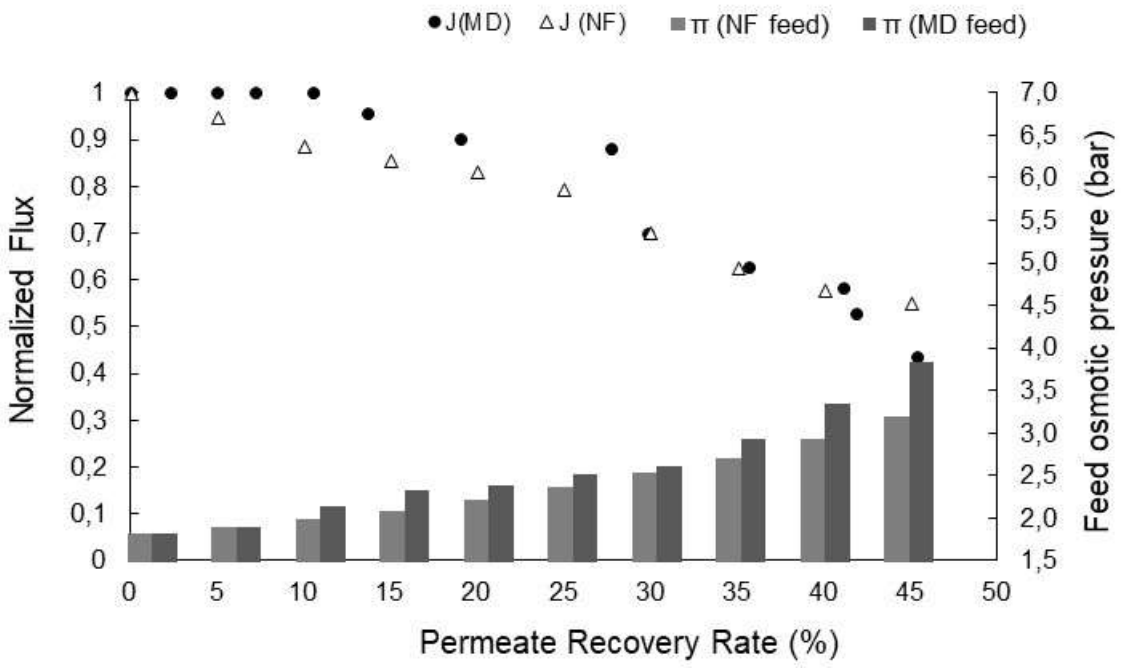

Figure 3:

Figure 3.3-1:Normalized permeate flux and feed osmotic pressure for NF and DCMD processes in a function of recovery rate.

NF exhibited a more pronounced initial flux decline compared to DCMD. For DCMD no flux decline was observed up to the permeate recovery rate of 10%. The delay in the onset of DCMD fouling may relate to the fact that DCMD is a non-pressure oriented process. The pressure in NF may decrease flux due to the higher solute flow through the membrane and compaction of the concentration boundary layer. Nevertheless, the flux values became similar for NF and DCMD when the permeate recovery rate exceeds 30%. The concentration polarization influences the performance of both processes reducing the driving force. In NF processes, concentration polarization increases the osmotic pressure at the membrane surface, thereby decreasing the driving force for mass transport. In DCMD, concentration polarization decreases the partial vapor pressure of water at the feed–membrane interface, thereby only slightly reducing the driving force for evaporation. Due to the high ion rejection in both processes, the feed solutions became more concentrated (Figure 3.3-1) and supersaturated as the experiment progressed, causing the precipitation of the soluble salts. This effect is more intense for DCMD because contaminants practically cannot be transported through the membrane. It can also be observed from Figure 3.3-1 that for permeate recovery rate of 45% the DCMD permeate flux decreased abruptly. Disparities in the flux decline rate between NF and DCMD can be attributed to differences in operating temperature and fouling mechanisms.

Regarding the composition of the feed solution, calcium sulfate ($CaSO_4$) is the most likely scalant (ANDRADE et al., 2017d). The form precipitated depends strongly on temperature. At 25°C, which is the operating temperature of NF, gypsum form is predominant (ANTONY et al., 2011; GRYTA, 2009), while at 60°C DCMD feed temperature, the anhydrite form is more common. Calcium sulfate solubility peak is around 40 °C (GRYTA, 2009), however, at typical DCMD feed temperature, it does not vary strongly. Furthermore, increasing temperature decreases the $CaSO_4$ nucleation induction time at a given saturation index (DUONG et al., 2016; NGHIEM; CATH, 2011), thus accelerating scaling and consequently reducing the maximum calcium sulfate concentration that DCMD can tolerate without scaling, compared to NF operated at 25ºC. The concentration of the calcium (Ca^{+2}) and sulfate (SO_4^{-2}) ions and the degree of saturation of the $CaSO_4$ salt were calculated in both the bulk of the solution (S_b) and on the surface of the membrane (S_m) as showed by (RICCI et al., 2015a). Results are shown in Figure 3.3-2.

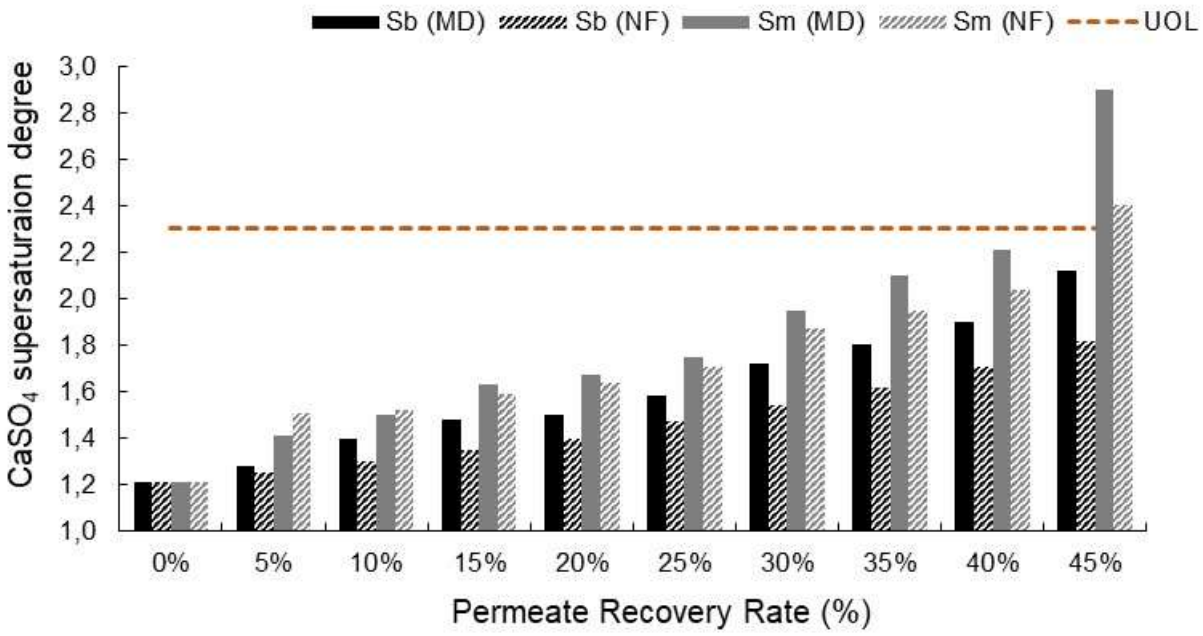

Figure 3.3-2: $CaSO_4$ supersaturation degree in the bulk (S_b) and at the membrane surface (S_m) for NF and DCMD processes in a function of recovery rate, with recommended upper operational limit (UOL) (HYDRANAUTICS, 2013).

As can be observed, the real gold mining effluent already presents a supersaturation degree S_b higher than 1, indicating the precipitation of $CaSO_4$ can happen spontaneously in this condition. With time, for both NF and DCMD, S_b and S_m increase as permeate recovery rate is increased, favoring, even more, the precipitation of this salt. The upper operational limit (UOL) suggested for $CaSO_4$ supersaturation degree is 2.3 (HYDRANAUTICS, 2013), after

which the use of anti scaling is recommended. In a general view, $CaSO_4$ supersaturation degree was higher for DCMD than for NF, which can be explained by the higher rejection of calcium and sulfate ions by DCMD. In the initial stage (permeate recover rate up to 10%) the S_m of NF was higher than that for DCMD corroborating the greater flux decline observed for NF compared to DCMD in this stage. Furthermore, the S_b and S_m value for DCMD at permeate recovery rate of 45% were above the recommended UOL value justifying the greater MD flux decline observed at this permeate recovery rate. In the DCMD the evaporating interface is in direct contact with the membrane pore allowing the occurrence of scaling at the pore entrance and consequently the inhibition of vapor flow through the membrane. The precipitation of $CaSO_4$ was already reported for MD systems. KESIEME; ARAL (2015) tested MD for treating an acid solution containing Al, Co, Cu, Ca, Fe, Mg, Mn, and Ni. The precipitation of $CaSO_4$ during MD was reported by those authors. To avoid this precipitation to occur in the surface of the MD membrane, a filter was installed in the feed line, allowing $CaSO_4$ to precipitate before entering the membrane cell.

In NF process, the total filtration resistance is composed of the resistance of membrane (R_m) and fouling resistance (R_f), while in the DCMD process there are still contributions of the resistance in feed boundary layer (R_{fb}) and resistance in permeate boundary layer (R_{pb}). The transport resistances were calculated for NF and DCMD processes and results are shown in Figure 3.3-3 (a) and (b) respectively. In the DCMD process, the transport resistance in the feed boundary layer played an important role corresponding to 41±3 % of the total filtration resistance. It can also be seen that fouling resistance was stable up to permeate recovery rate of 28% (R_f/R_t = 0.20 ± 0.03 %) and after that, it increased more rapidly. The increase of the fouling resistance can be related to $CaSO_4$ precipitation due to the severe S_b and S_m increase observed when permeate recovery rate exceeds 28% (Figure 3.3-2). At permeate recovery rate of 45%, the fouling resistance contribute to 39% of the total resistance, while for NF the fouling resistance contributes to 68% of the total resistance. These results suggest that although the permeate flux decline profiles are similar for DCMD and NF, the fouling potential in DCMD is lower, which brings practical benefits to the DCMD in relation to permeability recovery through cleaning. However, the membrane fouling in the DCMD process also affects mass transfer from the bulk feed stream to the membrane surface, since the R_{fb} resistance increased when permeate recovery rate exceeds 28%. The cake layer acts

reducing the heat transfer in the system due to the additional heat transfer resistance induced by this layer.

(a)

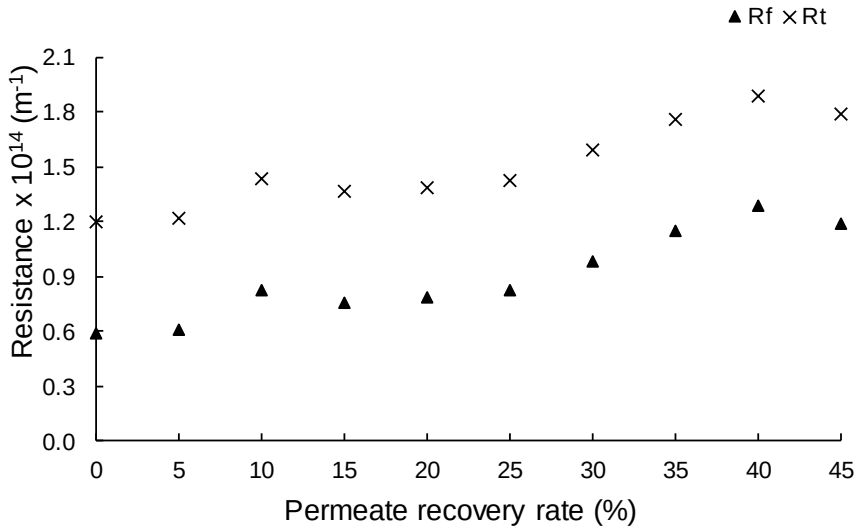

(b)

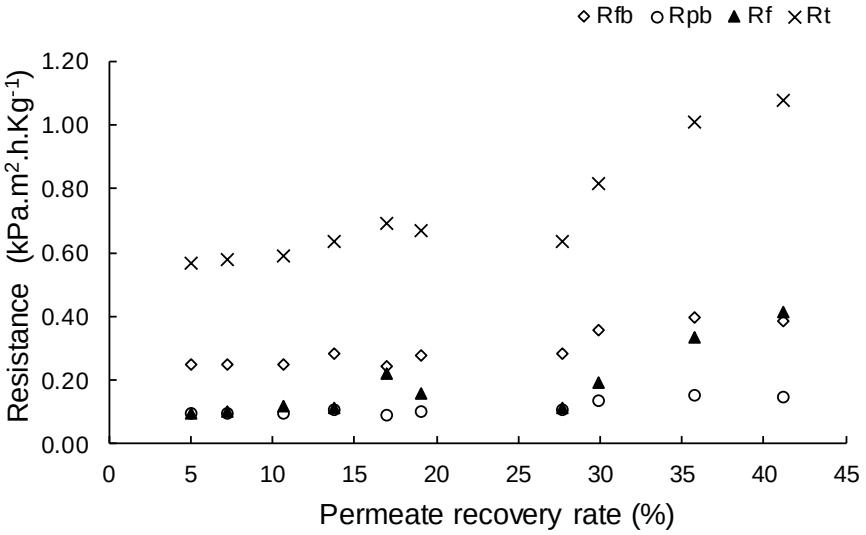

Figure 3.3-3: Resistance calculated for (a) NF and (b) DCMD systems. R_{fb}: feed boundary layer resistance; R_{pb}: permeate boundary layer resistance; R_f: Fouling resistance; R_t: Total resistance

To investigate the possible fouling mechanisms, Hermia's mathematical model was used for DCMD and NF membranes. Table 3.3-1 shows fitted parameters of Hermia's model and comparison between the experimentally measured permeate flux and the flux predicted.

Table 3.3-1: Evaluation of fouling mechanisms using Hermia's model for NF and DCMD processes treating a real gold mining effluent.

Model		NF	DCMD
Complete blocking filtration	J_o (L $m^{-2}h^{-1}$)	31.9	34.21
	k	0.07	0.077
	R^2	0.96	0.95
Standard blocking filtration	J_o (L $m^{-2}h^{-1}$)	32.4	35.79
	k	0.007	0.008
	R^2	0.94	0.93
Intermediate blocking filtration	J_o (L $m^{-2}h^{-1}$)	33.2	38.4
	k	0.003	0.004
	R^2	0.93	0.90
Cake filtration	J_o (L $m^{-2}h^{-1}$)	35.9	59
	k	0.0003	0.0003
	R^2	0.90	0.83

According to Hermia's model, for both technologies, the fouling mechanism that better explain the flux decline values obtained was the complete blocking filtration model, suggesting that for both processes the $CaSO_4$ crystals particles are larger than the pore size of the membrane sealing off the membrane and promoting the flux decline.

3.3.2 Permeate quality and water reuse

The salt rejection for DCMD and NF membrane was determined based on permeate conductivity. Figure 3.3-4 shows the rejection and permeate conductivity for both processes as a function of permeate recovery rate.

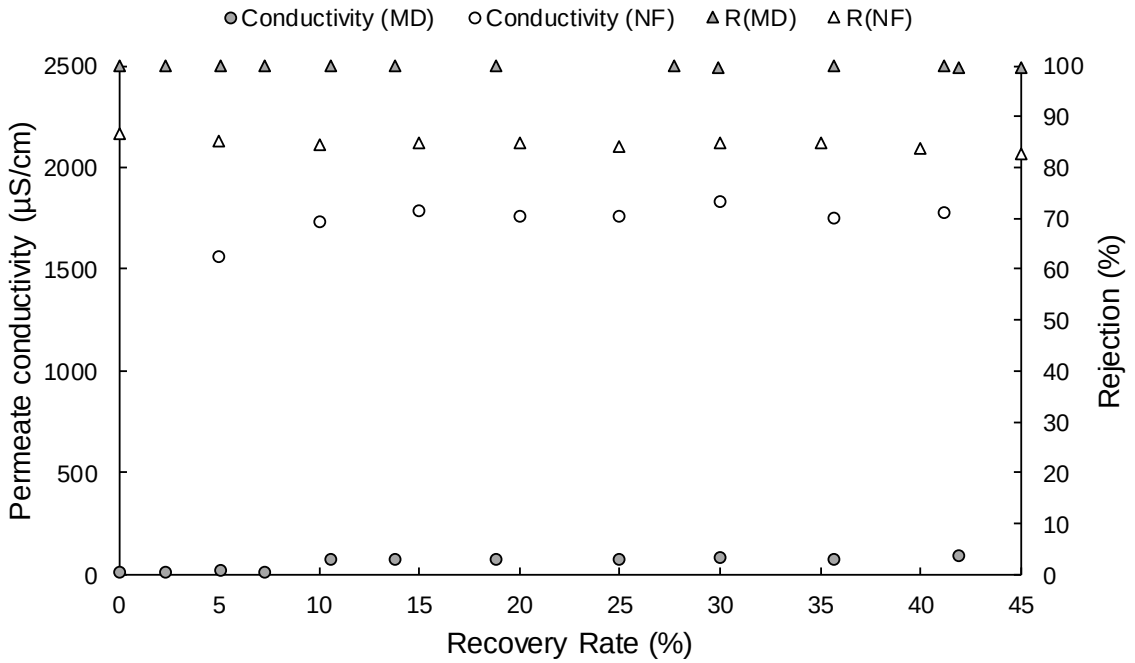

Figure 3.3-4: Rejection and permeate conductivity in a function of permeate recovery rate for NF and DCMD processes

As can be observed, in terms of conductivity, both processes presented high rejection rates. For NF, a rejection of 86% was observed at the beginning of the test, reaching 81% at a permeate recovery rate of 45%. This result is quite satisfactory, especially considering the composition of the effluent, rich in ions and acid. The DCMD, in turn, showed rejection above 99% throughout the test, demonstrating efficiency and robustness of the system in the removal of pollutants. Because it only allows the passage of vapor, the DCMD presents a theoretical rejection of 100%. However, when observing the conductivity of the permeate as a function of permeate recovery rate, it is possible to observe that there is a passage of solute to the distillate when permeate recovery rate exceeds 10%, indicating membrane wetting. In this work it was considered a lower limit of 20 µS/cm for the permeate conductivity, a reference already adopted by other authors (KESIEME; ARAL, 2015). Wetting was considered to occur when permeate showed conductivity higher than 20 µS/cm.

As membrane wetting was observed, wetting time and wetting rate were calculated. The wetting time is the time from which wetting of the membrane is observed and the wetting rate is given as a slope of the permeate conductivity as a function of time. By mass balance, the wetting rate can still be converted into salt permeate content (GUILLEN-BURRIEZA et al., 2016). The wetting time was estimated between 1.6 and 2 hours. The wetting time results reported in the literature are very relative, as it is reported since wetting times from the very

beginning of the test to days after the experiment began (GUILLEN-BURRIEZA et al., 2016). GUILLEN-BURRIEZA et al. (2016) performed several DCMD tests designed to prevent and understand the wetting phenomena (wetting processes related to scaling and Liquid Entry Pressure (LEP)). The authors found that in general, two factors can contribute to longer the wetting time: (a) high-temperature difference between feed and permeate; (b) low feed flow rate. In this situation, wetting time could take days to occur.

The result found in this work are in some extent against the general rule. Although the temperature difference and flux were high, and the feed flow rate was low, wetting time took less than 2 hours to occur. This result indicates that the wetting experienced by the membrane when treating gold mining effluent can be more related to scaling, as no pressure was applied in the system that could surpass the LEP of the membrane.

The wetting rate was 0.19 (slope of the curve) and it was calculated in terms of salt content giving a result of 0.10 mg salt per minute, or 6.25 mg/h. This value is higher than those found by (GUILLEN-BURRIEZA et al., 2016) and can be related to the wetting most probable cause: scaling. With scaling the membrane could have experienced faster wetting time and higher wetting rate.

Table 3.3-2 shows the physicochemical characterization of the raw effluent and the concentrate and permeate of both NF and DCMD processes. As can be seen, both NF and DCMD showed high ions rejection, but it is worth noting the better performance of DCMD compared to NF. DCMD produced better quality permeate with potential for reuse. Although it is expected 100% of contaminant retention in DCMD, the solute passage through the membrane confirms the membrane wetting. As previously mentioned, sulfate is one of the main ions that might have accumulated and precipitated on the membrane surface and it is present in high concentration in the effluent. Thus, the high concentration of this ion increases its diffusion capacity, causing it to pass through the membrane in greater quantity than other solutes. Arsenic species were efficiently removed by DCMD with 99% rejection. This is possible because the membrane rejection is independent of its charge, different from what happens in NF. These results corroborate with others found in the literature. By using DCMD in arsenic-containing water treatment, QU et al. (2009) were able to reduce the concentration of both arsenite and arsenate in an aqueous synthetic solution of arsenic to the maximum limit of the contaminant in water (10 μg/L). When treated by DCMD, the effluent concentrate retains almost all arsenic present and allows more possibilities of reuse for the permeate

produced since the consequent health and environmental risks presented by this metalloid were significantly reduced.

For NF, the high rejection of magnesium (Mg^{+2}) and calcium (Ca^{+2}) can be explained by the positive charge shown by the NF90 membrane at the effluent pH (1.95), causing repulsion of the ions of the same charge. Although sulfate ion has a negative charge (-2), this ion presents a relatively large ion radius and is retained by the NF membrane by size rejection but mainly to guarantee the electroneutrality of the feed, where Mg^{+2} and Ca^{+2} are retained, among others. Arsenic was the contaminant that presented the lowest removal rate by NF, because of its charge. Arsenate [As (V)] was removed in a higher rate than arsenite [As (III)], since, in aqueous matrices and effluent pH (1.95), the As (III) is present as H_3AsO_3, having a neutral charge, whereas As (V) is present in the negatively charged $H_2AsO_4^-$ form. Thus, As (V) is rejected not only by size but also by electrostatic repulsion. The As (III), on the other hand, has its diffusion proportional to its concentration (SEIDEL; WAYPA; ELIMELECH, 2001), moving more freely through the membrane.

Comparing the permeate characteristics with the water quality requirements for cooling systems and boilers (Table 3.3-2), it is observed that after pH adjustment the DCMD permeate quality is enough to fit all of the water quality standards for cooling systems and boilers. The NF permeate does not present sufficient quality to be reused in cooling systems or boilers since the concentration of sulfate and total dissolved solids (TDS) are above the water quality standards limit. However, this stream can be reused in other mining process stages, principally in uses that admit the use of water with low pH (2.52), thus reducing the cost involved with pH adjustment.

Table 3.3-2: Physicochemical characterization of raw effluent, concentrate and permeate from NF and DCMD, and their respective rejection between parenthesis ( )

Parameters	Raw effluent	NF		DCMD		Water reuse quality standards			
		Concentrate	Permeate	Concentrate	Permeate	Cooling water	Steam generator		
							Low pressure (<10 bar)	Medium pressure (10-50 bar)	High pressure (50 bar)
pH	1.95	2.51	2.52	1.47	6.27	6.9 - 9.0	7.0 - 10.0	8.2 - 9.0	8.2 - 9.0
Conductivity (µS/cm)	11.900	18.648	1.778 (85%)	19.777	84.1 (*99%*)	[c]	[c]	[c]	[c]
TDS[b]	7085	11.186	934 (86%)	11.725	124 (98%)	500	700	500	200
Total As (mg/L)	701	1.066	153 (*79%*)	1.167	2.1 (*99%*)	[c]	[c]	[c]	[c]
As 3 (mg/L)	*534*	*793*	*146 (73%)*	*889*	*1.4 (99%)*	[c]	[c]	[c]	[c]
As 5 (mg/L)	*45*	*70*	*7 (89%)*	*75*	*0.6 (99%)*	[c]	[c]	[c]	[c]
Sulfate (mg/L)	4852	7.9898	283 (*95%*)	7.999	131 (*96%*)	200	[c]	[c]	[c]
Calcium (mg/L)	258	428	< 2.50 (*99%**)	430	< 2.50 (*99%**)	50	[c]	0.4	0.01
Magnesium (mg/L)	134	225	< 1.25 (*99%**)	223	< 1.25 (*99%**)	0.5	[c]	0.25	0.01

[a](ASANO et al., 2007)

[b]*TDS: total dissolved solids*

[c]*accepted as received*

[d]*Calculated considering the detection limit value*

NF and DCMD generate a concentrate stream that also needs to be treated. For this, chemical precipitation can be a possible alternative as it is the process currently used in the industry. The concentration of the pollutants in a single stream, allowed by both NF and DCMD, represents an advantage even for the precipitation process. Since the volume of the stream to be treated suffers a considerable reduction, less volume of mud is formed after the chemical precipitation process. Excellent results were found by other authors (ANDRADE et al., 2018) using two-stage nanofiltration together with arsenic and calcium intermediate precipitation for gold mining effluent treatment

3.3.3 Energy requirements

As the effluent studied comes from a gas scrubber it has already high temperature (60°C) and heating the feed is not necessary. The high temperature of the effluent is advantageous for the MD process, but not for the NF process. NF membrane is limited to operate at a temperature higher than 45°C and its rejection performance is affected by temperature as showed by (ANDRADE et al., 2017a). The authors recommend operating the NF at a temperature around 20-25°C. Then, for the treatment of gold mining effluent by NF is necessary to cool the effluent. Thermal and electric energy were calculated for NF and DCMD system. For DCMD system two scenarios were considered: (1) use of residual heat of the effluent and then thermal energy is necessary only for cooling the recirculated distillate; thermal energy was calculated for the heat loss in the system, which was 2^{o}C maximum, and (2) the effluent at room temperature (25^{o}C); thermal energy is necessary for heating the feed and cooling the recirculated distillate. The second scenario aims to show the benefits of the use of the residual heat of the effluent. The results are shown in Table 3.3-3.

Table 3.3-3: Energy requirements and thermal and total energy efficiency for DCMD and NF system

	DCMD- scenario 1 (effluent fed at 60°C)	**DCMD - scenario 2 (effluent fed at 25°C)**	**NF**
Electric Energy (KWh m^{-3})	0,002	0.002	0.980
Thermal Energy (KWh m^{-3})	0.930	41.608	40.678
Total Energy (KWh m^{-3})	0.930	41.610	41.658
Thermal efficiency	1.19	0.07	-
Efficiency of MD system (ε_E or GOR)	1.19	0.07	-

Due to the demand for cooling the feed for NF, the energy requirement for NF was almost 40 times higher than for DCMD. The results also show the benefits of the use of the residual heat of the effluent for DCMD thermal efficiency, allowing the reduction of 98% on thermal energy consumption. The DCMD energy requirement in the scenario 1 can still be reduced if an alternative source of cooling fluid can be employed. For example, in the case of the gold mining studied, the treated effluent flow corresponds to about 50% of the total water demand in the industry, thus industrial water can be used as a cooling fluid instead of cooling and recirculation of the distillate.

3.3.4 Techno-economic comparison of DCMD and NF for gold mining effluent treatment

DCMD and NF show promising performance for gold mining effluent treatment, given that both systems were able to produce water for reuse from gold mining effluent. In this regard, the DCMD process is limited to operate up to permeate recovery rate of 40%, since severe fouling due to $CaSO_4$ precipitation, favored by the higher feed temperature, was observed when permeate recovery rate exceeds 40% (Figure 3.3-1). Although DCMD was susceptible to fouling and membrane wetting, fouling resistance contribution to total filtration resistance is lower than observed for the NF (Figure 3.3-3). Moreover, the DCMD produces a permeate with a superior quality without industrial use restriction (Table 3.3-2).

In relation to costs, Capex and Opex of the DCMD and NF systems were estimated for the treatment of 140 m^3/h of effluent at a permeate recovery rate of 40%. At this permeate recovery rate, a permeate flux of 18 $m^3/h.m^2$ and 16 $m^3/h.m^2$ was observed for NF and DCMD, respectively. For NF cost calculations, the cooling of the effluent to 25°C was considered, while for DCMD the use of the effluent residual heat was taking into account. Table 3.3-4 shows the characteristics of the DCMD and NF system considered for the calculation as well as the Capex for both systems.

Table 3.3-4: Characteristics considered for the cost estimation of the NF and DCMD treatment systems and the CapEx obtained

		Values		
	Description	**NF system**	**DCMD system**	**Units**
Summary of the system's characteristics	Annual System Capacity	1.226.400	1.226.400	m^3 $year^{-1}$
	Effluent temperature	60	60	°C
	Operating temperature	25	60	°C
	Average Permeate Flux	0.018	0.016	m^3 h^{-1} m^{-2}
	Required NF Membrane Area	3128	3544	m^2
	Design Plant Life	15	15	Years
	Membrane Lifespan	1-5	1-5	Years
	Brazil Investment Rate	14%	14%	
	Cleaning frequency	48	48	$year^{-1}$
	Cleaning cost	0.001	0.001	US$ m^{-3}
	Permeate pH adjustment cost*	0.25	0.01	US$ m^{-3}
	Maintenance cost	0.004	0.002	US$ m^{-3}
	Energy requirement	41.08	1.18	KWh m^{-3}
	Energy cost	1.64	0.05	US$ m^{-3}
CapEx	Treatment System	575,490.30	305,483.85	US$

**pH adjustment: NF (2.5 to 7) and DCMD (6.3 to 7.0)*

The NF estimated Capex was higher than that estimated for DCMD. Even the NF Capex without the cooling system (US$ 551,250.00), which has contributed to total NF Capex, was greater than that of DCMD. The lower value of the DCMD Capex value is due to the use of effluent residual heat that dismisses the installation of a cooling system.

The cooling of NF feed also adds considerable cost to the overall price of the reclaimed water because of its energy requirement. In addition, the NF permeate requires pH adjustment which is also expensive. Thus, it all contributes significantly to increase the final reclaimed water cost for the NF system.

The NF and DCMD Opex is also influenced by membrane lifespan and since the effluent has natural acidic characteristic it is expected relative low membrane lifespans. In this way, the NF and DCMD Opex were calculated for membrane lifespan from 1 to 5 years together with the contribution of each Opex components to the final value. Results are shown in Figure 3.3-5.

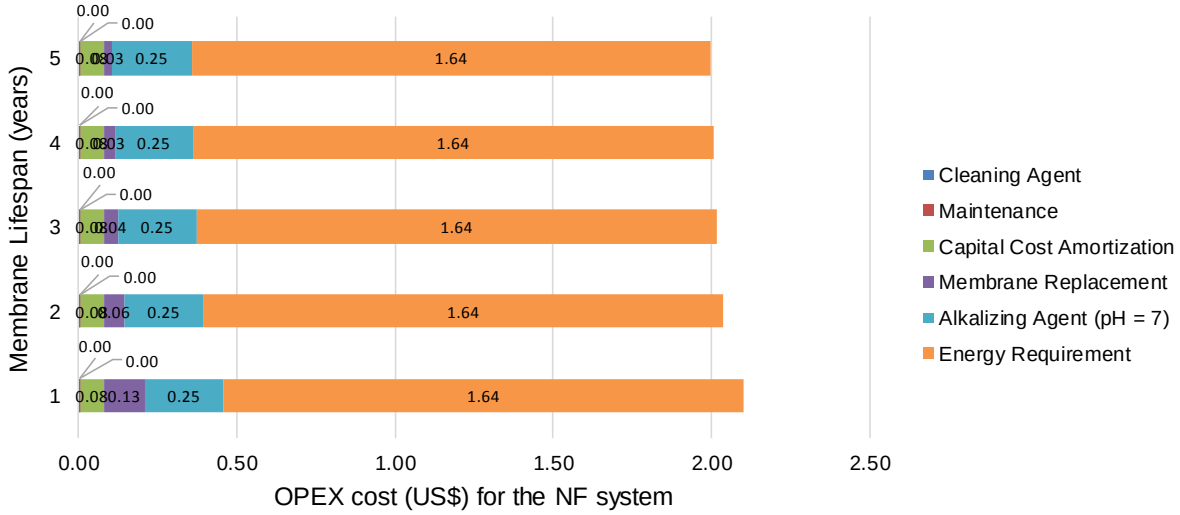

(a)

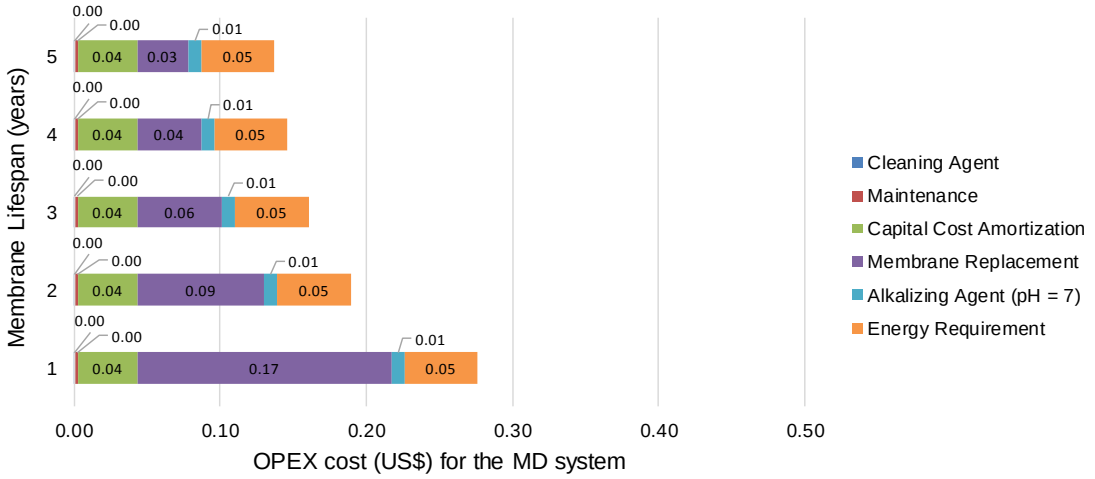

(b)

Figure 3.3-5: Contribution of Opex components to the final value in a function of membrane lifespan for (a) NF and (b) DCMD systems.

The NF Opex is less sensitive to the variation of the predictive membrane lifespan due to the greater contribution of energy (78%) and neutralization (13%) cost to the overall price of the reclaimed water. NF Opex varied from 2.00 – 2.10 US$/m^3 reducing the membrane lifespan from 5 to 1 year. The DCMD Opex was more sensitive to membrane lifespan, ranging from 0.13 to 0.27 US$/m^3 as membrane lifespan decrease from 5 to 1 year.

Energy requirement and membrane replacement were the most expressive components of the DCMD Opex. Energy requirement varied from 17 – 35% and membrane replacement from 26 – 64%. For the lowest membrane lifespans (1, 2 and 3 years), membrane replacement contribution was higher while at membrane lifespan of 4 and 5 years, energy requirement was the most expressive component.

Cleaning agent and maintenance showed similar contributions for NF and DCMD systems. They represented the Opex components with less expression, with percentages of 0.7 – 1.5% for maintenance, 0.3 – 0.7% for the cleaning agent. The DCMD Opex was more sensitive to the capital cost amortization than NF Opex; even in absolute value, capital cost amortization contribution was lower than that found for the NF system, as the Capex of the DCMD system is lower. The capital cost amortization ranged from 15 to 30% of the DCMD Opex as membrane lifespan increased.

Thus, besides DCMD allowed for the production of a higher quality permeate, that can be applied for more noble uses than NF permeate, it also showed lower susceptibility to scaling and lower associated costs (Capex and Opex), demonstrating greater potential as an alternative for gold mining effluent treatment and water reclamation. The permeate reuse would reduce water consumption by 490,560 m^3 $year^{-1}$, which represents almost 50% of the industrial water demand. Considering the current cost of fresh water (0.18 US$ m^{-3}), the permeate reuse would represent savings of US$ 88,300.80 per year.

3.4 CONCLUSION

Both NF and DCMD showed promising performances for gold mining effluent reclamation, showing high pollutants removal rate, which is an environmental and economic interesting aspect. DCMD presented a lower flux than NF (18 $kg/m^2.h$ and 16 $kg/m^2.h$ for NF and DCMD, respectively, at a recovery rate of 40%) and was limited to operate up to permeate recovery rate of 40% due to severe fouling caused by to $CaSO_4$ precipitation. Although DCMD was susceptible to fouling, fouling resistance contribution to total filtration resistance is lower than observed for the NF. Furthermore, DCMD produces a permeate with a superior quality and with no restriction for reuse.

The economic analysis revealed that due to the recovery of the natural high effluent temperature, the DCMD showed low energy requirement. In addition, due to the high DCMD contaminant rejection, a permeate of higher quality is produced, with a low demand for pH adjustment. Thus, the application of DCMD process for gold mining effluent reclamation could result in more significant annual cost savings if compared to NF process.

DCMD showed to have a very high efficiency for the treatment of gold mining effluent and it represents a promising industrial application as the thermal efficiency of the process was very high due to the fact that no heating energy requirement is necessary for the feed, decreasing drastically the treatment related costs. However, the heat loss by conduction in the DCMD process is very high compared to other MD configurations and an alternative configuration should also be tested.

3.5 ACKNOWLEDGEMENTS

The authors thank the Coordination of Improvement of Higher Education Personnel (CAPES), the National Council for Scientific and Technological Development (CNPq) and Foundation for Research Support of Minas Gerais (FAPEMIG) for the scholarships and financial resources provided.

CHAPTER 4:

THE FEASIBILITY OF VACUUM MEMBRANE DISTILLATION (VMD) FOR SULFURIC ACID PLANT WASTEWATER RECLAMATION

4.1 INTRODUCTION

The low quality of available mineral ores together with the high international mineral demand make the mining industry dependency on the water resource increase each day (KESIEME, 2015). The higher consumption of water for mineral processing also lead the production of large volumes of wastewaters that are often contaminated with heavy metals, representing a great challenge for its proper treatment. This, together with increasing stricter discharge standards, environmental legislative pressure and conflicts related to water supply, have intensify the search for effective techniques for wastewater treatment (KESIEME; ARAL, 2015). The proper treatment of contaminated effluents is becoming not only an interesting option by an environmental point of view, but also economic (KESIEME; ARAL, 2015), as it allow for the minimization of hazardous waste production as well as water reuse, decreasing the industry water demand.

The treatment process highly depends on the characteristics of the wastewater and the objective of the treatment. In order to produce high quality water for reuse, membrane distillation (MD) is highlighted as it has certain advantages both in relation to conventional distillation systems and pressure-driven membrane separation processes (ALKHUDHIRI; DARWISH; HILAL, 2012). This technology has the potential to concentrate solutions to its saturation without any significant decline in permeate flow and its performance is little affected by salinity compared to other membrane technologies (DRIOLI; ALI; MACEDONIO, 2015; WANG; CHUNG, 2015). As the feed stream must be hot, the main energy demand of the MD systems refers to the feed solution heating process (ZUO et al., 2011). Thus, the treatment of mining effluents that present high temperatures, as the gas scrubber effluent from the gold mining industry represents a great field for MD application.

From the configurations available for MD, direct contact MD (DCMD) is the most used, presenting several applications (ALKHUDHIRI; DARWISH; HILAL, 2012; CHEN et al., 2013; KESIEME; ARAL, 2015; MAHDI; SHIRAZI; KARGARI, 2015; QU et al., 2009; SHIM et al., 2015; YUN et al., 2006). The performance of this process on the treatment of the gold mining effluent was tested and compared to Nanofiltration (Chapter 3) and the results obtained proved its feasibility for this purpose, allowing even for lower treatment costs compared to Nanofiltration.

However, despite its operational simplicity, a source of clean water is required for the application of DCMD to compose the distillate. This stream need to be recirculated, requiring energy for its cooling. In addition, the presence of a cool stream on the permeate side lead to a higher heat loss in DCMD process when compared to other MD systems (QTAISHAT; BANAT, 2013).

Vacuum membrane distillation (VMD), on the other hand, is a process that uses only the vacuum on the permeate side, exhibiting a very low heat loss by convection, reduced resistance to mass transfer and allows the obtaining of a pure permeate at low operating temperatures (MAHDI; SHIRAZI; KARGARI, 2015; SIVAKUMAR; RAMEZANIANPOUR; O'HALLORAN, 2013). This configuration has been pointed out as a promising technology for the treatment of aqueous solution that can compete with well-established technologies (CHIAM; SARBATLY, 2014).

VMD is widely used for the removal of volatile compounds and water desalination (CHIAM; SARBATLY, 2014; MAHDI; SHIRAZI; KARGARI, 2015). This process have shown high efficiency on water decontamination, including for arsenic (both arsenite and arsenate) (CRISCUOLI; BAFARO; DRIOLI, 2013; DAO; LABORIE; CABASSUD, 2016), and also metal (Ca, Mg, Fe and Al) removal from coal mining water treatment (SIVAKUMAR; RAMEZANIANPOUR; O'HALLORAN, 2013).

Despite the publication of several works evaluating the technical feasibly of VMD, authors highlighted that the development of VMD in industrial scale is still lacking, as well as the evaluation of its performance with complex, more realistic multicomponent water matrixes (CHIAM; SARBATLY, 2014). In this way, the evaluation of VMD process as an alternative for gold mining effluent treatment is a very promising approach that can contribute to the increase the knowledge of VMD applications on the mining industry sector. In adittion, as it is a high temperature effluent, the energy costs of the treatment can be drastically reduced as heating represents almost 90% of the total energy demand of VMD systems (CABASSUD; WIRTH, 2003). The reduction of the energy demand for heating can drastically increase the thermal efficacy of MD processes, as shown in Chapter 3, enabling the industrial application of those processes.

Thus, the objective of this study was to evaluate the feasibly of VMD in the treatment of gold mining effluent and to select the best operational conditions that can allow for the production of high quality permeate for industrial reuse.

4.2 MATERIALS AND METHODS

4.2.1 Sampling

VMD tests were performed at the National Institute of Applied Sciences (INSA) of Toulouse (France). As the effluent studied in this work is contaminated with arsenic and because high volumes are necessary for the tests, VMD tests could not be made using the real effluent. Thus, a synthetic solution that simulate the characteristics of a gold mining effluent was prepared. For this, salts containing the major components of this effluent (Ca, Mg, Fe, Zn, chloride, sulfate) were added to distillate water using as source of those components the salts $CaSO_4$, $FeSO_4$, $MgSO_4$, Na_2SO_4, $Al_2(SO_4)_3$, KCl and $ZnCl_2$. The salts were dissolved in hot distillate water under agitation and its pH was adjusted to 2.0 using sulfuric acid (H_2SO_4). This solution was called Synthetic solution 1 (SS1).

Due to the acidic characteristic of the effluent and the fact that it can reduce the membrane lifespan another solution (SS2) was also prepared by adjusting the pH of SS1 to 5.0 using sodium hydroxide (NaOH) and the supernatant was used as feed solution.

Despite the arsenic is one of the major components of the gold mining effluent it was not used on the synthetic solution preparation because of its toxicity and because, as shown in NF tests and in other works (ANDRADE et al., 2017d), it does not influence on the membrane performance in terms of fouling and permeate flux decrease. The physicochemical characterization the synthetic solutions are described on Table 4.2-1.

Table 4.2-1: Physichochemical characterization of the gold mining effluent and synthetic solutions SS1 and SS2.

Parameter	Unit	Gold Mining Effluent	Gold Mining Effluent (adjusted pH)	Synthetic solution 1 (SS1)	Synthetic solution 2 (SS2)
pH		1.7 ± 0.2	4.9 ± 0.2	2.0 ± 0.1	5.0 ± 0.1
Conductiviy	(mS/cm)	11.5 ± 2.3	6.9 ± 0.3	7.8 ± 0.5	5.64 ± 0.6
Total Sulfate	(mg/L)	4191 ± 1180	4338 ± 439	6000 ± 3000	4316 ± 432
Total Arsenic	(mg/L)	668 ± 210	691 ± 70	-	-
Total Calcium	(mg/L)	518 ± 213	399 ± 40	600 ± 30	432 ± 43
Total Magnesium	(mg/L)	274 ± 134	259 ± 26	300 ± 15	216 ± 22
Total Iron	(mg/L)	102 ± 20	79 ± 8	100 ± 5	72 ± 7
Total Aluminium	(mg/L)	100 ± 14	78 ± 8	100 ± 5	72 ± 7
Total Zinc	(mg/L)	73 ± 30	57 ± 6	80 ± 4	58 ± 4
Total Chloride	(mg/L)	62 ± 24	48 ± 5	60 ± 3	43 ± 3
Total Sodium	(mg/L)	32 ± 13	31 ± 3	40 ± 2	29 ± 2
Total Potassium	(mg/L)	40 ± 6	32 ± 3	40 ± 2	29 ± 2

4.2.2 VMD Experimental setup

All the tests were carried out with a bench-scale batch pilot plant as described in details by (JACOB; LABORIE; CABASSUD, 2018) and showed on Figure 4.2 1. An initial volume of 4 L of feed solution was fed into a thermostatic feed tank and was heated by a hot water bath under agitation using a magnetic stirrer (350 rpm) to prevent salt precipitation in the tank. Feed was fed into the membrane module (Re = 2534) by a magnetic pump. The internal feed side channel of the membrane module was 87.6×47.5×0.5mm (l×w×d) and 8 mm of edge radius.

The required vacuum pressure was applied in the permeate side by a vacuum pump (Vacuubrand (1000–3 mbar)). The vacuum pipe was heated to prevent vapor condensation and a cold trap was placed after the vacuum pump to condense the permeate. A flow meter was used to measure the inlet liquid feed flow rate (0–250 L/h), which was kept at 125 L/h in this work. The permeate flow rate was measured by a mass flow meter (Bronkhorst, 0–60 g/h) and a water trap was placed before it to protect the equipment in case of liquid leak on the

vacuum pipeline. Temperature and pressure sensors were used to measure feed module inlet and outlet parameters and permeate properties and recorde in the data acquisition system. The frequency of data acquisition was set for 6 s for most of the tests, except for the recovery rate test, which was 30 s.

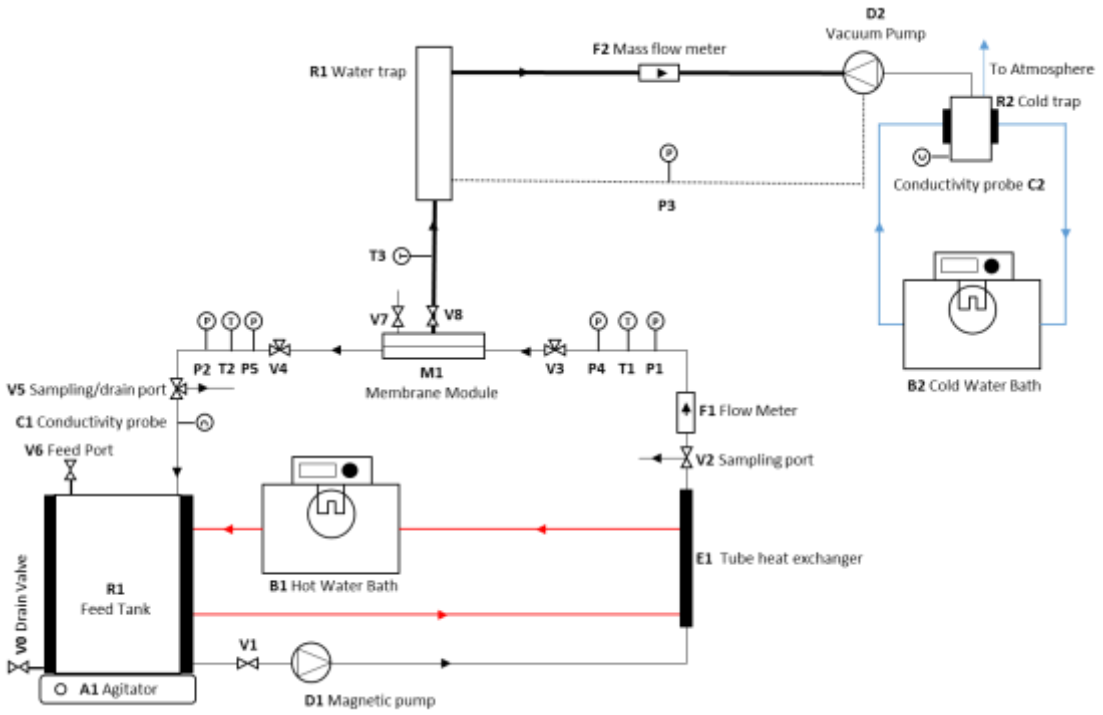

Figure 4.2-1: Schematic diagram of the VMD unit (JACOB; LABORIE; CABASSUD, 2018).

Before each test a virgin hydrophobic PTFE flat-sheet membrane (Fluoropore), provided by Millipore Corporation, France, was placed in the membrane cell. This membrane has a nominal pore size of 0.22 µm, 70% of porosity and the effective membrane area was 0.00416 m^2.

4.2.3 VMD experimental procedure

VMD tests were carried out with the synthetic solutions under different feed temperatures, vacuum pressures, feed pH and recovery rate. The tests were performed in batch mode with recirculation of the concentrate and with a feed flow rate of 125 L/h, as this value guarantees a Reynolds number equivalent to transient regime.

The permeability of the membrane was calculated by measuring the water vapor flow through the membrane using distillate water as feed. Membrane water permeability (K_M) was

calculated by the Temperature Variation (TV) Method described by (DAO et al., 2013) The water permeate flux was measured at feed temperatures from 40°C to 50°C. This measurement was made in 3 different vacuum pressures (64, 67 and 70 mbar). Membrane permeability was measured for virgin membranes and membranes that went through more than 24 h of test or any changes on permeate flux was observed during the test. Results were expressed in the temperature reference T_{ref} = 20°C, to facilitate comparison with the literature.

Different feed temperatures were evaluated in an interval that ranged from the natural minimum temperature of the gold mining effluent (40°C) to a maximum temperature (50°C) in which the feed can be maintained by using solar heating (with an increment of 1°C from 40 to 50°C by using a heat exchanger), so that the energy costs related to heating could be reduced, and the pilot plant system could be maintained stable.

4.2.3.1 Effect of pressure on VMD performance

A preliminary test was conducted using the synthetic solution (SS2) as the feed, as this solution had a lower salt concentration and was less aggressive to the membrane and system in general. The permeate flux was measured for the vacuum pressures of 61, 64, 67 and 70 mbar and with the feed temperature varying from 40 to 50°C. Results were compared with those obtained by using distillate water as feed.

With the results obtained from this test, it was chosen the vacuum pressure that provides the best cost benefit in relation permeate flux and energy consumption. The vacuum pressure chosen was used for the VMD system for the synthetic solution treatment.

4.2.3.2 Influence of the feed temperature in the permeate flux

The temperature influence on the permeate flux was analyzed by performing VMD tests with a fixed feed temperature. The feed temperatures chosen was 40 °C and 50°C, as it represents the highest and the lowest temperatures on the feed temperature range evaluated. The vacuum pressure applied was that chosen in the previous test. The test was conducted until an accumulated permeate volume of 100 mL was collected and results were used to choose the most suitable temperature for the VMD test.

4.2.3.3 Influence of the feed pH in the permeate flux

The feed pH influence on the permeate flux was also analyzed. For this, VMD tests were conducted using SS1 and SS2 as feed solution. Tests ran for 24 h and were performed using

the same vacuum pressure chosen in the first test and with the feed temperature chosen in the previous test.

After 24 h of permeation the volume of permeate obtained was measured and the same volume of distillated water at the same temperature of the feed was added to the feed tank to verify if any changes observed in the permeate flux with time could be restored. The test continued to run for more 2 hours.

After the end of the test, the membrane passed through physical cleaning by circulating distillate water for 5 min at a feed flow of 1.2 liters per minute (LPM). After the physical cleaning the membrane water permeability was measured. The membrane was taken out of the membrane cell and was left to dry at room temperature. The results found on this test were used to choose the feed pH more suitable for the VMD treatment.

4.2.3.4 Recovery rate test

After selection of the operational conditions for VMD (vacuum pressure, feed temperature and feed pH) a recovery test was performed. The test ran until a sharp decrease of the permeate flux was observed and a small value of permeate flux was obtained.

After the end of the test the same procedure done on the previous test was used. A volume of distillate water referred to the total volume of permeate obtained in the test was added to the feed tank and the system ran for 2 hours. After this, membrane passed through physical cleaning with distillate water and has its water permeability measured. The membrane was also taken out of the membrane cell and left to dry at room temperature.

4.2.4 Computer simulation

For the determination of the solution density and water activity for the synthetic solution at the beginning of the test and at different recovery rates, the software PHREEQC (PHREEQC Version 3 - A Computer Program for Speciation, Batch-Reaction, One-Dimensional Transport, and Inverse Geochemical Calculations) was used. The estimation of the permeate flux, the feed temperature and salt concentration at the membrane surface, the Reynolds number and the necessary potency of the pumps for circulation and vacuum application was performed using the model proposed by (MA; AHMADI; CABASSUD, 2018).

4.2.5 Analytical Methods

The mining effluent and permeates were characterized in terms of the following physicochemical parameters: pH (pHmeter Qualxtron QX 1500); conductivity (Hanna conductivity meter HI 9835); calcium and magnesium cations (Dionex ICS-1000 ion chromatograph equipped with AS-22 and ICS 12-A columns); and sulfate (4500-SO42) and chloride(4500-CL) (APHA, 2017).

4.2.6 Calculation

In the VMD system, the flow meter installed in the pilot plant gives the water vapor flow (Q_w) in g.h^{-1} in a function of time. In this way, the permeate flux [$J_{P(VMD),t}$] is calculated according to Equation (1):

$$J_{P(VMD),t} = \frac{\left(\frac{Q_{w,t}}{1000}\right)}{A_m} \quad (1)$$

Where A_m is the area of the membrane (in m^2). The recovery rate [RR_{VMD}] is calculated by Equation (2):

$$RR_{VMD,t} = \frac{V_{p,Tt}}{V_{fi}} . 100 \quad (2)$$

Where $V_{p,Tt}$ corresponds to the total volume of permeate (in L) in a time t and V_{fi} to the initial volume of feed (in L). The $V_{d,t}$ is calculated by the sum of all the permeate obtained until the time t:

$$V_{p,Tt} = \sum_{i=0}^{t} V_{p,i} \quad (3)$$

The volume of permeate in in a given time ($V_{p,ty}$) is calculated as demonstrated in Equation (4), where $Q_{w,ty}$ is the vapor flow (in g.h^{-1}) measured at that same time (t_y, in h) and t_x is the time where the last measurement of vapor flow was made (in h).

$$V_{p,ty} = Q_{w,ty} * (t_y - t_x) \quad (4)$$

In this study the measurement made by the water vapor flow meter was made in a frequency of 6 s, except for the recovery rate test, which was 30 s.

The rejection [R(%)] of pollutants and conductivity was calculated using Equation 5, considering the conductivity/pollutant concentration of the feed (C_f) and permeate (C_p) streams. The rejection [$R(\%)$] was calculated on the basis of its concentration in the permeate.

$$R(\%) = \frac{C_f - C_p}{C_f}.100 \quad (5)$$

The specific energy consumption (SEC) was defined by the relation between the rate of work done by the pump (W_{pump}) and permeate flow rate (Q_p) (Zhu et al., 2009), as follows:

$$SEC = \frac{W_{pump,VMD}}{Q_p} \quad (6)$$

$W_{pump,VMD}$ is calculated considering the work done for the circulation of the streams and the vacuum application, both calculated as proposed by (MA; AHMADI; CABASSUD, 2018).

Membrane resistance (R_m) and feed boundary layer resistance (R_{fb}) were calculated as shown by Equations (7) and (8) (SRISURICHAN; JIRARATANANON; FANE, 2006). The permeate boundary layer resistance (R_{pb}) was ignored as compared to the other resistances (CHIAM; SARBATLY, 2014).

$$R_m = \frac{P_{f,m} - P_{p,m}}{J_{p(VMD)}} \quad (7)$$

$$R_{fb} = \frac{P_{f,b} - P_{f,m}}{J_{p(VMD)}} \quad (8)$$

Where $P_{f,m}$ and $P_{p,m}$ are the vapor pressure at the membrane surface of the feed and permeate sides, respectively, and $P_{f,b}$ is the vapor pressure at the feed bulk. As shown by other authors (DAO et al., 2013), in VMD systems the $P_{p,m}$ can be considered as the vacuum pressure applied on the permeate side.

To calculate the vapor pressures ($P_{f,b}$ and $P_{f,m}$), Antoine's Equation was used considering the temperature of the feed bulk ($T_{f,b}$), given by the thermometer installed on the pilot plant, and at the feed membrane surface ($T_{f,m}$), calculated using the model proposed by (MA; AHMADI; CABASSUD, 2018).

$$P_{f,b} = EXP\left(23.238 - \frac{3841}{T_{f,b}-45}\right) \quad (9)$$

$$P_{f,m} = EXP\left(23.238 - \frac{3841}{T_{f,m}-45}\right) \quad (10)$$

As the feed used refers to a solution, to better estimate the vapor pressures, the value obtained by Equations (9) and (10) were multiplied by the activity of the water (α) and the molar fraction of water of the solution (M_{H20}) (CHIAM; SARBATLY, 2014; ZHAO et al., 2011), as follows:

$$P'_{f,b} = P_{f,b} * \alpha * M_{H20} \quad (11)$$

$$P'_{f,m} = P_{f,m} * \alpha * M_{H20} \quad (12)$$

M_{H20} is calculated by Equation 13, where ρ_{sol} is the density of the solution (in kg.L^{-1}), C_{sol} is the is the concentration of salt in the solution (in kg.L^{-1}), MM_{H2O} is the molar mass of water (in kg.mol^{-1}) and MM_{salt}, the molar mass of salt in the solution.

$$M_{H20} = \frac{\frac{(\rho_{sol} - C_{sol})}{MM_{H2O}}}{\frac{(\rho_{sol} - C_{sol})}{MM_{H2O}} + \frac{C_{sol}}{MM_{salt}}} \quad (13)$$

The ρ_{sol} was calculated using the software PHREEQC and the MM_{salt} was calculated as follows:

$$MM_{salt} = \frac{C_{m,total\ salt}}{C_{n,total\ salt}} \quad (14)$$

Where $C_{m,total\ salt}$ and $C_{n,total\ salt}$ are the mass concentration (in kg.L^{-1}) and the molar concentration (in mol.L^{-1}) of all the salts in the solution.

The differences in osmotic pressure ($\Delta\pi$) between the concentrate and permeate for different permeate recovery rates were estimated by the Equation of Van't Hoff, described in Equation (7).

$$\Delta\pi = RT\Delta\Sigma(C_c - C_p) \quad (7)$$

For this, it is used the universal gas constant (R), temperature of permeation (T) and the sum of the difference of the molar concentration of the main dissolved species that are present in the concentrate (C_c) and permeate (C_p) at each RR. In this study, data of pH and concentration of sulfate, calcium and magnesium were used to calculate the osmotic pressure.

The concentration of salt in at the membrane surface (C_m) was calculated using the molar concentration of the same salt in the concentrate (C_c) and permeate (C_p), the permeate flux ($J_{p(VMD)}$, in $m^3\ h^{-1}\ m^{-2}$) and the mass transfer coefficient (k), as indicated by (NOBLE; STERN, 1995):

$$\frac{C_m - C_p}{C_r - C_p} = \exp\left(\frac{J_{p(VMD)}}{k}\right) \quad (13)$$

k was calculated as demonstrated by (RICCI et al., 2015a). Considering the set of conditions used in this study, the numerical value obtained for sulfate (SO_4^{-2}) was 7.56×10^{-5} $m.s^{-1}$ and for calcium (Ca^{+2}), 5.92×10^{-5} $m.s^{-1}$.

4.3 RESULTS AND DISCUSSION

4.3.1 Comparison between water and gold mining synthetic solution as VMD feed

4.3.1.1 Pressure and temperature variation test (PTV test)

To evaluate the feasibility of the VMD system to treat an effluent with this characteristics a preliminary test was conducted using the synthetic solution (SS2) as the feed. The permeate flux was measured for the vacuum pressures of 61, 64, 67 and 70 mbar and with the feed temperature varying from 40 to 50°C and it was compared with the fluxes obtained when using distillate water as feed (Figure 4.3-1).

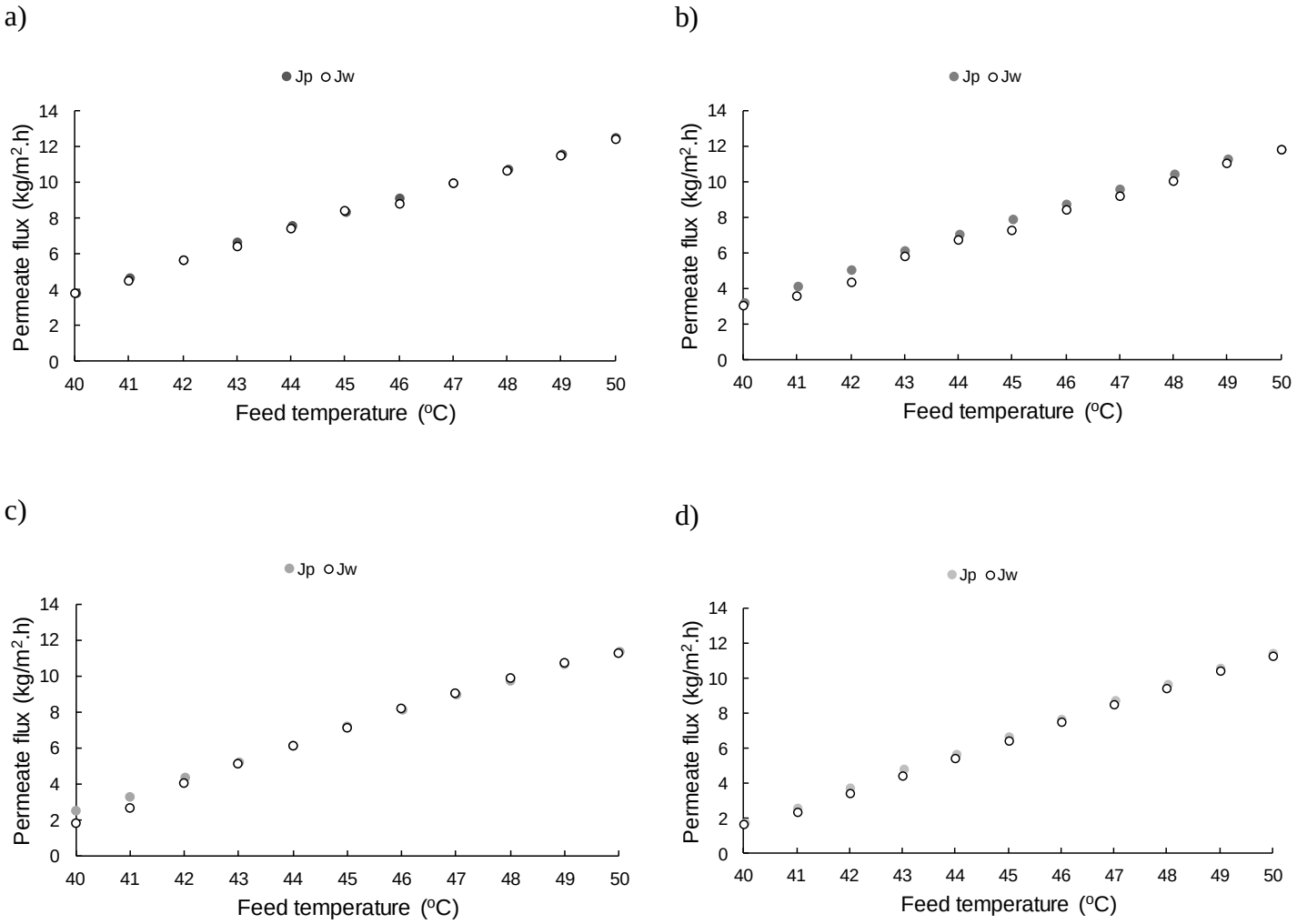

Figure 4.3-1: Comparison between the SS2 permeate flux (Jp) and distillate water flux (Jw) obtained with VMD at vacuum pressures of (a) 61 mbar; (b) 64 mbar; (c) 67 mbar; (d) 70 mbar.

As it can be observed, the permeate flux obtained for all vacuum pressures were very similar for the synthetic solution and distillate water. The VMD performance can be directly affected by the feed concentration but it also depends on the feed solution's chemical nature (CHIAM; SARBATLY, 2014), and as discussed before, the main application of VMD is for desalination, where usually feed presents high concentration of salts. The results found showed that, despite the composition of the feed used in this work, its moderate concentration (in terms of mass salt concentration) can explain the high permeate fluxes obtained. Thus, results indicate that VMD can be a suitable technology for treating the gold mining effluent.

The permeate flux obtained experimentally for the synthetic solution was compared for all the evaluated pressures and temperature to allow for best comparison between those operational conditions. The results are shown in Figure 4.3-2.

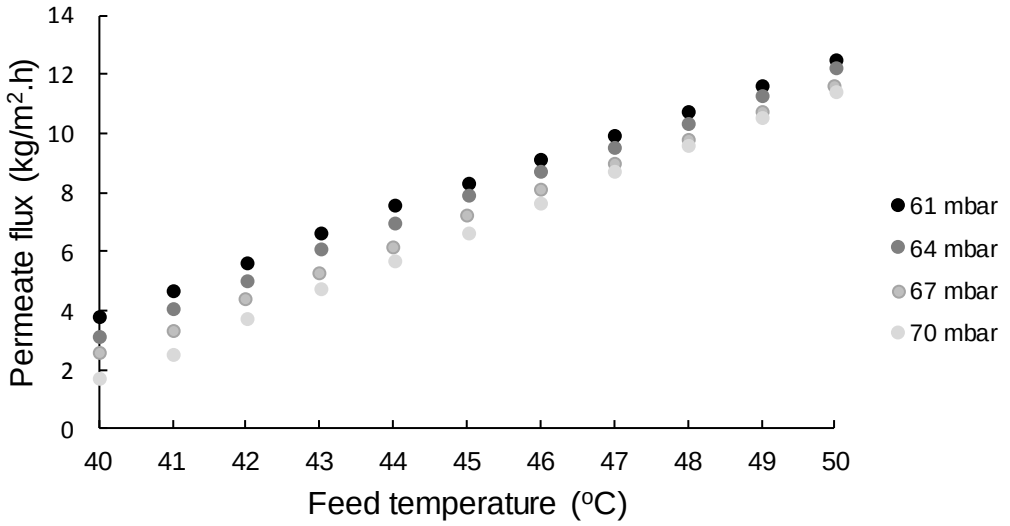

Figure 4.3-2: Permeate flux for VMD treating SS2 at temperatures from 40 to 50°C and vacuum pressures of 61, 64, 67 and 70 mbar.

As expected, for all vacuum pressures evaluated, the permeate flux increases as the feed temperature also increases. The increase on the feed temperature leads to an increase of the feed partial vapor pressure, increasing the driving force of VMD, thus a higher permeate flux is obtained.

It was also observed that the difference between the permeate flux obtained in the evaluated vacuum pressures decreases with the feed temperature increase. Thus, the increase on feed temperatures have a more pronounced effect on permeate flux than the increase of vacuum pressure, especially for high temperatures. Those results are in accordance with other authors that found that the sensibility of the permeate flux to vacuum pressure is higher at lower temperatures (BANAT; AL-RUB; BANI-MELHEM, 2003). As the gold mining effluent to be treated already presents a high temperature, the feed temperature of 50°C was chosen as the best feed temperature for VMD test performance.

For the vacuum pressure, it was chosen the one that allowed for a better stability of the system and higher permeate flux without a high increase on the energy demand. In this way, the

energy consumption for the vacuum pump was calculated for all vacuum pressures evaluate at the feed temperature of 50°C and results are shown in Figure 4.3-3.

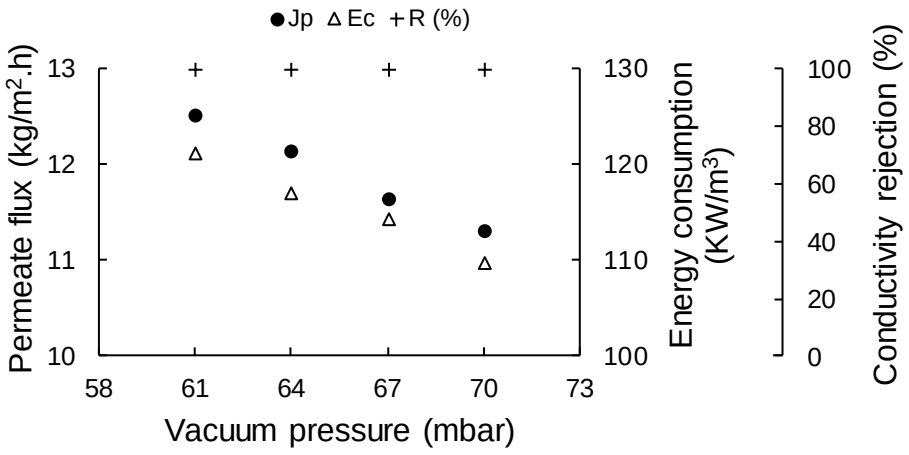

Figure 4.3-3: Permeate flux (Jp) and Energy consumption (Ec) in a function of the vacuum pressure applied (T_{feed} = 50°C).

As can be observed, the permeate flux showed a linear variation with the vacuum pressure, as reported (WANG et al., 2012). Regarding the process efficiency on conductivity removal, it remained the same (100%) for all pressures evaluated. With the decrease of the vacuum applied, both permeate flux and energy consumption decreases. However, the permeate flux decreases in a higher intensity than energy consumption. Thus, the vacuum pressure of 64 mbar was chosen for the next tests as it presents a high permeate flux with good stability of the system and not high relative energy consumption.

The computer simulation for flux prediction was also performed using the same conditions of the tests to evaluate if the model built for saline solutions in this pilot plant can also be used for a complex water solution that contains several different ions. Figure 4.3-4 shows the ratio between experimental data and simulation data.

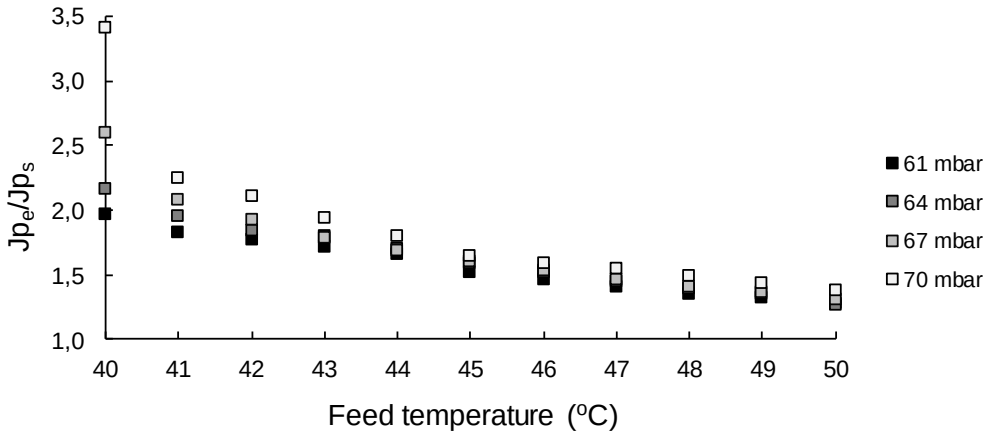

Figure 4.3-4: Ratio between the permeate flux obtained by experimental data (Jp_e) and computer simulation (Jp_s) of VMD treating synthetic solution SS2 for all feed temperatures and vacuum pressures evaluated.

As it can be observed, the permeate flux predicted by the simulation model was above the real permeate flux obtained experimentally, as all ratios were higher or equal to 1.2. Regarding the different pressured evaluated, it can be seen that the higher the vacuum applied, the closer the simulation data were from the experimental data obtained. In terms of feed temperature, it is observed that a more realistic permeate flux prediction could be made at higher feed temperatures. In addition, the ratio between experimental data and simulation data for different vacuum pressures was more similar to each other as feed temperature increase.

In this way, it can be concluded that the computer simulation can be used to predict the permeate flux for the synthetic effluent studied in this work, especially at higher temperatures. For the following tests, in order to eliminate the influence of this difference, the simulated permeate flux was multiplied by the ratio between the experimental and the simulated flux obtained for the specific test at the time 0. This will allow analyzing the difference between the fluxes predicted in a function of the concentration of the feed solution to that obtained experimentally.

4.3.2 Influence of the feed temperature in the permeate flux membrane performance

Although it was observed that higher feed temperatures allows for high permeate flux, the temperature variation (TV) test was performed in a short period, not allowing to evaluate if this flux would remain stable for longer. Thus, the feed temperature influence on the permeate flux was analyzed by performing VMD tests with a fixed and constant feed temperature (40

and 50°C) and vacuum pressure (64 mbar) (Figure 4.3-5). Experimental permeate flux data was compared to those predicted by the computer simulation and corrected multiplying it to specific Jp_e/Jp_s ratio found for the vacuum pressure of 64 mbar and feed temperature of 40°C ($[Jp_e/Jp_s]_{(40oC)}$ = 2.2) and 50°C ($[Jp_e/Jp_s]_{(50oC)}$ = 1.3).

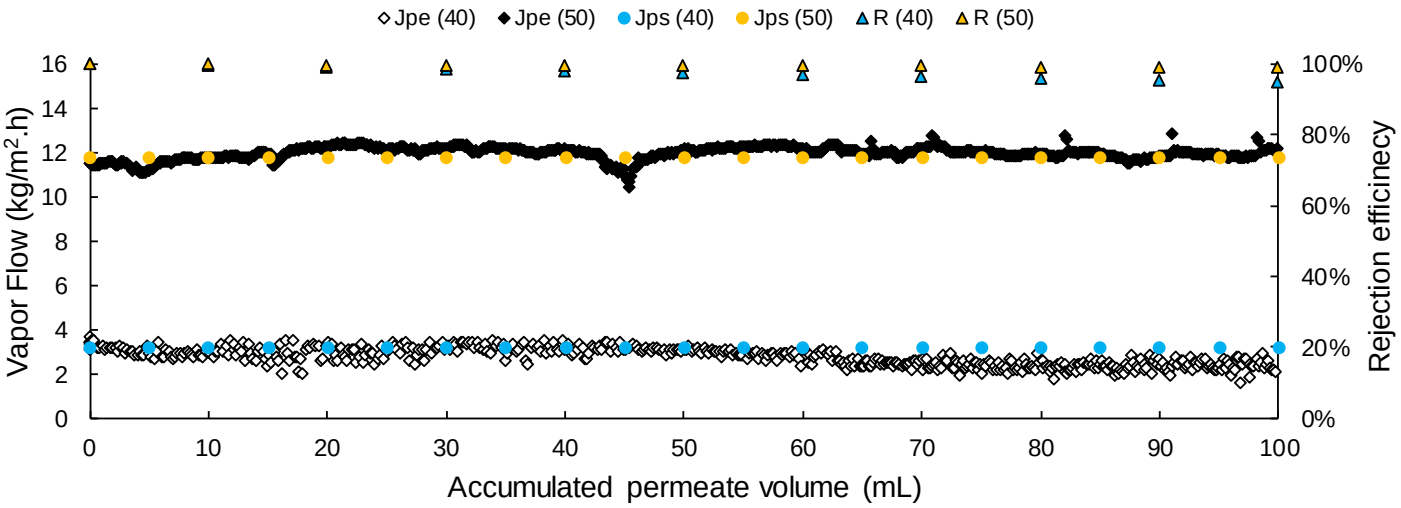

Figure 4.3-5: Experimental (Jpe) and corrected simulated (Jps) permeate flux for VMD treating SS2 in a function of total permeate volume for the feed temperature of 40°C and 50°C (P_v = 64 mbar).

As can be observed, in general, for both feed temperatures the permeate flux remained constant and the system was stable during the whole test. For the feed temperature of 40°C, a discreet decay was observed in the end. The fluxes obtained were very close to that of the computer simulation (corrected), showing that the values found in this test were similar to that obtained on the TV test.

The VMR rejection efficiency for both feed temperatures was calculated and it can be observed that for both feed tests presented high the conductivity rejection, with an efficiency higher than 95%. The test at 50°C presented a rejection efficiency of 99% and it was maintained until the end of the test. For the test at 40°C, by the other hand, membrane wetting was observed and the efficiency decreased from 99% to 95%. This result is in accordance to other authors (SRISURICHAN; JIRARATANANON; FANE, 2006) that discussed that higher feed temperatures can provide higher permeate fluxes and longer the wetting time experienced by the membrane.

Thus, because it allowed for the highest permeate flux and a high removal efficiency the feed temperature of 50^{o}C remained the chosen operational condition for the gold mining effluent treatment using VMD.

4.3.3 Influence of the feed pH in the permeate flux

The feed pH can have a high influence on the performance of membrane treatment and this was easily observed on the results obtained for Nanofiltration (Chapter 2). Even MD being a system not much influenced by the pH of the feed solution, considering the acid nature of the gold mining effluent, the VMD performance was also tested for an acid solution (SS1). At lower pH, the feed contains more dissolved salts that tend to precipitate with the pH adjustment. The higher concentration of salts can reduce the permeate flux and the feed acidity can reduce membrane lifespan. On the other hand, higher pH can favor salt precipitation on the membrane surface, increasing the fouling. This can consequently reduce permeate flux and in case of irreversible fouling, compromise the integrity of the membrane.

In this way, VMD was tested for two synthetic solutions: SS1 (pH = 2) and SS2 (pH = 5). These pH were chosen as they represent the pH of the real gold mining effluent (around 2.0) and the maximum pH to which the effluent pH could be adjusted without producing a sludge contaminated with arsenic, as discussed in the pH influence on the Nanofiltration performance (Chapter 2). Tests with the pH in between was not possible to me performed due to the time available for concluding the VMD tests. The permeate flux obtained and that one predicted by computer simulation (and corrected) were compared and results are presented on Figure 4.3-6. By the end of the test (24 hours) hot water was added to the concentrate to recovery the feed initial conditions and check for permeate flux behavior.

a)

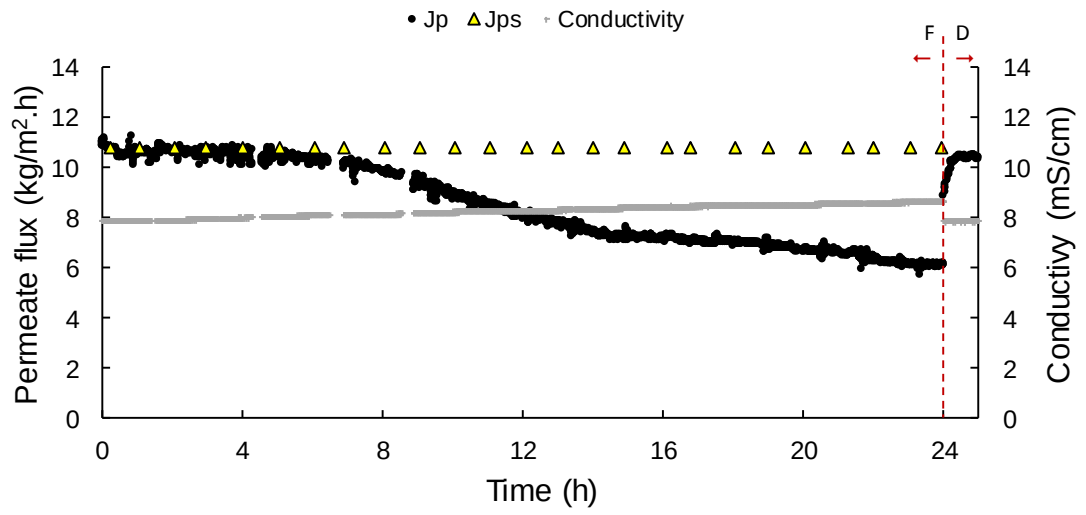

b)

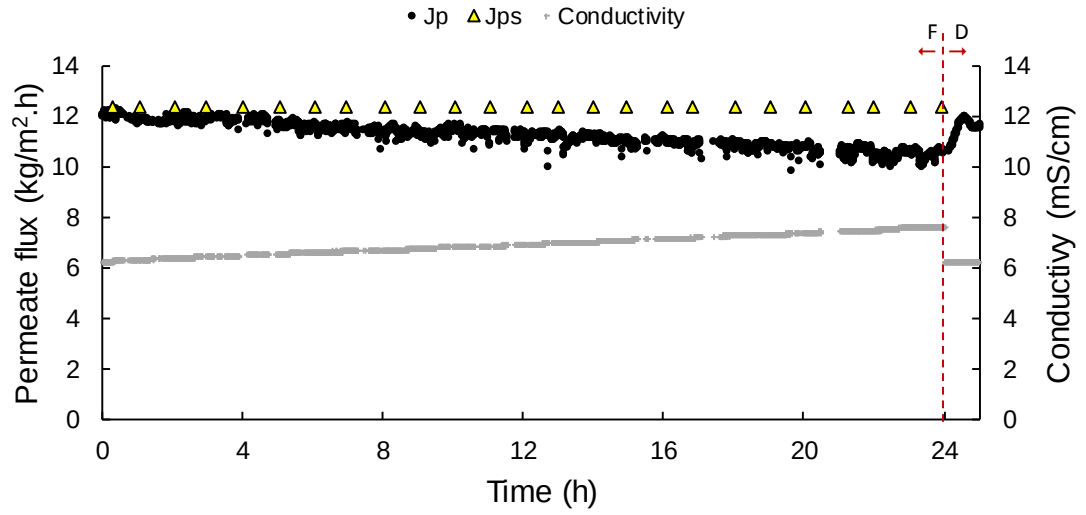

Figure 4.3-6: Experimental (Jp) and simulation predicted (Js) permeate flux and conductivity for VMD treating (a) SS1; and (b) SS2; before (F) and after (D) the dilution of the concentrate, indicated by the red line (P_v = 64 mbar; T_{feed} = 50°C).

As it can be observed, the permeate flux obtained was very different for each feed solution. It is important to highlight that the maximum permeate recovery rate (RR) achieved by both tests in 24 hours was similar, 19% for SS1 and 21% for SS2. The VMD showed a rejection of 99% for both of the solutions, showing that the feed pH had no influence on the system efficiency. Different from the nanofiltration, in which the feed pH affect both the feed solution and the ion rejection by altering the membrane surface charge (as discussed in Chapter 2), in VMD the feed pH itself does not affect the membrane rejection. This is because in VMD the ion rejection is given by the permeation of water vapor through the pores of the hydrophobic membrane while the non-volatile compounds such as salts remain dissolved in

the feed solution. Thus, the membrane property responsible for an effective rejection in VMD is its hydrophobicity that is not altered by the feed solution pH.

For the SS2 (Figure 4.3-6b), it can be observed that the permeate flux obtained was the same obtained in the previous tests and a gradual decrease of permeate flux was observed with time ($\Delta Jp/\Delta t$ = -0.069). At the end of the test and dilution of the concentrate, the feed conductivity went back to initial condition and the permeate flux could be restored close to the initial value as well. This result showed that the flux decline is related to the feed concentration, which increases the concentration polarization at the membrane surface, and possible fouling. With the dilution of the concentrate the permeate flux could be restored without the need of a physical cleaning with water.

On the other hand, for the SS1 (Figure 4.3-6a), a very different result was obtained. As can be observed, the permeate flux predicted remained practically constant with time, even considering the increase on the feed concentration. It shows that the decrease on the permeate flux is not related to the feed concentration alone, but other factors related specifically to the pH, as ions speciation and their respective fouling potential.

The permeate flux obtained for SS1 remained stable up to approximately 6 h of test (RR = 6%), with a very low permeate flux decay rate ($\Delta Jp/\Delta t$ = -0.061) similar to that obtained for SS2 but slightly lower. After 6h the permeate flux of SS1 showed a sharp decay ($\Delta Jp/\Delta t$ = -0.387) until approximately 15 h of test (RR = 14%). After 15 h, the permeate flux showed a more stable behavior again with a gradual decrease ($\Delta Jp/\Delta t$ = -0.148) until the end of the test. The dilution of the concentrate after the end of the test allowed for the permeate flux to be restored close to the initial value, without the need for a physical cleaning procedure with water. As it can be seen, the permeate flux could be restored for both of the tests by the dilution of the concentrate, but this process was faster in the VMD test with SS1 as feed.

Due to the concentration of calcium and sulfate on the feed, the results found on the Nanofiltration evaluation (Chapter 2) and previous work (ANDRADE et al., 2017d; MERICQ; LABORIE; CABASSUD, 2010), calcium sulfate ($CaSO_4$) is the most likely scalant and its precipitation is expected to represent a risk factor for membrane fouling. To evaluate the concentration of this salt during the VMD test of solutions SS1 and SS2, the supersaturation degree of $CaSO_4$ in the feed bulk (S_b) and at the membrane surface (S_m) was calculated (Figure 4.3-7).

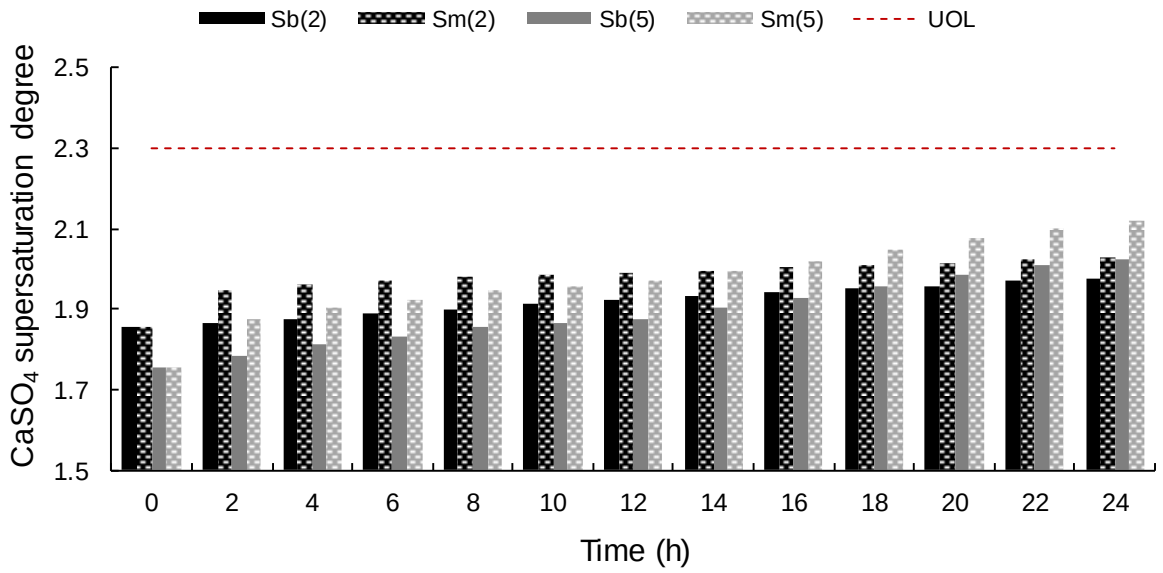

Figure 4.3-7: $CaSO_4$ supersaturation degree in the feed bulk (Sb) and at the membrane surface (Sm) for VMD treating SS1 [$S_{b(2)}$ and $S_{m(2)}$] and SS2 [$S_{b(5)}$ and $S_{m(5)}$] and upper operational limit (UOL) recommended for Nanofiltration (HYDRANAUTICS, 2013) (P_v = 64 mbar; T_{feed} = 50°C).

As can be seen, the $CaSO_4$ supersaturation degree is higher than 1 for both solutions even at the beginning of the test, similar to what happens to the real effluent (Chapter 2), indicating the high chances of $CaSO_4$ precipitation. Together with the high concentration it is important to highlight that, different from other salts, the solubility and nucleation time of calcium sulfate decrease with temperature increase (MERICQ; LABORIE; CABASSUD, 2010), with a solubility peak around 40°C (GRYTA, 2009) that does not vary strongly at the temperature that VMD was performed (50°C). This represents an aggravating factor for $CaSO_4$ precipitation, especially that at the membrane surface (S_m), increasing the risks of membrane scaling with time, and consequent supersaturation degree increase.

The increase on S_m was more intense for SS2 but no drastic changes on its the permeate flux was observed. The highest value found for both SS1 and SS2 solutions did not achieved the upper operational limit recommended for nanofiltration, but the S_m higher than 1 together with the high temperature of the feed solution already represents a high risk for calcium sulfate precipitation. As showed in previous work the scaling cause by the $CaSO_4$ can be physically reversible (MERICQ; LABORIE; CABASSUD, 2010). In this way, despite no drastic changes on the concentration of $CaSO_4$ could explain the permeate flux decay for SS1, the highest values of the supersaturation degree found for SS2 may explain the longer permeate flux restore time observed for SS2.

The increase of the salt concentration of the feed with time also causes an increase of the feed osmotic pressure, especially considering the efficiency of the system. The increase on the osmotic pressure leads to a decrease on the vapor pressure of the solution, decreasing the driving force of the VMD process. As the solutions tested have different pH and salt concentrations, the osmotic pressure is also different and its increase can reflect in different permeate flux decay behavior. Thus, the feed osmotic pressure was calculated for both feed solution as demonstrated by (RICCI et al., 2015b) considering all the salts in the solution and also the most abundant ions in the solution (calcium and sulfate). Results are shown in Figure 4.3-8.

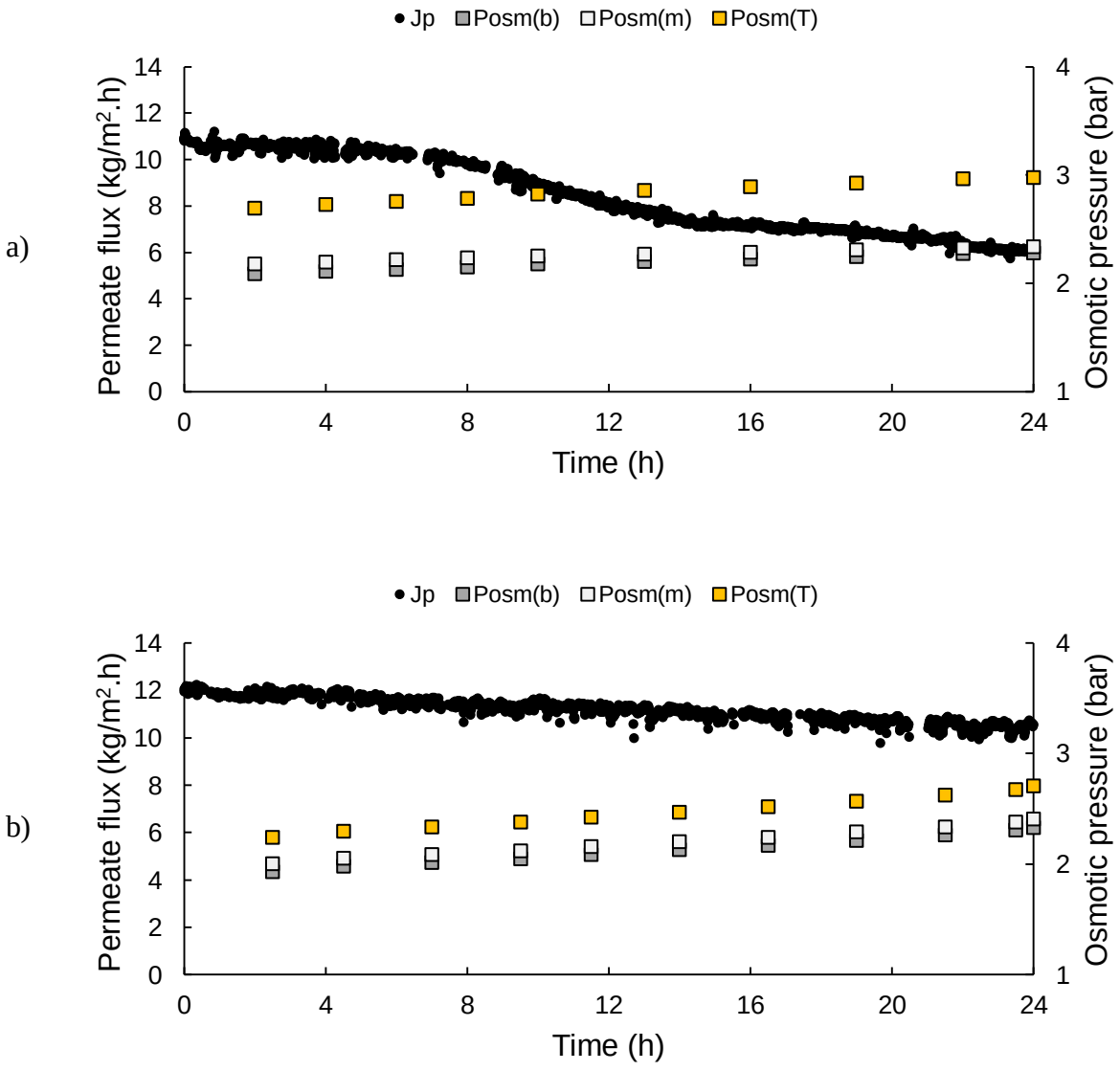

Figure 4.3-8: Experimental permeate flux (Jp) and feed osmotic pressure of total salts in the bulk ($P_{osm(T)}$) and of $CaSO_4$ in the bulk ($P_{osm(b)}$) and at the membrane surface ($P_{osm(m)}$) for VMD treating (a) SS1; and (b) SS2 (P_v = 64 mbar; T_{feed} = 50°C).

As it can be observed, the initial osmotic pressure for both solutions is similar regarding the ions calcium and sulfate, but the osmotic pressure referred to all salts in solution is higher for the SS1. The $CaSO_4$ osmotic pressure represents approximately 90% of the total osmotic pressure of SS2, while, for SS1, this contribution is 80%. By the results of supersaturation degree and osmotic pressure, it is clear that despite the salt concentration of SS1 being higher than that of SS2, the difference related to calcium and sulfate ions is not very pronounced, nor for the osmotic pressure and neither for $CaSO_4$ supersaturation degree. This shows that when the pH of SS1 is adjusted to 5.0, $CaSO_4$ is not the salt that precipitates the most to form the sludge.

With time, the feed osmotic pressure of the solutions showed similar increase behavior and that for calcium and sulfate was also similar in values, not explaining the permeate flux decay of SS1. However, regarding the values of the total salt osmotic pressure of SS1, it can be seen that by 6 h of test it reached 2.76, a value that SS2 did not reach in 24 h (maximum value for SS2 feed osmotic pressure was 2.71).

The permeate flux decay found for SS1 could be explained by precipitation of the calcium sulfate enhanced by the high osmotic pressure of the feed solution together with its high temperature. For SS2, despite the supersaturation degree found for $CaSO_4$ was higher than that obtained for SS1, this process could not have occurred because of the lower concentration of salts of the solution compared to SS1. Besides the scaling caused by $CaSO_4$, its precipitation at the membrane surface must be avoided, as this salt can also act as nuclei for the precipitation of other salts (MERICQ; LABORIE; CABASSUD, 2010) increasing even more the membrane scaling and drastically decreasing the permeate flux.

As discussed before, the increase on the osmotic pressure consequently decrease the vapor pressure of the solution. In this way, the vapor pressure on the bulk and at the membrane surface was also calculated for both SS1 and SS2 solutions, considering all dissolved salts, as it is directly affected by the osmotic pressure. Results are shown in Figure 4.3-9.

a)

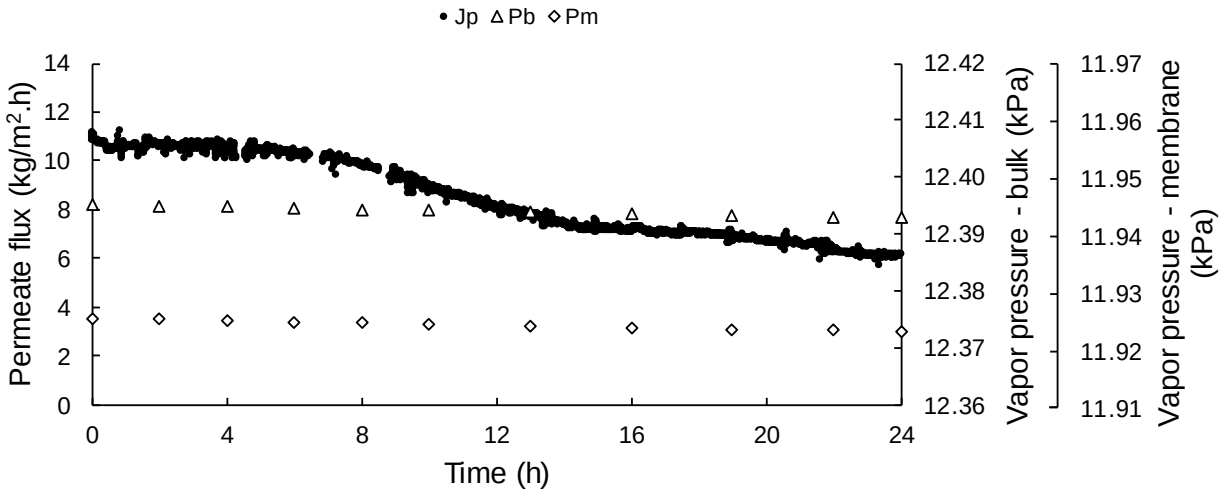

b)

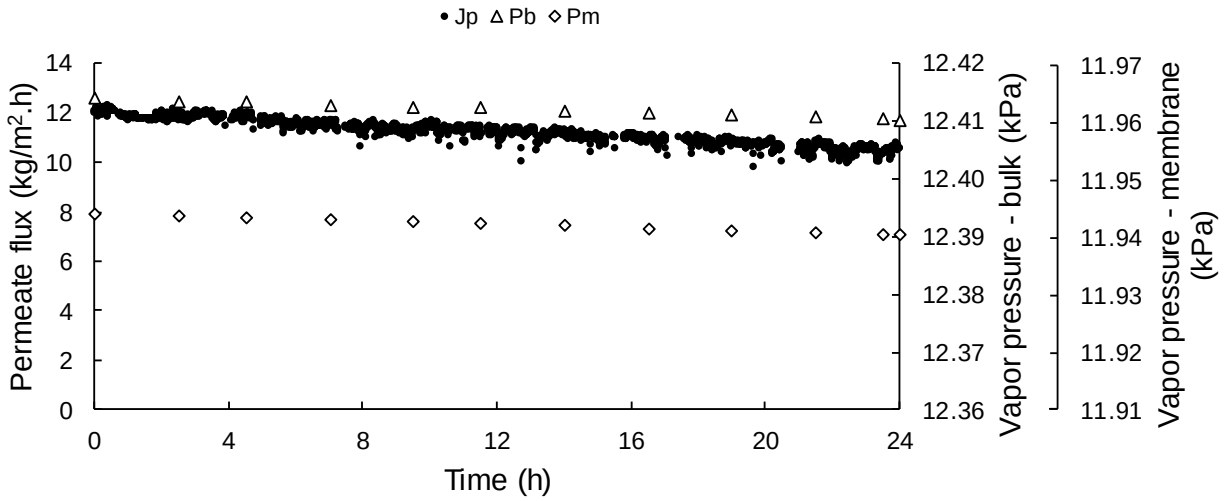

Figure 4.3-9: Experimental permeate flux (Jp) and vapor pressure in the bulk (P_b) and at the membrane surface (P_m) for VMD treating (a) SS1; and (b) SS2 (P_v = 64 mbar; T_{feed} = 50°C).

The mass transfer resistances were also calculated for both solutions at different times of the tests (Figure 4.3-10). It was observed that despite the different physicochemical characteristics of SS1 and SS2 the initial resistances for both was similar, with a fouling resistance slightly higher for SS1. With time, the resistances obtained for SS2 did not presented much variation, expect for a small and gradual increase on R_f especially after 14 h which explains the also gradual permeated flux decay observed. The maximum ratio between the R_f and R_t found in the end of the SS2 test was 5%.

a)

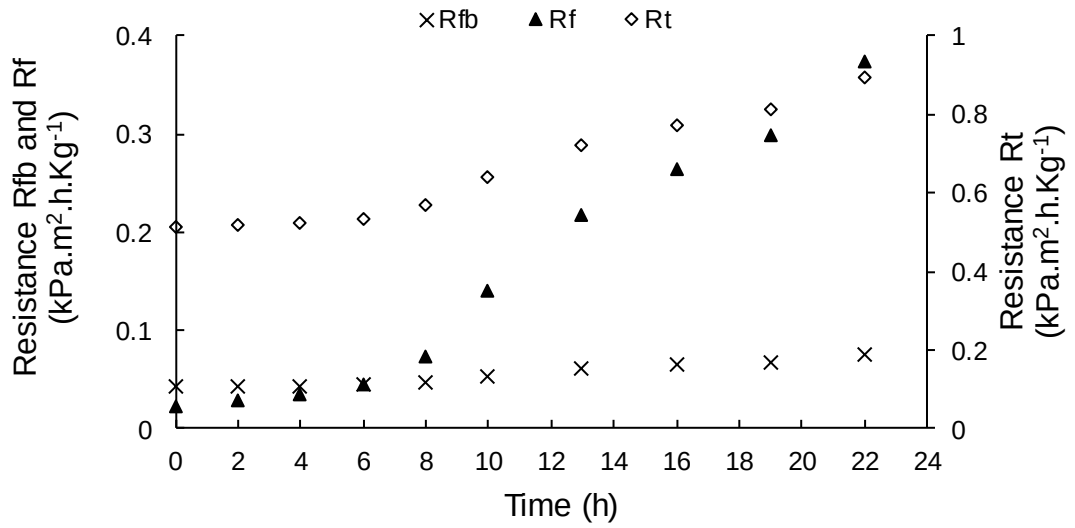

b)

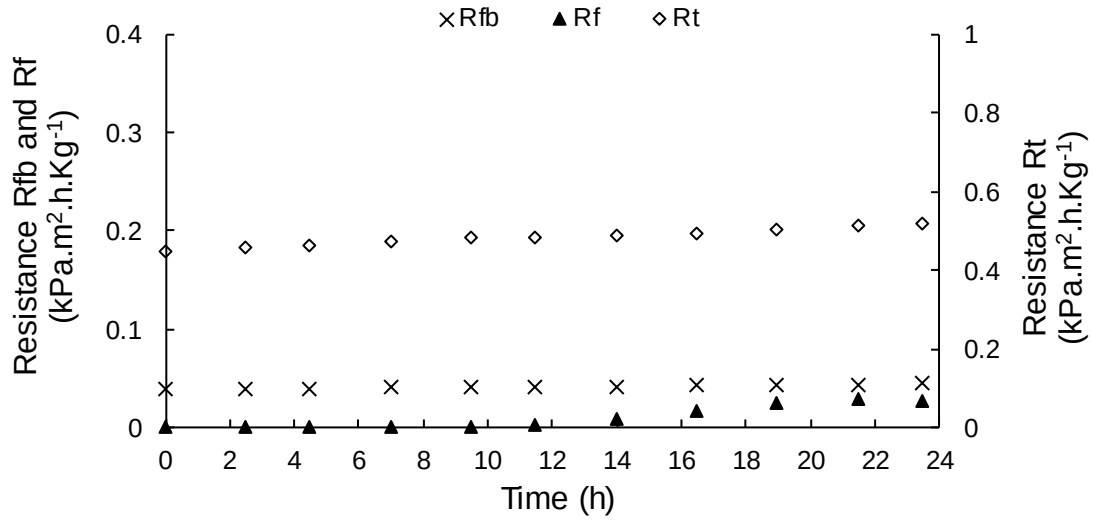

Figure 4.3-10: Feed boundary layer resistance (R_{fb}), fouling resistance (R_f) and total resistance (R_t) for (a) SS1; and (b) SS2 in a function of time.

For SS1, it can be observed a faster and more intense increase of the R_f, which also led to an increase of the R_t, explaining the sharp decay showed by the permeate flux after 6 h. The more pronounced permeate flux decay started to occur at a R_t around 0.53-0.56 kPa.m^2.h.kg^{-1} and R_f ranging from 0.05 to 0.07 kPa.m^2.h.kg^{-1}. R_f and R_t continued to increase even after 15 h, when the permeate flux showed a less intense decrease. The R_t increased 76% after 24 h of test with SS1, and the ratio between the R_f and R_t increased from 5% to 42% in the end of the test, showing the influence of this resistance on performance of the system . Thus, it can be observed that the main cause of the permeate flux decline for VMD treating SS1 was the membrane fouling. The R_{fb} remained practically constant for both solutions as the temperature

at the bulk and at the membrane surface remained constant and also the molar fraction and activity coefficient of the water, as the concentration of the solution is not very high.

Hermia's model adapted to cross-flow filtration mode (SRISURICHAN; JIRARATANANON; FANE, 2006) was applied to the experimental data obtained for VMD in order to elucidate possible mechanisms of fouling. The model was applied for the test with SS1 in three different blocks that showed different permeate flux decay (Table 4.3-1), as for test of SS2 as a whole as flux decreased gradually from the beginning to the end of the test (Table 4.3-2).

Table 4.3-1: Evaluation of fouling mechanisms using Hermia's model for VMD treating SS1 for 24h.

Time range (h)	Jf/Ji	Model											
		Complete blocking filtration			Standard blocking filtration			Intermediate blocking filtration			Cake filtration		
		Jo ($L\ m^{-2}h^{-1}$)	k	R^2	Jo ($L\ m^{-2}h^{-1}$)	k	R^2	Jo ($L\ m^{-2}h^{-1}$)	k	R^2	Jo ($L\ m^{-2}h^{-1}$)	k	R^2
0-6	0.97	10.8	0.00650	0.94	10.8	0.00099	0.94	10.8	0.00061	0.94	10.8	0.00011	0.94
7-15	0.80	10.1	0.04979	0.98	10.1	0.00836	0.97	10.1	0.00561	0.97	10.2	0.00127	0.96
15-24	0.85	7.5	0.02084	0.95	7.5	0.00404	0.94	7.5	0.00313	0.94	7.6	0.00094	0.93

Jf: final permeate flux
Ji: initial permeate flux
Jo: original permeate flux (predicted by the model)
k: coefficient depending on the flow rate and solution properties
R^2: regression coefficient

As can be observed, for VMD treating SS1 the fouling mechanisms found for each block was different. In the first moment (0-6 h). the permeate flux decrease was very low and all the fouling models had a similar adjust to the experimental data (around 95%). This results indicate that all fouling mechanisms should have occurred in the same proportion in this period, but in small scale and intensity as seen by the lowest mass transfer coefficient found for all models.

For the second moment (7-15 h), in which the highest decay was observed for the permeate flux, the model that showed the best adjustment was the complete blocking filtration (98%) with the highest mass transfer coefficient obtained. It is important to highlight that the data form this part of the test were those that best fit the models' equations as the influence of fouling in the permeate flux was very pronounced. Results indicate that most of the $CaSO_4$ that precipitated at the membrane surface acted by completely blocking the pores,

consequently decreasing the available pore area, explaining the sharp decay observed for the permeate flux.

Finally, for the third moment (15-24 h), when a less pronounced decrease is observed for permeate flux, the adjust of experimental data to the complete blocking filtration still presents the higher value found (95%), lower than that found previously. This result can be explained because this was the mechanism that was more intense in the second moment (7-15h) and still represents the main fouling mechanism. However, with time, the deposited salts at the membrane surface could have prevent other formed crystals from completely blocking the pores, allowing for a lower decrease on the permeate flux.

Table 4.3-2: Evaluation of fouling mechanisms using Hermia's model for VMD treating SS1 for 24h.

Time range (h)	Jf/Ji	Model											
		Complete blocking filtration			Standard blocking filtration			Intermediate blocking filtration			Cake filtration		
		Jo ($L\ m^{-2}h^{-1}$)	k	R^2	Jo ($L\ m^{-2}h^{-1}$)	k	R^2	Jo ($L\ m^{-2}h^{-1}$)	k	R^2	Jo ($L\ m^{-2}h^{-1}$)	k	R^2
0-24	0.87	12.3	0.00584	0.95	12.3	0.00086	0.95	12.3	0.00051	0.95	12.3	0.00009	0.95

Jf: final permeate flux
Ji: initial permeate flux
Jo: original permeate flux (predicted by the model)
k: coefficient depending on the flow rate and solution properties
R^2: regression coefficient

For the test with SS2, on the other hand, as no pronounced decay of permeate flux was observed, the same adjust was observed for all the models to experimental data, with very low mass transfer coefficient, showing the respective fouling mechanisms should have the same contribution on the permeate flux reduction with time and they occurred in small scale.

After the end of the 24 h test and diluting of the concentrate, both of the membranes went through a physical cleaning procedure with distillate water. Results showed that water membrane permeability (K_M) remained the same for the membrane used for the test with SS2 (K_M/K_{M0} = 1.01) but a decrease was observed after the test with the acid synthetic solution (SS1) (K_M/K_{M0} = 0.87). It indicates that the fouling that occurred during the test could not be removed physically, being chemically reversible or irreversible. This result differs from that obtained by other authors (MERICQ; LABORIE; CABASSUD, 2010) that found that the scaling cause by $CaSO_4$ was physically reversible. This difference can be due to the different

composition and pH of the feed solutions, higher concentration of calcium and sulfate in the solutions studied in this work, and longer monitoring time of the test.

Thus, results showed that the despite the VMD membrane performance is not directly influenced by the feed pH. it can highly influence the composition of the feed solution. The use of an acid solution as feed showed some drawbacks as lower permeate flux, fast and sharp permeate flux decay (at a recovery rate of less than 5%), and irreversible or chemically reversible membrane fouling. Thus, the adjustment of the pH to 5.0 makes the solution less aggressive to the membrane and equipment integrity and also allowed for a better performance of the VMD.

4.3.4 Determination of the optimal VMD permeate recovery rate

After the selection of the best operational conditions for VMD (vacuum pressure, feed temperature and feed pH) a recovery test was performed. The test ran until a sharp decrease of the permeate flux was observed and / or a small value of permeate flux was obtained. After the end of the test, the same procedure of diluting the concentrate performed on the previous test was done and permeate flux was checked. During the test, the difference between the feed inlet and outlet pressure was checked and the ratio of the pressure difference at each recovery rate and the initial pressure plotted together with the permeate flux in Figure 4.3-11.

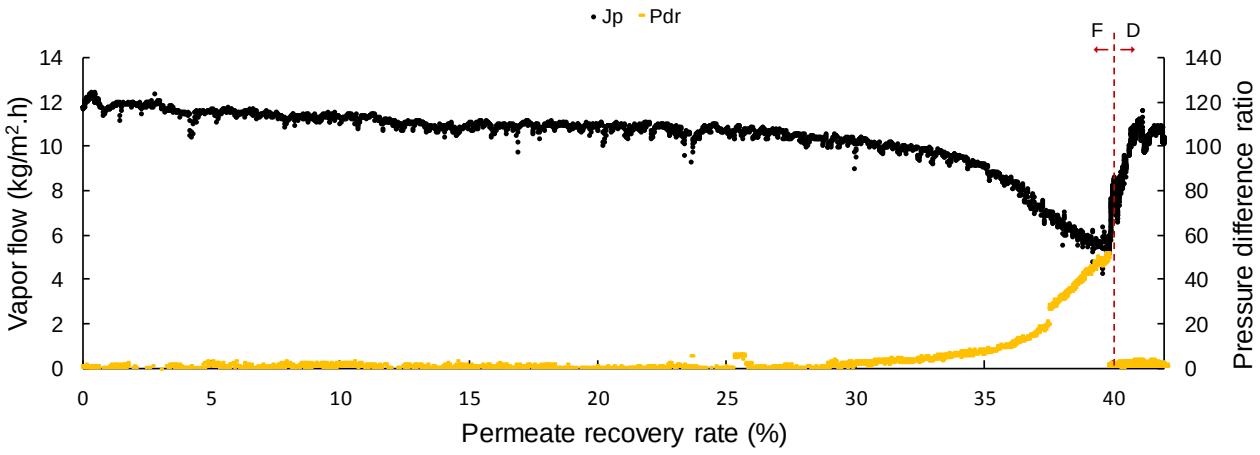

Figure 4.3-11: Permeate flux (Jp) and pressure difference ratio (Pdr) in a function of time for VMD using SS2 as feed before (F) and after (D) the dilution of the concentrate (indicated by red line)

As can be observed, the permeate flux remained practically constant until the permeate recovery rate of 30-35%. with a discreet decrease on the flux ($\Delta Jp/\Delta t$ = -0.057), very similar

to that obtained in the previous test (SS2 for 24h). From the beginning of the test to this point the permeate flux decreased approximately 17% from its initial value. After this, a sharp decrease was observed ($\Delta Jp/\Delta t$ = -0.521), reducing the permeate flux to half of the value observed at 35%. Simultaneously, it could be observed that the pressure difference ratio remained constant and close to 1 until the permeate recovery rate of 30%, after which the ratio of the pressure inlet and pressure outlet started to increase. It means that the pressure inlet started to increase as permeate recovery rate increased and this was more intense after the recovery rate of 35%. As the feed flow rate was kept constant during the test, the increase on the pressure difference may be associate to the increase on the osmotic pressure of the feed.

In order to understand the role played by the calcium sulfate on membrane fouling, its supersaturation degree was calculated for the bulk and membrane surface in different permeate recovery rates and results are shown in Table 4.3-3.

Table 4.3-3: $CaSO_4$ supersaturation index for the feed bulk (Sb) and membrane surface (Sm) in a function of the permeate recovery rate (pH = 5; T_{feed} = 50°C; P_v = 64 mbar).

Permeate recovery rate (%)	**0**	**5**	**10**	**15**	**20**	**25**	**30**	**35**	**40**
S_b	1.42	1.45	1.48	1.51	1.55	1.59	1.64	1.72	1.74
S_m	1.42	1.52	1.55	1.58	1.63	1.67	1.72	1.78	1.78

As can be observed, the supersaturation degree of the calcium sulfate was very high, as expected, because of the initial concentration of the feed and the high rejection showed by VMD. Despite up to 45% of permeate recovery rate, the $CaSO_4$ supersaturation degree remained below the critical value of 2.3 considered as the upper operational limit for nanofiltration (HYDRANAUTICS, 2013), considering the effect of the temperature on $CaSO_4$ solubility discussed previously, the values found showed that the conditions were very favorable for the precipitation of this salt. In this way, the permeate flux decay observed after 30-35% permeate recovery rate can be directly liked to scaling caused by calcium sulfate.

As the osmotic pressure can be related to the permeate flux decay for SS1 solution, it was also calculated for different recovery rates and values were compared. Figure 4.3-12 shows the osmotic pressure and conductivity rejection in a function of the permeate recovery rate.

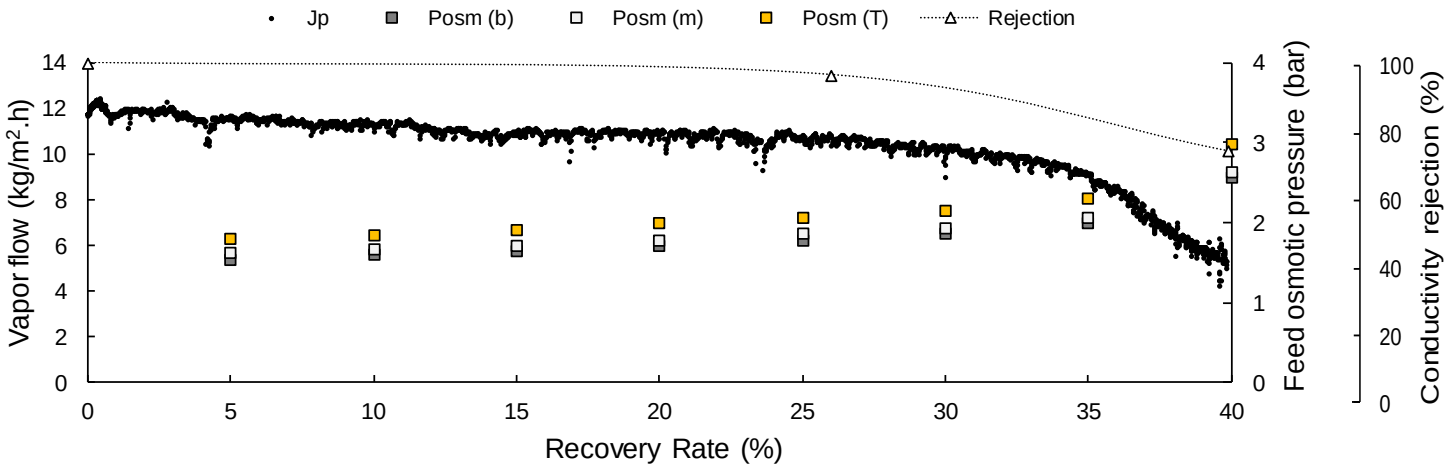

Figure 4.3-12: Permeate flux (Jp). conductivity rejection and feed osmotic pressure of total salt in the bulk ($P_{osm(T)}$) and of $CaSO_4$ in the bulk ($P_{osm(b)}$) and at the membrane surface ($P_{osm(m)}$) in a function of permeate recovery rate for VMD using SS2 as feed (pH = 5; T_{feed} = 50°C; P_v = 64 mbar).

As expected, the osmotic pressure increased with feed concentration. The permeate flux sharp decay took place between 30% and 35% of permeate recovery rate, where the total salt osmotic pressure was 2.16 and 2.35, respectively. This result differs from that observed in the previous test of VMD treating acid solution (SS1) when a sharp decay of the permeate flux was observed (P_{osm} = 2.76). As observed in this test (VMD treating SS1), the high osmotic pressure of the solution could have favor the $CaSO_4$ precipitation at the membrane surface, causing an intense permeate flux decrease. However, this precipitation only took place in the SS1 solution after the feed presented a higher osmotic pressure than that found for the SS2 at 30% of permeate recovery rate, showing that the pH of the solution can influence the maximum osmotic pressure supported before $CaSO_4$ precipitates.

The vapor pressure of the solution was also calculated for different permeate recovery rates (Figure 4.3-13). Results showed that until the permeate recovery rate of 30%, the vapor pressure calculated for both the feed and membrane surface presented a gradual slow decay and this decay becomes more pronounced after 30%. This is due to the increase in osmotic pressure, what can influence not only the driving force of VMD, but also membrane fouling and membrane wetting. After 30%, the permeate flux decreased sharply and the rejection efficiency of the system also reduced, showing it was a critical point.

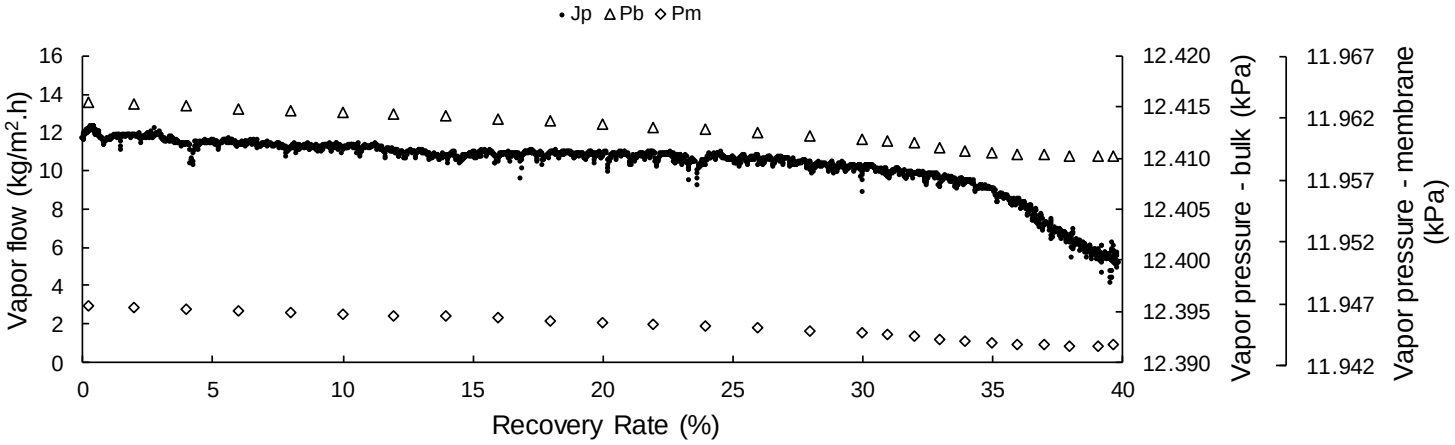

Figure 4.3-13: Permeate flux (Jp) and vapor pressure of the solution calculated for the bulk (Pb) and the membrane surface (Pm) in a function of permeate recovery rate for VMD using SS2 as feed (pH = 5; T_{feed} = 50°C; P_v = 64 mbar).

The resistances were also calculated for different permeate recovery rates (Figure 4.3-14). The result found was very similar for that found for the 24 h of SS2, with R_t of approximately 0.45 kPa.m^2.h.kg^{-1}, increasing gradually and slowly until the recovery rate of 30%, where the R_f started to increase. The increase of the R_f was very similar for that obtained for VMD treating SS1 for 24 h. At 30% of permeate recovery rate, the osmotic pressure reached 2.7 bar and, simultaneously, R_f started to increase, increasing the Rt until the end of the test. The sharpest decay of permeate flux occurred at a R_t of 0.53-0.56 kPa.m^2.h.kg^{-1}, a value similar to that found when an intense permeate decay was observed for VMD treating SS1, and R_f of 0.02-0.06 kPa.m^2.h.kg^{-1}.

R_t increased 125% compared to its initial value and 97% compared to R_t at the recovery rate of 30%. The R_{fb} remained practically constant until the recovery rate of 40% as the temperature at the bulk and at the membrane surface remained constant and also the molar fraction and activity coefficient of the water, as the concentration of the solution is not very high. After 35%, a discreet increase was observed as the permeate flux sharpest decay was observed in this recovery rate.

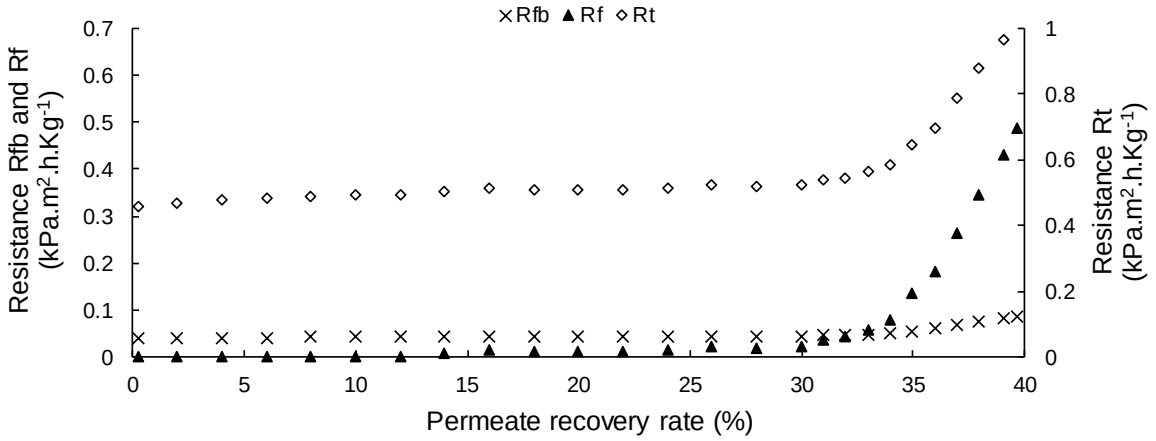

Figure 4.3-14: Feed boundary layer resistance (Rfb). fouling resistance (Rf) and total resistance (Rt) for VMD treating SS2 in a function of permeate recovery rate (pH = 5; T_{feed} = 50°C; P_v = 64 mbar).

Hermia's model was also applied for the permeate flux data obtained in the recovery rate test in two different moments (Table 4.3-4). The first, from the beginning of the test to the permeate recovery rate of 30%, in which a gradual and not pronounced flux decay was observed, the models showed low mass transfer coefficient and similar adjustments and the intermediate blocking filtration and cake filtration were the models that adjusted better to experimental data (91%). This result is consistent to those found for the VMD treating SS2 for 24 h, but the higher monitoring time of permeate flux data of the recovery rate test showed that the contributions of intermediate blocking and cake filtration are slighly higher.

Table 4.3-4: Evaluation of fouling mechanisms using Hermia's model for VMD treating SS1.

Recovery Rate range (%)	Jf/Ji	Model											
		Complete blocking filtration			Standard blocking filtration			Intermediate blocking filtration			Cake filtration		
		Jo (L m^{-2}h^{-1})	k	R^2	Jo (L m^{-2}h^{-1})	k	R^2	Jo (L m^{-2}h^{-1})	k	R^2	Jo (L m^{-2}h^{-1})	k	R^2
0-30	0.88	12.0	0.00476	0.90	12.0	0.00071	0.90	12.0	0.00042	0.91	12.0	0.00008	0.91
30-40	0.54	10.9	0.05918	0.95	11.1	0.01069	0.94	11.5	0.00777	0.92	12.8	0.00208	0.89

Jf: final permeate flux
Ji: initial permeate flux
Jo: original permeate flux (predicted by the model)
k: coefficient depending on the flow rate and solution properties
R^2: regression coefficient

The second moment, after 30% of permeate recovery rate, a sharp decay was observed. Hermia's model indicates that the fouling mechanism the most contributed to this process was

the complete blocking of the pores. The same result was found for the sharp decay observed for VMD treating SS1. From the results obtained is it possible to conclude that when treating the synthetic solutions evaluated here there is a critical point of salt concentration which enhance $CaSO_4$ precipitation at the membrane surface, completely blocking the pores and making the permeate flux drop drastically. The optimum operational recovery rate can be considered that point before this process starts. The test performed here indicates that this recovery rate would be around 30-33% when SS2 is used as feed solution at the temperature of 50^{o}C.

Thus. the results indicate that. for feed solutions with the composition used in this study, the performance of VMD may be limited by the feed osmotic pressure, with a critical maximum value close to 2.7. The increase of the osmotic pressure decreases the vapor pressure, decreasing the driving force of VMD, and also favor membrane scaling by the precipitation of calcium sulfate. This process can lead to the complete blocking of the pores, increasing the fouling resistance of the membrane and making the permeate flux decreases sharply.

4.4 CONCLUSIONS

VMD was tested for the treatment of gold mining effluent using a synthetic solution. Results showed that this technique can be successful applied for wastewater reclamation. Despite the composition of the feed. the flux initially observed for the solution was similar to those obtained with distillate water. showing that VMD is indeed a robust system and that it can provide high permeate fluxes. The influence of feed temperature. vacuum pressure. pH and recovery was tested.

As expected. the higher the feed temperature and the vacuum pressure. higher is the permeate flux. A feed temperature of 50^{o}C and a vacuum pressure of 64 mbar were chosen as the best operational conditions. maintaining the feed flow rate at 1.25 kg/h. The pH = 5.0 was chosen as the more suitable feed pH for this treatment. not only because it is less aggressive to the membrane. but as it allowed for a higher and more stable permeate flux and higher recovery rates without pronounced changes in the permeate flux.

Recovery rate test showed that a maximum recovery rate of 30% that could be achieved with a high rejection efficiency of the system (close to 100%) and a high permeate flux. After this rate the pressure inlet starts to increase and permeate flux can decrease sharply.

The $CaSO_4$ is the most likely scalant for the VMD membrane and its precipitation can be favorable both by the high temperature and high osmotic pressure of the feed solution. The precipitation of this salt seems to complete block the membrane pores causing sharp decay on the permeate flux.

As VMD tests were performed in France using a synthetic solution at pH 5.0 and showed promising results. those needed to be validated and compared to DCMD. so that an indicative its performance on the real contaminated gold mining effluent treatment could be accessed.

CHAPTER 5:

THE FEASIBILITY OF DIRECT CONTACT MEMBRANE DISTILLATION (DCMD) FOR SULFURIC ACID PLANT WASTEWATER RECLAMATION

5.1 INTRODUCTION

The evaluation of the feasibility of membrane distillation process (MD) on the treatment of gold mining effluent was already demonstrated for direct contact membrane distillation (DCMD) treating the real gold mining effluent at its natural pH (around 2.0) and its performance was compared to that obtained by the Nanofiltration in Chapter 3. It was showed that DCMD is a suitable and effective technology on the treatment of gold mining effluent.

In Chapter 4, another configuration of MD was also tested. The vacuum membrane distillation (VMD) showed a good performance on treating a synthetic solution with composition similar to that presented by the gold mining effluent at pH 5.0. However, as the tests were performed in France and the real effluent could not be tested as feed solution.

In order to compare the technologies tested in this work it is necessary to evaluate the performance of each on the treatment of the same feed solution, as its physicochemical characteristics, salt concentration and pH can directly influence the performance of membrane distillation. Thus, the objective of this study was to evaluate the use of DCMD on the treatment of the same synthetic solution used for VMD, selecting the best operational conditions and comparing the results obtained for both VMD and DCMD systems in terms of system rejection efficiency, membrane fouling, membrane wetting and permeate flux.

5.2 MATERIALS AND METHODS

5.2.1 Sampling

In order to compare the performance of the VMD on treating a synthetic solution with a composition similar to the gold mining effluent at pH = 5.0, DCMD tests were performed using as feed solution the same solution used for VMD.

For this, salts containing the major components of this effluent (Ca, Mg, Fe, Zn, chloride, sulfate) were added to distillate water using as source of those components the salts $CaSO_4$, $FeSO_4$, $MgSO_4$, Na_2SO_4, $Al_2(SO_4)_3$, KCl and $ZnCl_2$. The salts were dissolved in hot distillate water (40^oC) under agitation and its pH was adjusted to 2.0 using sulfuric acid (H_2SO_4). As the acid feed can reduce the membrane lifespan, the pH of the synthetic solution was adjusted to 5.0 using sodium hydroxide (NaOH) and the supernatant collected after precipitation of the solids and was used as feed solution. The physicochemical characterization of the gold mining effluent and the synthetic solution used on this work is presented on Table 5.2-1.

Table 5.2-1: Physicochemical characterization of the gold mining effluent and the synthetic solutions SS1 and SS2

Parameter	**Unit**	**Gold Mining Effluent**	*Acid Synthetic solution*	**DCMD feed** *(Synthetic solution after pH adjustment)*
pH		1.7 ± 0.2	2.0 ± 0.1	5.0 ± 0.1
Conductiviy	(mS/cm)	11.5 ± 2.3	7.8 ± 0.5	5.64 ± 0.6
Sulfate	(mg/L)	4191 ± 1180	6000 ± 3000	4316 ± 432
Arsenic	(mg/L)	668 ± 210	-	-
Calcium	(mg/L)	518 ± 213	600 ± 30	216 ± 22
Magnesium	(mg/L)	274 ± 134	300 ± 15	432 ± 43
Iron	(mg/L)	102 ± 20	100 ± 5	72 ± 7
Aluminium	(mg/L)	100 ± 14	100 ± 5	72 ± 7
Zinc	(mg/L)	73 ± 30	80 ± 4	58 ± 4
Chloride	(mg/L)	62 ± 24	60 ± 3	43 ± 3
Sodium	(mg/L)	32 ± 13	40 ± 2	29 ± 2
Potassium	(mg/L)	40 ± 6	40 ± 2	29 ± 2

* - not used on the synthetic solution

5.2.2 DCMD Experimental setup

MD assays were also performed on a laboratory scale in the filtration unit shown in Figure 5.2-1. MD module is composed of two compartments between which the membrane was disposed. In one of the compartments, the hot effluent is circulated and in the other, cooled water. The feed tank is followed by a thermometer, a peristaltic pump, and a rotameter before the membrane module. Before being recirculated to the feed tank, the concentrate passed through a heating system in order to maintain the effluent at the temperature of the test. The cold water reservoir (distillate tank) is placed on a digital balance and it is also followed by a thermometer, peristaltic pump, and a rotameter before the membrane module. The distillate passes through a cooling system (chiller) before being recirculated to the distillate tank.

The temperature differential is needed so that the permeate flux can be established. This flux was measured using the data collected in the digital balance as the increase in the distillate mass is provided by permeate production.

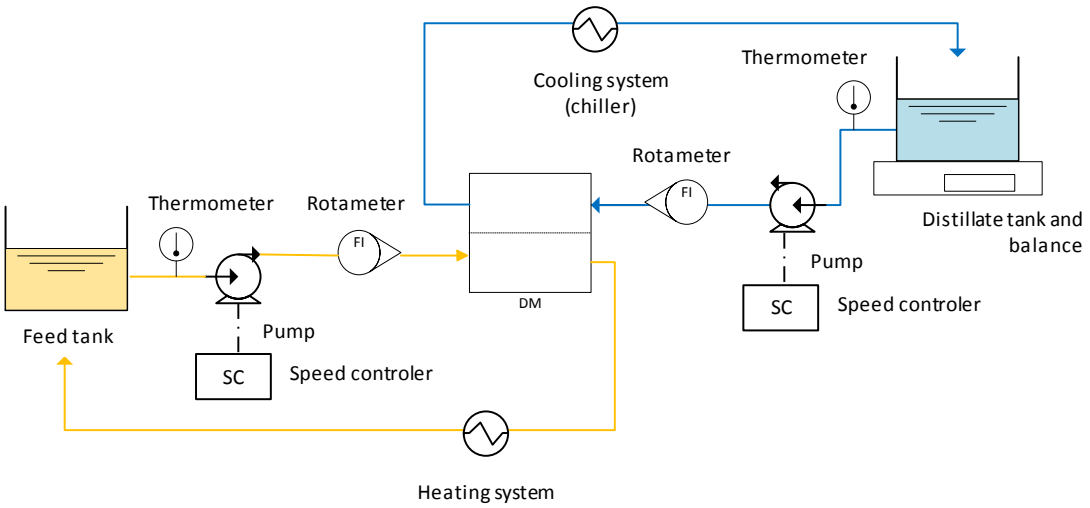

Figure 5.2-1: Schematic diagram of the MD system

For the membrane cell, a Sterlitech® (CF042D Crossflow Cell) cell was used, in which was positioned a new Sterlitech® PTFE microfiltration membrane. This membrane has an average pore size of 0.2 µm and for the experiment, the filtration area was 0.0042 m^2.

5.2.3 DCMD experimental procedure

Before the tests, a virgin membrane passed through a cleaning procedure in which it was submerged in a hydrochloric acid (HCl) 0.2% w/w solution for 20 minutes and then washed with distillate water. After chemical cleaning, water permeability was measured using distillate water as feed in three different temperatures, 40, 50 and 60^oC.

DCMD was used to treat the synthetic solution. The tests were performed in batch mode with recirculation of the concentrate. The distillate temperature was fixed at 25^oC which is the room temperature in Brazil so that in a full-scale application there is no need for distillate cooling other than cooling that may occur in the equalization tank. The influence of the feed temperature, feed flow rate and permeate recovery rate was studied.

For this, different feed temperatures were evaluated. The temperature was kept at 40 ± 1°C, 45 ± 1°C, 50 ± 1°C, 55 ± 1°C and 60 ± 1°C by heating up the synthetic solution on a hotplate. This temperature range was selected considering the following limits: the natural minimum temperature of the gold mining effluent (40°C) and a maximum temperature (60°C) in which the feed can me maintained by using solar heating, so that the energy costs related to feed heating could be reduced.

To evaluate the feed flow rate, three different feed flow rates was evaluated (0.55, 0.75 and 1.00 liters per minute (LPM)). This range was chosen as it can maintain the system in intermediate-turbulent state, in which concentration polarization can be minimized. Finally, for the maximum permeate recovery rate evaluation, DCMD was applied until the permeate flux was drastically reduced or the quality of the distillate could be compromised.

For all the tests, the permeate flux and feed and distillate conductivity were continuously measured and permeate samples were taken out at different times for physicochemical analysis.

5.2.4 Analytical Methods

The mining effluent and permeates were characterized in terms of the following physicochemical parameters: pH (pHmeter Qualxtron QX 1500); conductivity (Hanna conductivity meter HI 9835); calcium and magnesium cations (Dionex ICS-1000 ion chromatograph equipped with AS-22 and ICS 12-A columns); arsenic (DHAR et al.; 2004); and sulfate and chloride (APHA, 2017).

5.2.5 Calculation

In the DCMD system, the permeate flux [$J_{P(MD)}$] is calculated according to Equation (1):

$$J_{P(MD)} = \frac{m_{di} - m_{df}}{A_m.(t_i - t_f)} \quad (1)$$

Where m_{di} and m_{df} correspond to the mass (kg) of the initial and final distillate, respectively. A_m is the area of the membrane (in m^2), t_i and t_f correspond to the initial and final time, respectively.

The recovery rate [RR_{MD}] is calculated by Equation (2):

$$RR_{MD} = \frac{m_{df} - m_{di}}{m_{fi}} .100 \quad (2)$$

Where m_{fi} corresponds to the mass (kg) of the initial feed.

It is important to note that since the DCMD process is initiated with a determined volume of cold water and over time the permeate volume that is produced is added to the initial water

volume, the calculation of the concentration of a species in the permeate is made from Equation (3):

$$c_{p(MD)} = \frac{c_d . v_{td,y}}{v_{p,y}} . 100 \quad (3)$$

Being $c_{p(MD)}$ and c_d the concentration of the species in the permeate and the distillate, respectively. The $v_{td,y}$ is the total volume of distillate in time y and $v_{p,y}$ is the volume of permeate at the same time (y).

The rejection [R(%)] of pollutants and conductivity was calculated using Equation 4, considering the conductivity/pollutant concentration of the feed (C_f) and permeate (C_p) streams. The rejection [$R(\%)$] was calculated on the basis of its concentration in the permeate, not the distillate.

$$R(\%) = \frac{C_f - C_p}{C_f} . 100 \quad (4)$$

The specific energy consumption (SEC) was defined by the relation between the rate of work done by the pump (W_{pump}) and permeate flow rate (Q_p) (Zhu et al., 2009), as follows:

$$SEC = \frac{W_{pump}}{Q_p} \quad (5)$$

W_{pump} was calculated by multiplying the volumetric feed flow rate (Q_f) by ΔP, which is assumed to be equivalent to the permeate pressure

$$W_{pump} = \Delta P \times Q_f \quad (6)$$

By combining Equations 2, 5 and 6, the equation to determine SEC can be rewritten as follows:

$$SEC = \frac{\Delta P}{RR} \quad (7)$$

The differences in osmotic pressure ($\Delta\pi$) between the concentrate and permeate for different permeate recovery rates were estimated by the Equation of Van't Hoff, described in Equation (8).

$$\Delta\pi = RT\Delta\Sigma(C_c - C_p) \quad (8)$$

For this, it is used the universal gas constant (R), temperature of permeation (T) and the sum of the difference of the molar concentration of the main dissolved species that are present in the concentrate (C_c) and permeate (C_p) at each RR. In this study, data of pH and concentration of sulfate, calcium and magnesium were used to calculate the osmotic pressure.

The concentration of salt in at the membrane surface (C_m) was calculated using the molar concentration of the same salt in the concentrate (C_c) and permeate (C_p), the permeate flux ($J_{p(VMD)}$, in $m^3\ h^{-1}\ m^{-2}$) and the mass transfer coefficient (k), as indicated by (NOBLE; STERN, 1995):

$$\frac{C_m - C_p}{C_r - C_p} = \exp\left(\frac{J_{p(VMD)}}{k}\right) \quad (9)$$

k was calculated as demonstrated by (RICCI et al., 2015a). Considering the set of conditions used in this study, the numerical value obtained for sulfate (SO_4^{-2}) was 7.56×10^{-5} $m.s^{-1}$ and for calcium (Ca^{+2}), 5.92×10^{-5} $m.s^{-1}$.

Membrane resistance (R_m), feed boundary layer resistance (R_{fb}) and permeate boundary layer resistance (R_{pb}) were calculated as shown by Equations (10), (11) and (12) (SRISURICHAN; JIRARATANANON; FANE, 2006).

$$R_m = \frac{P_1 - P_2}{J_{p(MD)}} \quad (10)$$

$$R_{fb} = \frac{P_f - P_1}{J_{p(MD)}} \quad (11)$$

$$R_{pb} = \frac{P_2 - P_p}{J_{p(MD)}} \quad (12)$$

Those calculations were made considering values of vapor pressure at the feed (P_1) and permeate (P_2) membrane surface and at the bulk feed (P_f) and permeate (P_p), and $J_{p(MD)}$, the permeate flux.

Equation 13 was used to calculate the pressures and Equation 14 and 15 to estimate the temperatures at the membrane surface (SRISURICHAN; JIRARATANANON; FANE, 2006).

$$P = EXP\left(23.238 - \frac{3841}{T-45}\right) \quad (13)$$

$$T_{w,f} = \frac{h_m\left(T_p + \left({h_f}/{h_p}\right)T_f\right) + h_f T_f - J_{p(MD)}\Delta H_v}{h_m + h_f(1 + \frac{h_m}{h_p})} \quad (14)$$

$$T_{w,p} = \frac{h_m\left(T_f + \left({h_p}/{h_f}\right)T_p\right) + h_p T_p - J_{p(MD)}\Delta H_v}{h_m + h_p(1 + \frac{h_m}{h_f})} \quad (15)$$

Where $T_{w,f}$ and $T_{w,p}$ are the temperatures at interface for feed and permeate, respectively, calculated from the temperatures at the bulk for feed (T_f) and permeate (T_p), the convective heat transfer coefficient of the membrane (h_m), feed (h_f) and permeate (h_p), the vaporization heat (ΔH_v) and permeate flux ($J_{p(MD)}$).

As described in Chapter 4, as the feed used refers to a solution, to better estimate the vapor pressures, the value obtained by Equation (13) was multiplied by the activity of the water (α) and the molar fraction of water of the solution (M_{H20}) (CHIAM; SARBATLY, 2014; ZHAO et al., 2011), as follows:

$$P' = P * \alpha * M_{H20} \quad (16)$$

5.3 RESULTS AND DISCUSSION

5.2.6 Influence of the temperature on DCMD performance

It is well known that the increase on the feed temperature for a fix distillate temperature lead to a higher permeate flux as the temperature difference between the feed and permeate are the driving force of the DCMD process. Higher temperature difference can also increase the wetting time experienced by the membrane. On the other hand, high feed temperature can lead to an increase on the heating energy demand of the system, increasing its Opex. In this

way, the influence of the temperature was evaluated in order to choose the more suitable feed temperature for DCMD application (Figure 5.3-1).

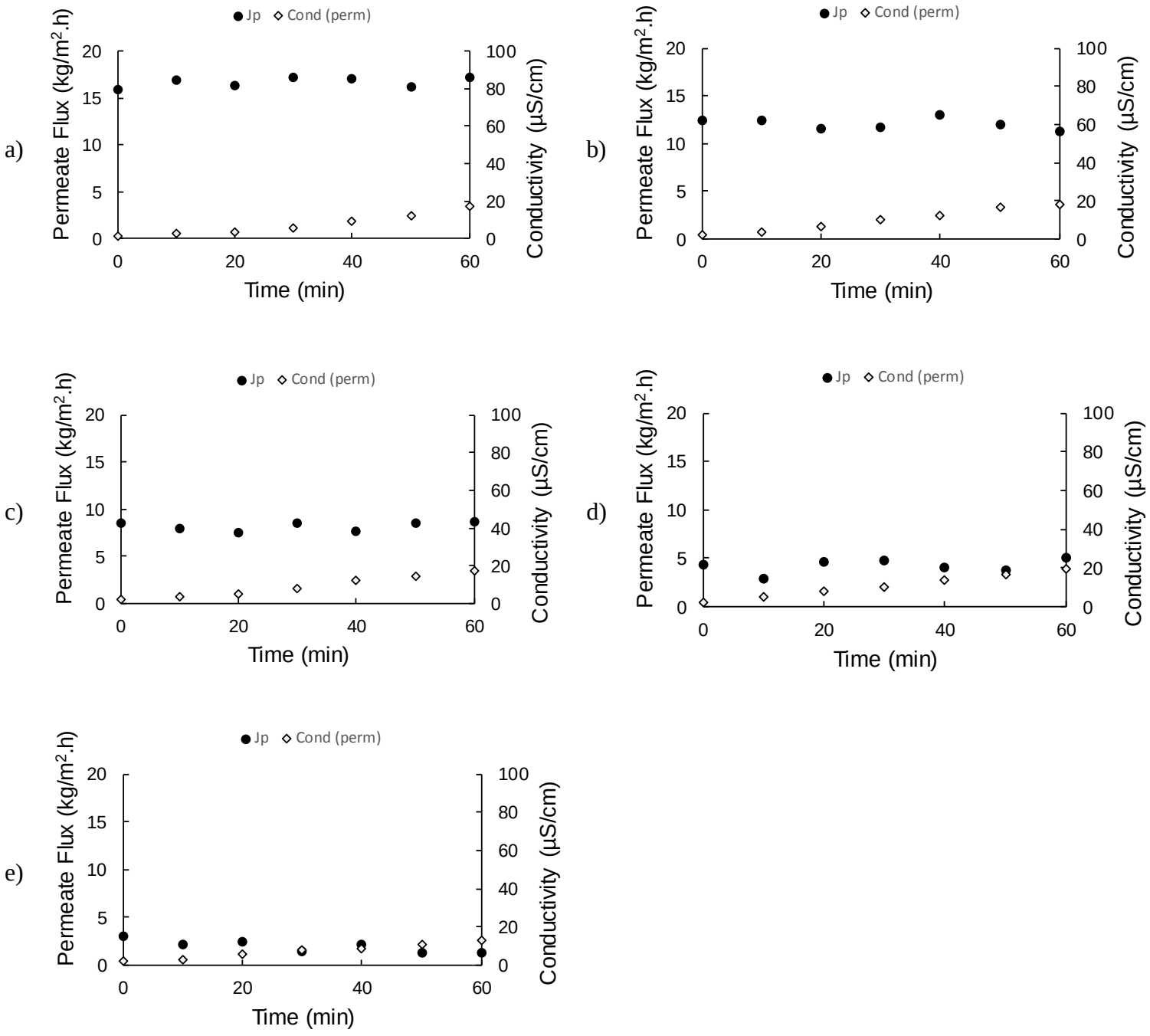

Figure 5.3-1: Permeate flux (Jp) and permeate conductivity [Cond (perm)] for DCMD treating synthetic solution at feed temperatures of (a) 60°C; (b) 55°C; (c) 50°C; (d) 45°C; and (e) 40°C (T_{dest} = 25oC; feed flow rate 0.55 LPM)

The permeate flux obtained for DCMD at high feed temperatures (55°C and 60°C) was relatively high compared to the other technologies tested, nanofiltration and vacuum membrane distillation. The permeate flux for DCMD at 55°C (12 kg/m².h) was very similar to

that obtained for VMD at 50°C and vacuum pressure of 64 mbar (11.7 – 12.5 kg/m^2.h). Despite DCMD is expected to have a lower permeate flux than VMD (DRIOLI; ALI; MACEDONIO, 2015), this result is possible as in both processes the feed solution used is the same and also the type of membrane in terms of material, porosity and nominal size of pores. Because in DCMD the heat loss is higher and permeate condensate right on the other side of the membrane, a higher feed temperature can be necessary to establish a permeate flux similar to that obtained in VMD.

The permeate flux observed at 60°C (16 kg/m^2.h) can be compared than that average permeate flux obtained by Nanofiltration (NF) applied to real gold mining effluent (pH 2.0, feed temperature of 25°C and transmembrane pressure of 10 bar) (18 kg/m^2.h), being slightly lower. This result shows that, despite NF being known for providing higher fluxes than MD, a permeate flux comparable to that obtained by NF could be obtained in DCMD, a non-pressure driven process, when high effluent temperatures are used. Considering that the temperature of the gold mining effluent studied in this work is already high, no heating is needed for the feed, increasing the thermal efficiency of the DCMD and allow its application in industrial scale due to the reduced costs.

The permeate flux obtained for all evaluated feed temperatures remained practically stable during all the experiment and, as can be observed, membrane wetting o in all tests. In this way, a wetting rate was calculated to each test in order to compare DCMD performance in terms of both permeated flux and membrane wetting.

The wetting rate is usually calculated by the slope of the curve of permeate conductivity in a function of time (SRISURICHAN; JIRARATANANON; FANE, 2006). But, as different temperature were evaluated and different permeate fluxes were obtained, another type of membrane wetting rate (wr*) was calculated as the slope of the curve of permeate conductivity in a function of the volume of permeate obtained. Results of permeate flux and wetting rate (wr*) in a function of feed temperature is presented on Figure 5.3-2.

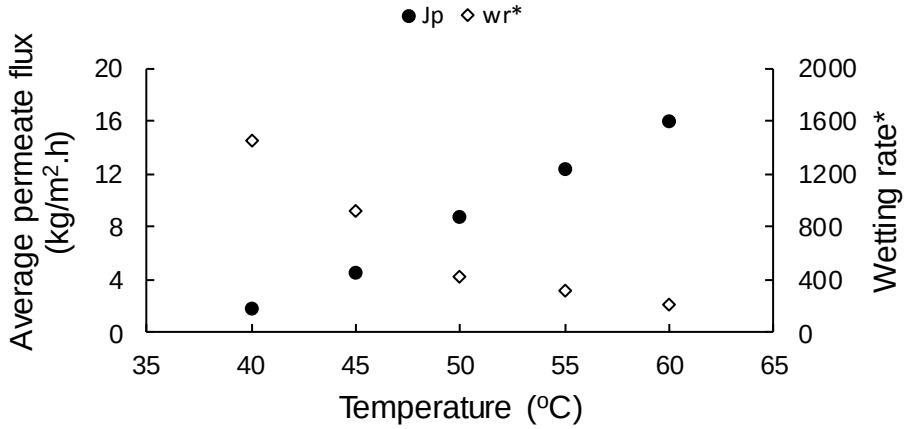

Figure 5.3-2: Permeate flux (Jp) and wetting rate (wr*) in a function of feed temperature (T_{dist} = 25°C; Feed flow rate = 0.55 LMP)

Comparing the results for all tested feed temperature it can be observed a linear increase in permeate flux with the increasing of feed temperature. This result was also observed for the VMD in Chapter 4 and can be explained by the direct relation between the temperature difference between the feed and the permeate stream and the driving force of the DCMD.

The wetting rate also showed an expected behavior, decreasing as the temperature increases. It is possible to observe that higher feed temperatures are more suitable for the operation of the DCMD since they allow obtaining higher flow and lower wetting rate (SRISURICHAN; JIRARATANANON; FANE, 2006). However, the wetting rate presented linear decay with intensity greater than 40 to 50°C and less than 50 to 60°C, so that when the temperature increases, the gain of permeate flow is not reflected in the decrease of the wetting rate.

Based on these results, it is possible to observe that 60°C was the temperature that showed higher permeate flux and lower wetting rate. Despite of this efficiency, as DCMD was performed using a synthetic solution in order to be compared to VMD, the feed temperature chosen was 55°C, since it allowed for a high permeate flux, similar to that obtained by VMD at its optimal operational conditions. It presented low wetting rate and this temperature can still be maintained in the feed tank by using solar heating.

5.2.7 Influence of the feed flow rate

The feed flow rate is another parameter important to be evaluated as it affects the flow regime inside the membrane cell, influencing the residence time of the feed in the cell and also the permeate flux, wetting and membrane fouling. Higher feed flow rates are expect to provide higher flux and membrane wetting time and to prevent fouling by promoting shearing stress

(WARSINGER et al., 2015). At the same time, very high feed flow rates generate pressure in the feed line, which can force the liquid against the pores, enabling membrane wetting or even break. In addition, as it is related to the work done by the circulation pump, higher feed flow rates also demand more energy. In this way, three different feed flow rates were tested and compared in terms of permeate flux, membrane wetting and energy consumption (Figure 5.3-3).

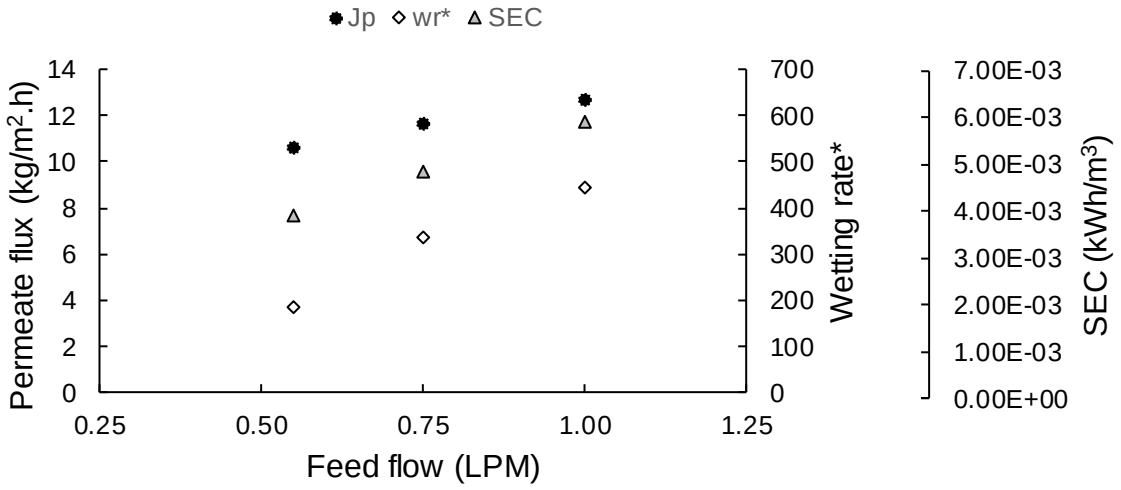

Figure 5.3-3: Permeate flux (Jp), wetting rate (wr*) and specific energy consumption (SEC) in a function of the feed flow rate (SEC).

As can be observed, the results indicate that the increase of the feed flow rate led to permeate flux increase. However, the membrane wetting rate and the specific energy consumption (SEC) were also increased. The feed flow rate of 0.75 LPM led to an increase of 10% of the permeate flux, but wetting rate and SEC increased 80% and 24%, respectively, compared to the feed flow rate of 0.55% . The feed flow rate of 1.00 LPM led to an increase of 8% of permeate flux compared to 0.75 LPM, but 32% of wetting rate and 23% of SEC. If compared to the feed flow rate of 0.55 LPM, this increase was of 19% of the flux, 138% of the wetting rate and 53% of the SEC.

Thus, 0.55 LPM was chosen as the most suitable feed flow rate for DCMD treating the synthetic effluent, since this provides a considerable permeate flow, lower wetting rate and lower SEC.

5.2.8 Determination of the optimal DCMD recovery rate

Since the main objective of DCMD is to obtain water for reuse, the evaluation of the permeate recovery rate is of extreme importance in order to evaluate the optimal recovery rate which provided relatively high permeate flux and permeate with quality sufficient for reuse. Despite MD systems in general being known for supporting higher feed concentration than other membrane processes (DRIOLI; ALI; MACEDONIO, 2015), the composition of the feed can influence the MD performance. As shown in the previous chapters, the high concentration of calcium and sulfate salts on the gold mining effluent (Chapters 2 and 3) and synthetic solutions used to simulate its characteristics (Chapter 4) favor membrane scaling at moderate mass salt concentrations as $CaSO_4$ is a powerful scalant (GRYTA, 2008, 2009; MERICQ; LABORIE; CABASSUD, 2010; WARSINGER et al., 2015).

Thus, the performance of DCMD was evaluated regarding the permeate flux and the rejection efficiency in a function of permeate recovery rate. As with the increase on the permeate recovery rate, the concentration of the feed can favor membrane fouling, decreasing of permeate flux, at the end of the test hot water was added to dilute the concentrate back to initial feed conditions. With this, the capacity of recovery of the initial permeate flux with the dilution of the concentrate was also evaluated. Results are shown in Figure 5.3-4.

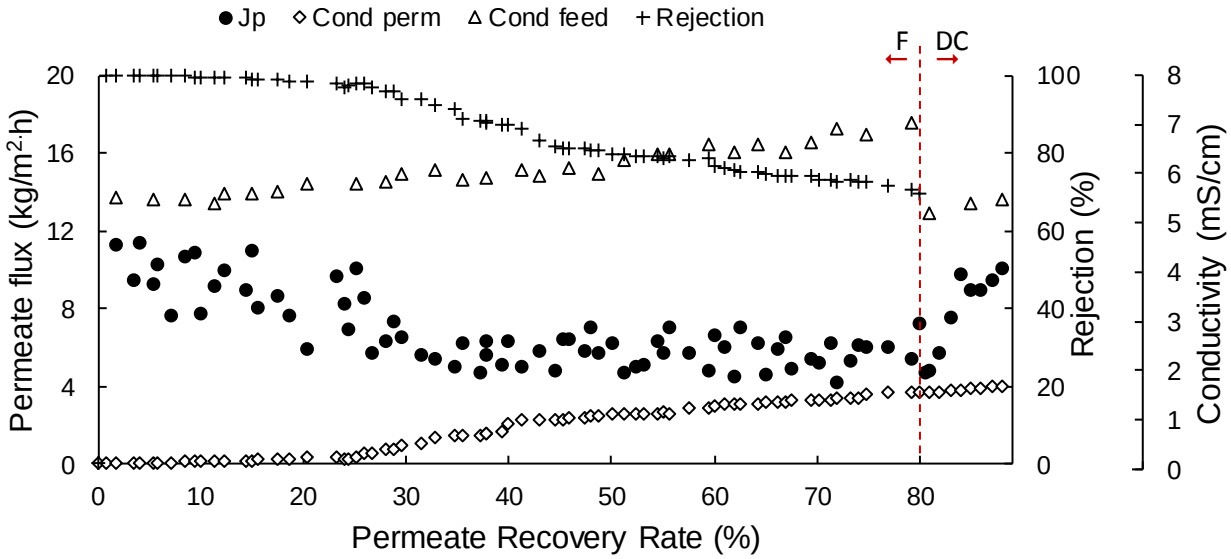

Figure 5.3-4: Permeate flux (Jp), feed and permeate conductivity (Cond) and conductivity rejection in a function of permeate recovery rate before (F) and after (DC) the dilution of the concentrate.

It can be observed that the flux started at a relative high value (around 12 kg/m^2.h) but a decrease was percept already in the beginning of the test, up to 30% of recovery rate. After this point, even with the increasing concentration of the feed, permeate flux remained practically constant around 5 kg/m^2.h until the end of the test, at a recovery rate of 80%.

Regarding conductivity, it is expected that there will be an increase in the feed and, if membrane wetting occur, also in the permeate. As observed from Figure 5.3-4, permeate conductivity remained very low until the recovery rate of 25%, when membrane wetting occurred. As permeate flux was gradually decreasing until 30% of permeate recovery rate while rejection was kept high, it can be inferred that with time and concentration of the feed, membrane fouling was occurring, with concentration of salts in the membrane surface. Around 25% of permeate recovery rate, membrane wetting occurred (wetting time = 8.8 h) and salts started to pass to the permeate side and as feed became more concentrated, the driving force for the passage of salts increased, increasing the conductivity on the permeate side, gradually lowering the quality of permeate at higher permeate recovery rates.

In relation to DCMD performance, in order to guarantee a permeate of high quality it is clear that the ideal maximum permeate recovey rate would be 30%. However, as permeate flux remained stabilized until the recovey rate of 80% it would be interesting to repeat the test more times to check if the wetting time would remain the same, or if it can be increased. If so, DCMD could be applied using higher permeate recovery rates even with the decrease on the permeate flux.

From Figure 5.3-4 it becomes evident that when diluting the feed, there is a recovery of the permeate flow. This is an advantage to be highlighted from the process, as there was a recovery of the permeate flux without the need to interrupt the process for cleaning the membrane. This becomes an economically viable practice with regard to continuous treatments and demonstrates that membrane fouling is reversible because the diluted feed acts as a natural washing system, removing the denser fouling on the membrane surface.

Because of the feed concentration and considering its composition, the feed osmotic pressure was calculated for different recovery rates. It was considered the osmotic pressure caused by the main salts in solution and also that cause by the ions calcium and sulfate, the most abundant ions in solution. Results are shown in Figure 5.3-5.

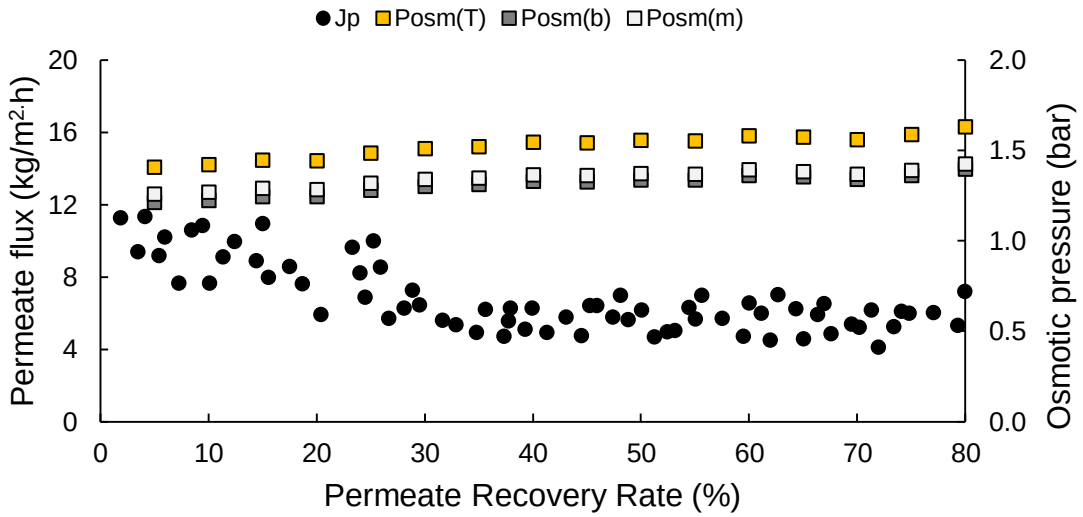

Figure 5.3-5: Permeate flux (Jp) and osmotic pressure caused by the main salts in solution [Posm(T)] and by calcium and sulfate ions in the bulk [Posm(b)] and at the membrane surface [Posm(m)] in a function of permeate recovery rate (T_{feed} = 55°C; T_{perm} = 25°C; Feed flow rate = 0.55 LPM).

As expected, the osmotic pressure of the feed increase as the permeate recovery rate increase, with a higher rate up to 30%. This happens because the permeate flux was higher and also the rejection efficiency of the system, which caused a more intense concentration of the feed at the beginning. After 30%, with membrane wetting, part of the salts that were supposed to be retained in the concentrate passed to the permeate. This, together with lower permeate flux made the increase on the osmotic pressure occur with less intensity than in the beginning of the test. At the wetting time, the osmotic pressure of the solution was at 1.5 bar.

The supersaturation of calcium sulfate was also calculated for both the bulk (Sb) and membrane surface (Sm) (Figure 5.3-6). It can be observed that the supersaturation degree increased with the increase of permeate recovery rate and Sm was always higher than Sb as the concentration of salts is higher at the membrane surface. Still, even with the high recovery rate of 80%, the supersaturation degree of $CaSO_4$ did not reach the upper operation limit recommended for this salt for nanofiltration (HYDRANAUTICS, 2013). Nevertheless, as discussed in the previous chapters (Chapter 3 and Chapter 4), the calcium sulfate presents an inverse solubility with temperature (WARSINGER et al., 2015) which favor its precipitation at the temperature in which DCMD was performed, especially when the feed solution is concentrated.

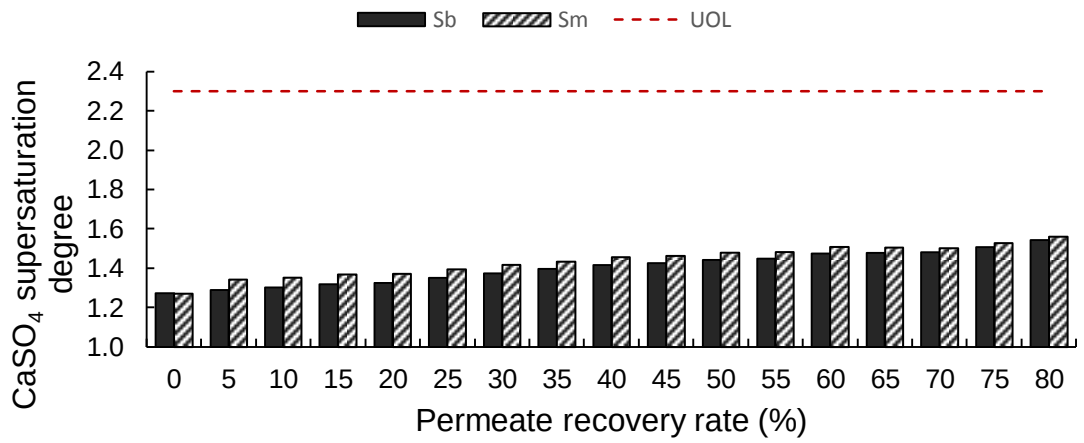

Figure 5.3-6: Supersaturation degree of $CaSO_4$ at the bulk (S_b) and at the membrane surface (S_m) in a function of permeate recovery rate.

Resistances were calculated for DCMD treating the synthetic effluent and results are shown in Figure 5.3-7. As can be observed, the R_{pb} remained practically constant, being the lower resistance presented by the system. The R_{fb} presented a slightly increase up to 30% of permeate recovery rate, after which it remained stable. The R_f was the resistance that presented the higher increase, which was already expected as DCMD permeate flux decreased right after the beginning of the test. After 30%, the permeate flux was stabilized and R_f seems to be maintained at a constant value too.

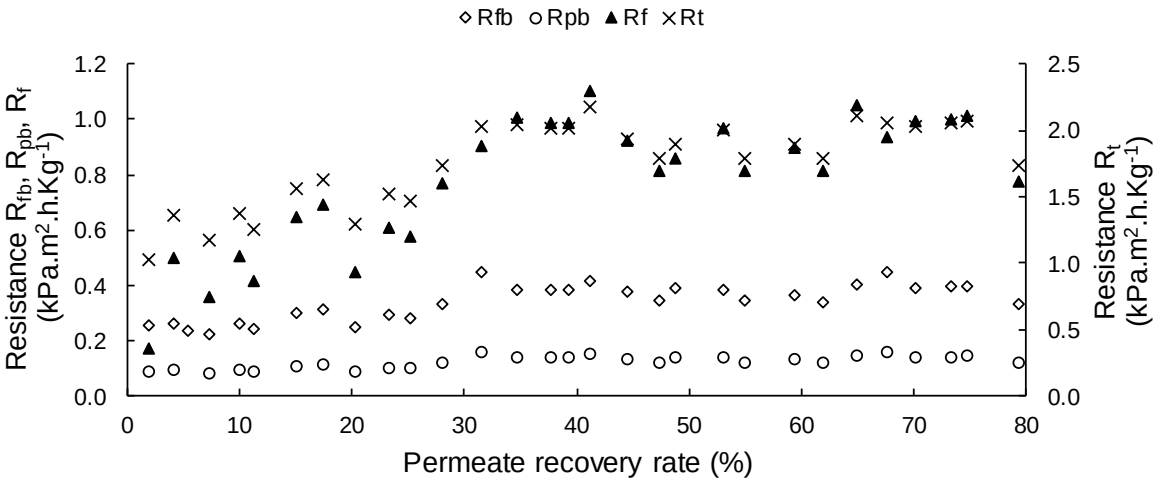

Figure 5.3-7: Feed boundary layer resistance (R_{fb}). fouling resistance (R_f) and total resistance (R_t) for DCMD treating the synthetic solution in a function of permeate recovery rate (T_{feed} = 55°C; T_{perm} = 25°C).

Hermia's model adapted to cross-flow filtration (SRISURICHAN; JIRARATANANON; FANE, 2006) was applied to the experimental data of DCMD in order to better elucidate the fouling mechanisms (Table 5.3-1).

Table 5.3-1: Evaluation of fouling mechanisms using Hermia's model for DCMD treating synthetic .

Recovery Rate range (%)	Jf/Ji	Model											
		Complete blocking filtration			Standard blocking filtration			Intermediate blocking filtration			Cake filtration		
		Jo ($L\ m^{-2}h^{-1}$)	k	R^2	Jo ($L\ m^{-2}h^{-1}$)	k	R^2	Jo ($L\ m^{-2}h^{-1}$)	k	R^2	Jo ($L\ m^{-2}h^{-1}$)	k	R^2
0-30	0.18	12.3	0.07286	0.88	12.7	0.01271	0.87	13.2	0.00893	0.85	15.7	0.00225	0.82
35-80	0.87	5.2	0.00790	0.70	5.2	0.00177	0.69	5.2	0.00159	0.69	5.2	0.00064	0.68

The results showed that at the first hours of test, then permeate flux showed a decrease, the complete blocking filtration was the model that presented the better regression factor, indicating this was the main fouling mechanism. After the permeate recovery rate of 35%, the adjust of the models was not very high as the permeate flux remained practically constant and fouling could not be easily observed, as shown by the low mass transfer coefficients found. Still, complete blocking filtration remained the main fouling mechanism. This result is consistent to that obtained for VMD (Chapter 4). With $CaSO_4$ precipitation, pores started to be blocked completely by the salt crystals that are formed at the membrane surface. The increase pore blocking gradually decrease the permeate flux until the crystals are not able to reach the membrane surface because of the salt already precipitated there, allowing for a more stable permeate flux.

5.4 CONCLUSION

DCMD has proven to me a very efficient technology for gold mining effluent treatment. As this effluent already present high temperature, the performance of DCMD allows for the recovery of this heat, dismissing any heater system for the feed. As the permeate temperature remained at room temperature, costs with cooling can also be decreased as, in industrial scale, alternatives abundant water sources can also be used as a permeate or to cool down the permeate temperature after the membrane cell.

When treating the synthetic solution with similar characteristics as the real effluent in pH 5.0, DCMD showed great performance. Tests with different temperatures showed that the higher the feed temperature, the higher the permeate flux and the lower the membrane wetting rate. The temperature of 55^{o}C was chosen as the best feed temperature as it can provides high permeate flux and lower wetting rate and it can be maintained by a solar heating system. For the feed flow rate, it was observed that the feed flow range tested in this study didn't show very high variation, so 0.55 LPM was chosen to be the best feed flow rate as it guaranteed a transient flux without destabilizing the system of increase the pressure inlet on the membrane module.

Regarding the recovery rate, a maximum permeate recovery rate of 30% was chosen as after this, the wetting took place and the rejection efficiency of the system started to decrease. Up to 30% of permeate recovery rate, the DCMD showed an efficiency of 96% of rejection, providing a permeate with quality enough for reuse in the industry. Thus, DCMD is a suitable and efficient technology for gold mining effluent reclamation.

The results found in this work show that DCMD, VMD and NF are effective processes on gold mining effluent treatment and depending on operational conditions can provide quite similar permeated fluxes, being comparable in terms of performance. They can also produce water for industrial reuse, decreasing the water demand of the industry, and by concentrating the effluent, minimize the waste production by its precipitation. Despite the advantages achieved with this technologies, as the gold mining effluent studied in this work is contaminated with arsenic, the precipitation of the concentrate produced by MD, DCMD or VMD would still represent a hazardous waste. However, if the arsenic can be recovered with high purity from the effluent or the concentrate of those systems, it can be reused in the industry, becoming a valuable by-product other than a hazardous waste. Thus, other treatments such as solvent extraction can be tested for the arsenic recovery.

CHAPTER 6:

THE FEASIBILITY OF SOLVENT EXTRACTION (SX) TO REMOVE ARSENIC FROM THE GOLD MINING EFFLUENT

6.1 INTRODUCTION

Solvent extraction (SX) is a process widely used in metallurgy, especially in hydrometallurgical processes where metals are extracted in aqueous media from the materials containing them. The increasingly lower quality levels of the minerals that have been found and to the growing concern with the environment, the application of hydrometallurgy has been greatly increased establishing a very effective competition to against pyrometallurgical processes (MIHOVILOVIC, 2001). The production of gold is one of the traditional applications of hydrometallurgy, as well as the production of alumina, uranium, zinc, nickel, copper, titanium, rare earths, etc (HAVLIK, 2008).

Because it represents a technique that provides the purification of metals, SX also began to be used in the production processes of copper by pyrometallurgy for the removal of interfering metals (impurities). In the pyrometallurgical process of copper, which provides 80% of all the copper commercialized in the world, copper plates are produced from the electrethine of copper electrolytic solutions (SCHLESINGER 2011). However, this usually contains several impurities, such as antimony, selenium, tellurium, bismuth and arsenic (BALLINAS et al., 2004), the latter being capable of causing the most serious damage to copper cathodes (SAITUA; GIL; PADILLA, 2011) and thus must be removed.

In order to remove the arsenic from the electrolytic solutions, SX applied to arsenic was first proposed and it is already used on industrial or pilot scale in several countries (IBERHAN; WIŚNIEWSKI, 2003). Today, lots of extracts with different properties and selectivity are found in the market. For the removal of arsenic, the use of neutral (eg Cyanex® 923, TBP), acid (eg Cyanex® 301) and basic extracts (eg TOA, Aliquat 336) has already been proposed. This is because arsenic may be present in aqueous solutions in either the ionic, anionic or cationic form.

The use of commercial solvents has already been tested by several authors in order to remove arsenic from water (BEY et al., 2010), from effluents such as water produced (LOTHONGKUM et al., 2011; PANCHAROEN; POONKUM; LOTHONGKUM, 2009; PRAPASAWAT et al., 2008) and also acid solutions, generally simulating copper electrolytic solutions (IBERHAN; WIŚNIEWSKI, 2003).

In this way, SX is a promising technology for the removal of arsenic from mining effluents. Removal of this metal is interesting from an environmental and health point of view, as it represents a toxic contaminant. However, if recovered with sufficient purity, this metal can be reused in the industry, representing no more a waste but a valueable by-product. Thus, the removal and recovery of arsenic presents environmental and also economic advantages, contributing to the ecoefficiency of the mining sector.

It is important to note that the SX process is economically feasible when the solute concentration to be withdrawn is high. In this context, alternative technologies, such as membrane distillation (KESIEME; ARAL, 2015) and nanofiltration, may be necessary/interesting to concentrate the solution for acid or metal recovery, and still allow obtaining water for reuse. Therefore, the objective of this work was to evaluate the feasibility of solvent extraction in the removal of arsenic from mining effluent.

6.2 MATERIAL AND METHODS

6.2.1 Synthetic solution preparation

In order to eliminate the influences of other metals and ions present in the raw effluent, synthetic solutions (Xss1 and Xss2) containing arsenite [As (III)] and arsenate [As (V)] were prepared using $NaAsO_2$ e and $Na_2AsO_4.7H_2O$ as sources of As (III) and As (V), respectively. Those reagents were diluted in deionized water to provide the concentration of 600 mg L^{-1} of total arsenic, [500 mg As (III) L^{-1} and 100 mg As (V) L^{-1}].

The pH was adjusted to 2 using sulfuric acid (H_2SO_4), so it was the only source of sulfate, resulting on a concentration of 2000 mg.L^{-1} (Xss1). In order to increase the concentration of sulfate without increasing the concentration of arsenic, the salt sodium sulfate (Na_2SO_4) were added until the concentration of sulfate to 6000 mg.L^{-1} (Xss2). A third solution was also prepared by adjusting the pH of Xss1 to 5.0. The supernatant was defined as Xss3.

6.2.2 Extractants

To investigate the effect of extractant type in arsenic extraction, six different extractants were tested: LIX 841, Cyanex 272, Cyanex 923 Aliquat 336 and Alamine 336 (Table 6.2-1). These extractants were used as such without any purification and kerosene was used as solvent to dilute all the extractants above.

Table 6.2-1: Properties of the extractants used in this work

Extratante	**Lix 84**	**Cyanex 272**	**Cyanex 923**	**Aliquat 336**	**Alamine 336**
Chemical nature	acid	acid	neutral	basic	basic
Composição	2-hydroxy-5-nonylbenzophenone	bis(2,4,4-trimethylpentyl) phosphinic acid	mixture of tertiary octyl and hexyl phosphine	$(R_3NCH_3)^+Cl^-$, R=octyl/decyl	tri-octyl/decyl amine
Density (g/cm³)	0.89-0.91	0.92	0.88	0.88	0.81
Superficial tension (dyn./cm³)	-	-	9	28	53

6.2.3 Experimental procedure

6.2.3.1 Dispersive solvent extraction

For the dispersive solvent extraction experiments, A/O relation were set at 1. 15 mL of aqueous phase (effluent or synthetic solution) and 15 mL of organic phase (extractant and diluent) are added in 125 mL Erlenmeyer flasks. These were brought to shaking at 250 rpm in an incubator at controlled temperature for 60 minutes. The flasks were sealed in order to avoid contact of the reaction medium with the external medium, avoiding the increase of interferences in the analysis. The organic phase were composed of extractant 33% in kerosene.

After the extraction, the mixture was transferred to separation funnels for complete phase separation. Samples were collected from the aqueous phase, where pH, arsenic concentration and, where relevant, sulfate concentration were measured. The concentration of solutes in the organic phase were determined by mass balance.

The extraction efficiency [E(%)] is calculated by Equation 1:

$$E\ (\%) = \frac{[y]_{aq\,i} - [y]_{aq\,f}}{[y]_{aq\,i}} \qquad (1)$$

Where $[y]_{aq\,i}$ represents the initial concentration of y in aqueous phase and $[y]_{aq\,f}$ represents the concentration of that same specie y in aqueous phase after the extraction.

6.2.3.2 Selection of solvents for arsenic extraction

For a previous selection of potential extractants for the extraction of arsenic, all extractants were tested for total arsenic extraction using as aqueous phase the synthetic solution Xss1. This solution was chosen as it presents the acidity the gold mining effluent with a lower concentration of sulfate, allowing for a better analysis of the affinity of the extractants for arsenic. As the gold mining effluent presents high temperature, tests were performed at the temperature of 50^{o}C. Extractants that showed a minimum of 40% of arsenic removal were selected for the next tests.

6.2.3.3 Activation of amines

Alamine 336 and Aliquat 336 were tested for initial activation. For this, the organic phase (composed by the extractant and kerosene) were first put in contact with an acid solution prepared with distillate water and H_2SO_4 to pH = 2.0 under agitation of 250 rpm for 30 minutes. The phase were separated and the organic phase were used on dispersive extraction experiment. The efficiency of arsenic extraction were measured for the activated amines and compared to the results obtained by the non-activated ones.

6.2.3.4 Evaluation of the influence of the pH on arsenic extraction

The pH can influence the extraction of arsenic by changing the conditions of the aqueous media, which can also change the form of the species in solution. The gold mining effluent studied in this work have acid pH and its adjustment to 5.0 can be necessary for the performance of some treatments, as the vacuum membrane distillation. In this way, the influence of the pH on arsenic extraction was evaluated by performing SX using solutions Xss1 and Xss3.

6.2.3.5 Evaluation of the influence of sulfate concentration on arsenic extraction

To evaluate the influence of the sulfate concentration on arsenic extraction, dispersive extraction testes were performed with the extractants selected previously and the synthetic solutions Xss1 and Xss2. The extraction efficiency of each extractant was analyzed for arsenic and sulfate.

6.2.3.6 Evaluation of the influence of the temperature on arsenic extraction

Despite the effluent presents a high temperature, temperature fluctuations can be often observed on industry effluents. In addition, solvent extraction can be applied to streams that present room temperature, as the nanofiltration concentrate, for example. In this way, the

extraction of arsenic was also tested at room temperature (25°C) for both synthetic solution (Xss1 and Xss2). The extraction efficiency of each extractant was analyzed for arsenic and sulfate and results were compared to those obtained at 50°C. The higher arsenic extraction obtained were selected as the optimal dispersive extraction condition and the respective extractant, synthetic solution and extraction temperature was chosen to be tested for the next test.

6.2.3.7 Evaluation of the influence of extraction time on arsenic extraction

The variables selected on the previous test (extractant, synthetic solution and extraction temperature) were used to test the influence of extraction time on arsenic removal. For this, 2 tests were performed, one performed on the shaker used for the previous test and another performed in a jacket becker using a mechanic agitator, both keeping the system at the same agitation (250 rpm) and at the temperature 50°C. The organic phase was composed of extractant 30% in kerosene and aqueous phase of synthetic solution Xss1.

The test in the shaker was performed putting 14 flasks on the shaker and taking one at a time until the end of test (120 minutes). The test in the jacket becker were performed with an initial volume of 1 L (A/O = 1:1) from which aliquots were taking at different times. Arsenic concentration was measured at each sampling time.

6.2.4 Analytical methods

The samples collected were analyzed for pH (pHmeter Qualxtron QX 1500); total arsenic, As (III) and As (V) (DHAR et al., 2004); and sulfate (APHA, 2017).

6.3 RESULTS AND DISCUSSION

6.3.1 Selection of extractants for arsenic extraction

Different extractants were tested for their affinity to arsenic and, consequently, the efficiency on the extraction of arsenic. The results are shown in Figure 6.3-1.

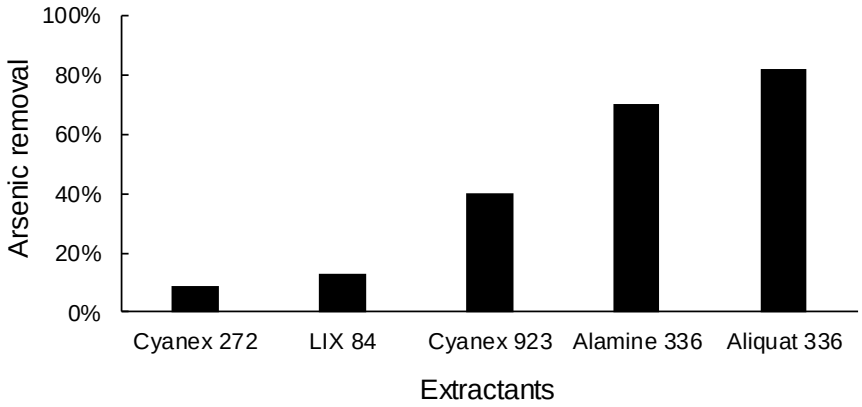

Figure 6.3-1: Extraction efficiency of all evaluated extractans for total arsenic present in acid synthetic solution (Xss1) (A/O = 1; extractant 33% in kerosene, Agitation = 250 rpm, t = 60 min; T = 50^{o}C).

It can be observed that, despite of their chemical nature, all extractants tested were capable of extracting arsenic from an acid medium. Cyanex 272 and LIX 84 were the extractants that showed the lowest efficiency. Despite the extraction of arsenic has already been observed for acid extractants, some might present a better affinity for metals in cations forms (AHMED, 2013). In acid medium, the most common forms of arsenic are H_3AsO_3 [As (III)] and $H_2AsO_4^-$ [As (V)] and Cyanex 272 and LIX 84 did not show good affinity for those.

Cyanex 923 presented a moderate extraction efficiency for arsenic (approximately 40%), showing a good affinity for this metal. The extraction of arsenic by Cyanex 923 were already described by other authors for produced water (PANCHAROEN; POONKUM; LOTHONGKUM, 2009; PRAPASAWAT et al., 2008) and also acid synthetic solutions (WISNIEWSKI, 1997) containing arsenic.

Alamine 336 and Aliquat 336 were the extractants that presented the highest efficiencies for total arsenic extraction, 70% and 82%, respectively. Several authors in the literature reported the removal of arsenic by Aliquat 336 from different mediums such as produced water (LOTHONGKUM et al., 2011; PANCHAROEN; POONKUM; LOTHONGKUM, 2009; PRAPASAWAT et al., 2008); distillate, tap and river water (GÜELL et al., 2011); and also acid synthetic solutions (BEY et al., 2010), with high efficiency.

The high efficiency showed by Alamine 336 can be explained by the similarity between the chemical nature of this extractand and Aliquat 336. As observed, Alamine 336 is also a good extractand for arsenic removal from acid synthetic solutions. The extractants Cyanex 923,

Alamine 336 and Aliquat 336 were selected to perform the next tests due to their affinity to arsenic and high potential of removal both arsenite and arsenate.

6.3.1.1 Activation of amines

As Alamine 336 and Aliquat 336 are amines, they might need to be activated before used on solvent extraction. In this way, those two extractants were tested for initial activation with acid solution (Figure 6.3-2). The results found were very similar to that obtained without previous activation, showing that the acidity of the effluent alone was already sufficient for the amines activation during the extraction.

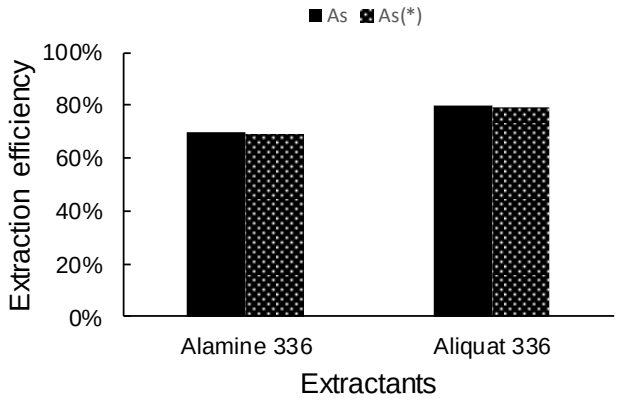

Figure 6.3-2: Extraction efficiency of Alamine 336 and Aliquat 336 non-activated and activated (*) with acid solution and non for total arsenic present in acid synthetic solution (A: Xss1; O: extractant 33% in kerosene; A/O = 1; Agitation = 250 rpm, t = 60 min; T = 50^{o}C).

6.3.1.2 Evaluation of the pH influence on arsenic solvent extraction

Despite the pH of the gold mining effluent is close to 2.0, the SX can be also applied for other streams produced during the treatment if this effluent such as the concentrate for NF. In this way, the influence of the pH was tested for arsenic removal by performing the solvent extraction in a solution at pH 2.0 (Xss1) and other at pH 5.0 (Xss2) (Figure 6.3-3). The pH 5.0 was chosen as it is the maximum value to which the effluent pH can be adjusted without producing a sludge contaminated with arsenic. This adjustment was necessary for a better performance of some treatments, as VMD. In this way, it is important to test if arsenic can be removed from those solutions with the same efficiency.

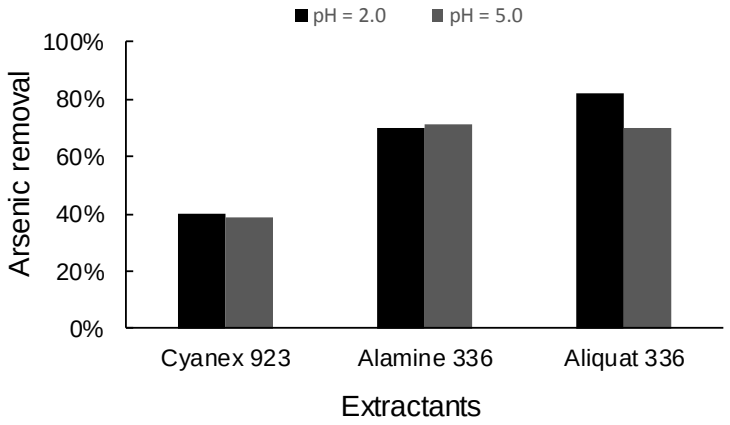

Figure 6.3-3: Arsenic extraction efficiency of Cyanex 923, Alamine 336 and Aliquat 336 from (a) Xss1; and (b) Xss3 (O: extractant 33% in kerosene; A/O = 1; Agitation = 250 rpm, t = 60 min; T = 50^{o}C).

It was observed that the adjustment of the pH from 2.0 to 5.0 did not changed much the arsenic removal efficiency of the evaluated extractants, except for Aliquat 336. Even with a decrease on its removal efficiency, Aliquat 336 still present a great performance on the extraction of arsenic at pH 5.0 (70%). This result indicates that fluctuations on pH in the range of 2.0 to 5.0 have no drastic consequences on the extraction performance and that SX could be applied for the vacuum membrane distillation concentrate as well.

6.3.1.3 Evaluation of the sulfate concentration on arsenic extraction

As reported by other authors, the concentration of sulfate can influence the arsenic extraction as a co-extraction of sulfuric acid can occur together with arsenic (BALLINAS et al., 2003; IBERHAN; WIŚNIEWSKI, 2003) or an increase of arsenic removal can be observed with the increase of this acid (WISNIEWSKI, 1997). As the gold mining effluent studied in this work presents high sulfate concentration, the extractants Cyanex 923, Alamine 336 and Aliquat 336 were tested for arsenic removal using two synthetic solutions that present different sulfate concentrations. The arsenic and sulfate extraction were evaluated and results are shown in Figure 6.3-4.

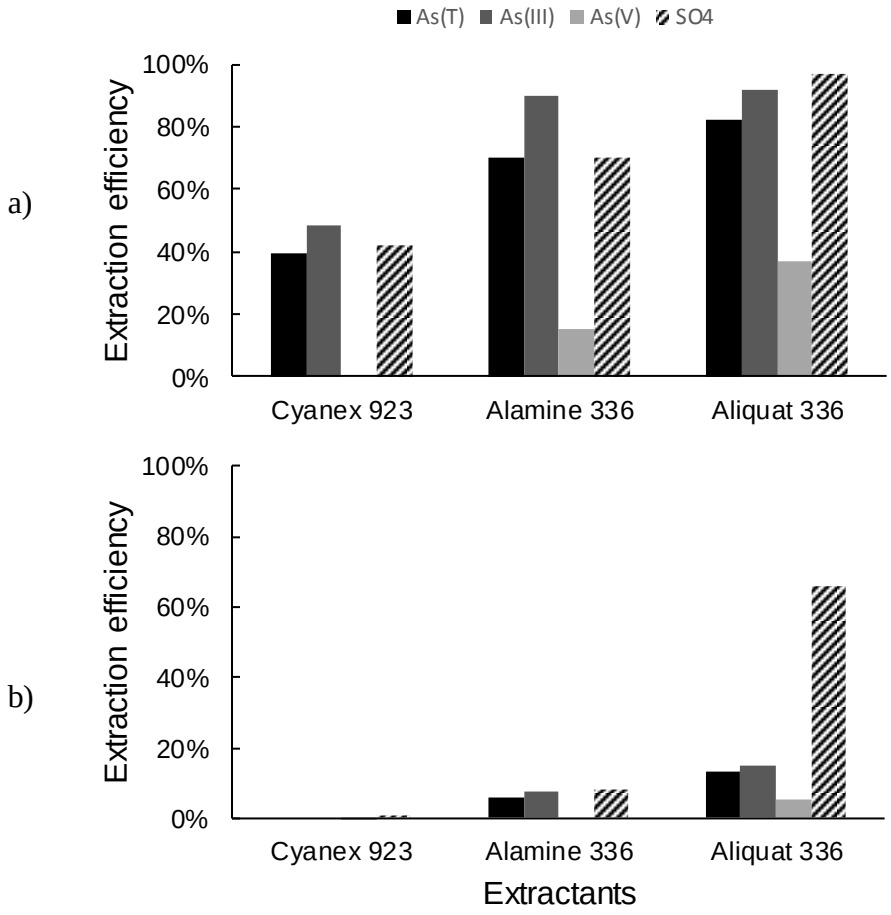

Figure 6.3-4: Arsenic and sulfate extraction by Cyanex 923, Alamine 336 and Aliquat 336 from (a) Xss1; and (b) Xss2 (A/O = 1; O: extractant 33% in kerosene; Agitation = 250 rpm, t = 60 min; T = 50^{o}C).

As it can be observed, the extractants have different affinity and abilities to extract arsenic depending on its speciation form. Cyanex 923 showed high affinity for As (III) but not for As (V), a result that differs from those obtained by other authors (WISNIEWSKI, 1997) that observed the removal of both arsenic species from a sulfuric acid media.

Aliquat 336 could extract both arsenite and arsenate and this is due to its ability to react to undissociated and dissociate forms, as $H_2AsO_4^-$ (MARINO; FIGOLI, 2015). According to (GÜELL et al., 2010), the kinetics of the extraction of Aliquat 336 is higher for As (V) than for As (III), making it a more suitable extractant for arsenate. However, in this work the removal of arsenite was higher than for arsenate. This result can be explained by the higher concentration of As (III) in the solution, increasing the driving force of its extraction.

Regarding the influence of the sulfate concentration, the higher concentration of sulfate in solution Xss2 led to a high decrease of arsenic extraction efficiency for all the evaluated

extractants, including Alamine 336 which is reported to extract sulfuric acid from sulfate solutions (MANAA; LASHEEN, 2016). The competition between arsenic and sulfate for the link site of the extractant can occur as arsenic species and sulfuric acid are often co-extracted, as reported by other authors (BALLINAS et al., 2003). This same effect was observed in this work.

It is observed that the removal efficiency decrease not only for the arsenic but also to the sulfate. However, the concentration of sulfate is 3 times higher, so a lower removal for sulfate, as presented by the Aliquat 336 does not represent a decrease of the efficiency of the extracting on removing sulfate, the decrease was just proportional as the concentration of sulfate increases and the extract has a saturation limit, which could have been reached.

It is important to highlight that solution Xss2 has a sulfate concentration similar to the gold mining effluent. Thus, this result showed that in order to guarantee the arsenic extraction from the gold mining effluent or from the concentrate of membrane separation processes as nanofiltration and membrane distillation, it is important that these streams pass through a pre-treatment for lowering the sulfate concentration.

6.3.1.4 Influence of the temperature on arsenic extraction

The influence of the temperature on arsenic extraction was also tested as temperature fluctuation often occur in industrial effluents and solvent extraction can be applied to the nanofiltration concentrate stream, which is produced in room temperature. In addition, even for high temperature streams, as the removal of arsenic is of sum importance, the cooling of the effluent can be an option to be considered if the the efficiency of arsenic removal is improved in lower temperatures. Results of arsenic extraction from solution Xss1 and Xss2 at room temperature are shown in Figure 6.3-5.

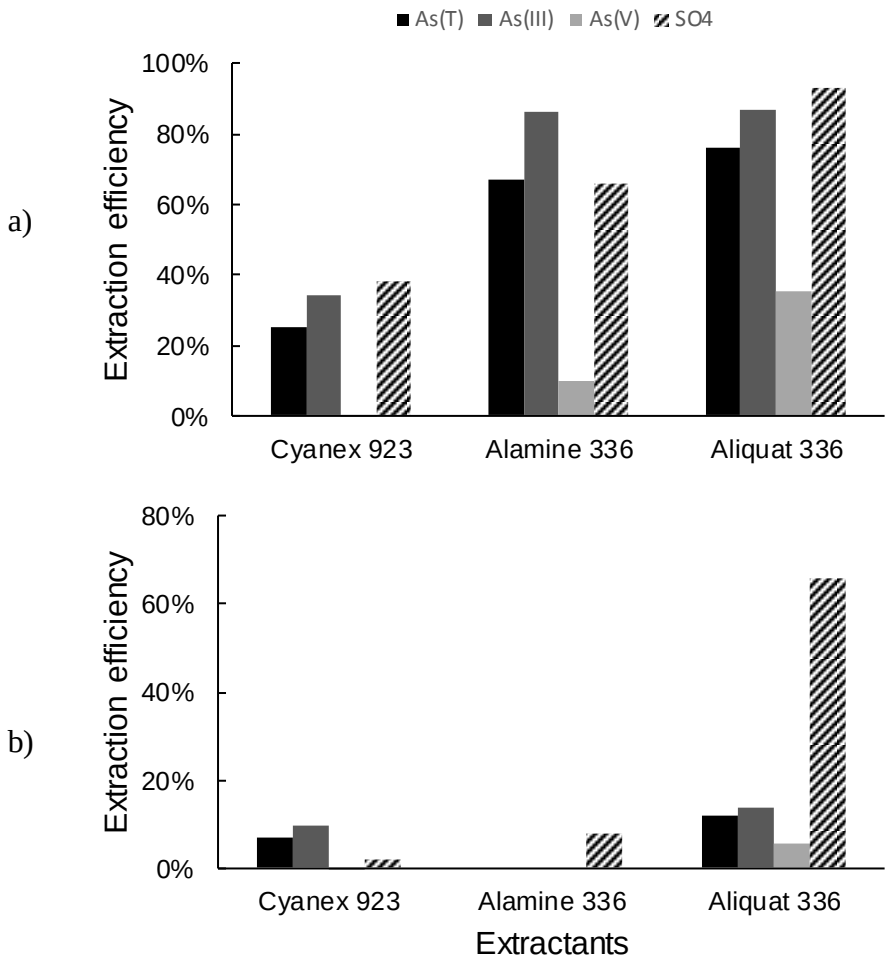

Figure 6.3-5: Arsenic and sulfate extraction by Cyanex 923, Alamine 336 and Aliquat 336 from (a) Xss2; and (b) Xss3 (A/O = 1; O: extractant 33% in kerosene; Agitation = 250 rpm, t = 60 min; T = 25^{o}C).

As it can be observed, at room temperature (25^{o}C), the results observed for arsenic extraction from solution Xss1 did not differ much from those obtained at 50^{o}C. This indicates that practically the same arsenic removal efficiency can be achieved in different temperatures, allowing this process to be applied in the real effluent at its natural temperature or in other streams containing arsenic that can be produced in temperatures close to the room temperature.

6.3.1.5 Influence of extraction time and mixing condition on arsenic extraction

The optimum time for arsenic removal is an operational parameter of great importance. The metal extraction is based on chemical reaction can take long time to achieve its best result of even happen in a very short period and lose its efficiency with time. In this way, arsenic

extraction were analyzed for different reaction times in two different systems, shaker and jacket beker, presenting different mixing conditions (Figure 6.3-6).

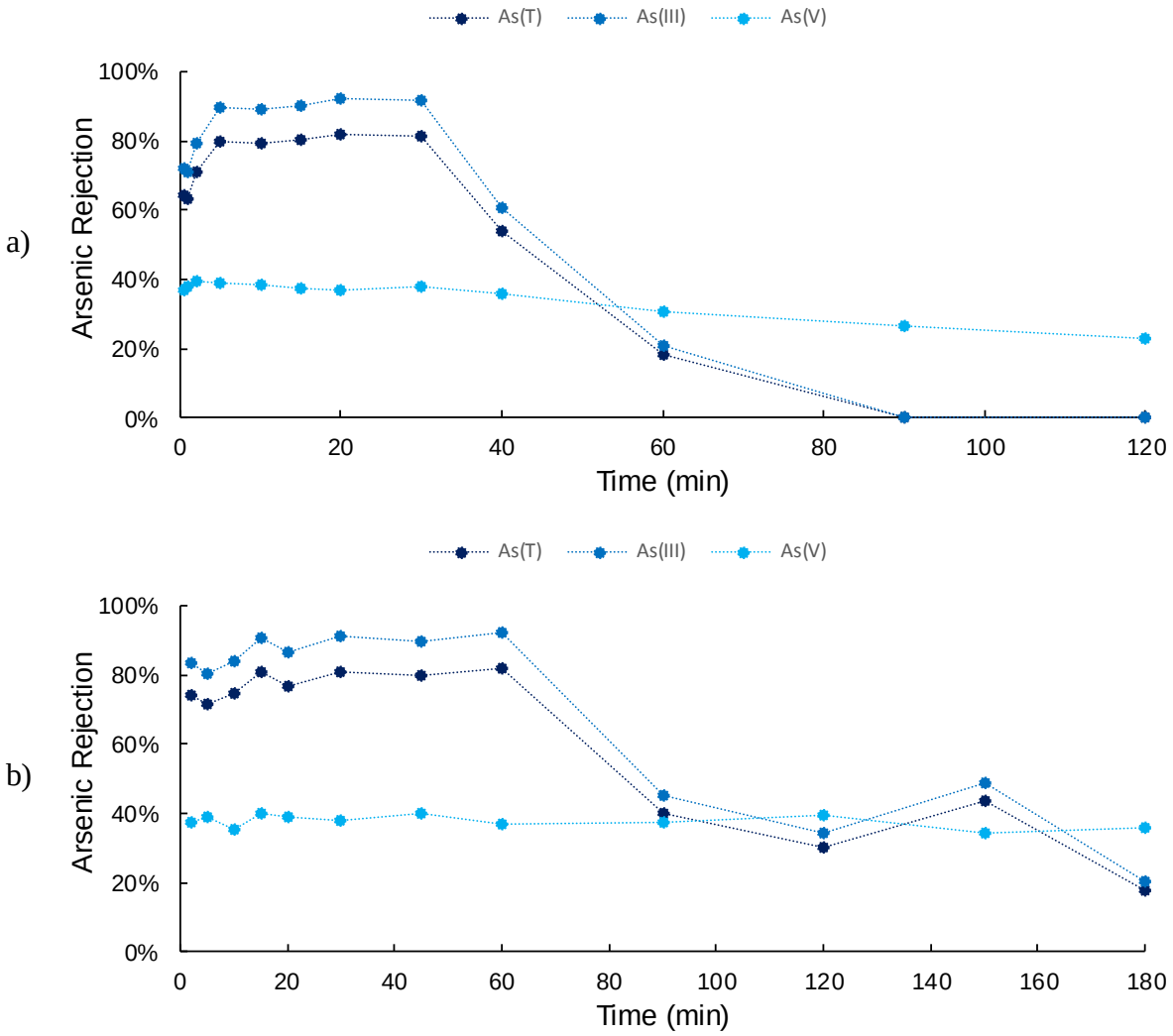

Figure 6.3-6: Arsenic extraction efficiency in a function of reaction time in (a) shaker; and (b) jacket becker (A: Xss2; O: Aliquat 336 33% in kerosene; A/O = 1; Agitation = 250 rpm, T = 50^{o}C).

Asi t can be observed, the two systems showed different behavior for arsenic removal with time. In the first one, the highest efficiency was achieved after 5 minutes of reaction. This efficiency was maintained until 30 minutes, after which it started to decrease. At the end of the test, practically no arsenic removal was observed.

For the jacket becker system, the highest efficiency was achieved after 15 minutes of reaction and it was maintained until 60 minutes, after which it started to decrease, as observed for the

shaker. At 180 minutes of test only 20% of arsenic extraction was observed. The difference between the results obtained can be related to the mixing conditions of each system. In the jacket becker, the mechanical agitation provided by the mixer can maintain the extraction reaction for a longer time.

These results showed that the chemical reaction for arsenic extraction by Aliquat 336 in acid medium occur relatively fast, achieving its efficiency generally within 15-20 minutes depending on the mixture procedure. The time necessary to achieve the maximum efficiency will depend on the conditions of the system but it generally takes a short time (from 5 to 15 minutes).

The results found in this work showed that arsenic can be efficiently removed from acid medium using Aliquat 336. It is important to test the reaction optimum time before designing an extraction system to achieve better and faster results.

6.4 CONCLUSIONS

Different extractions were tested for the extraction of arsenic and the influence of temperature, sulfate concentration and extraction time were also evaluated. Results showed that Cyanex 923, Alamine 336 and Aliquat 336 were the extractants that showed the best performance, removing 40%, 70% and 82% of the arsenic in solution.

The sulfate concentration in the aqueous solution have a big influence on arsenic extraction lowering the efficiency of the system when this ion is present in high concentrations. In this way, a pre-treatment of streams with high content of sulfate is necessary to achieve good arsenic removal efficiencies.

Despite high temperatures had allowed for better results, the difference between the removal efficiencies observed in $50^{o}C$ and $25^{o}C$ was not pronounced in a way that the solvent extraction of arsenic can be applied in streams with different temperatures for arsenic removal, as the concentrate of nanofiltration (room temperature) or gold mining effluent and membrane distillation concentrates (high temperature).

Arsenic solvent extraction is a suitable process for removing the arsenic from acid aqueous medium. This removal is interesting not only for solving the contamination problem of mining effluents but also to allow for arsenic recovery. The recovery of arsenic in high purity

can allow for its industrial reuse, making this hazardous metal that is usually seen as a toxic contaminant to become an economical valuable material.

CHAPTER 7:

FINAL CONSIDERATIONS

Three different membrane processes were tested for gold mining effluent reclamation. NF proved to be a suitable technology for the treatment of the sulfuric acid plant wastewater contaminated with arsenic. It allowed the generation of a permeate of sufficient quality for industrial reuse. The best operating conditions observed were the original wastewater feed pH (pH ~ 2), feed temperature of 25^{o}C, transmembrane pressure of 10 bar and recovery rate of 45%, above which the quality of the permeate became much lower.

Regarding the retention mechanisms, for the NF90 membrane and the studied sulfuric acid plant wastewater, the retention of higher valence counterions to balance the retained co-ion loads was the most important, more than the Donnan effect or the retention by size. No drastic changes were observed in the removal of pollutants or in the permeate flux in NF even when the feed pH was close to the membrane IEP.

The main mechanism responsible for the linear decay of the permeate flux with the increase of the recovery rate was the increase of the filtration resistance, caused by the increase of the concentration of solutes near the surface of the membrane and development of incrustation. Osmotic pressure increasing reduces the driving force for permeation.

When comparing the efficiency of NF and direct contact membrane distillation (DCMD) for the treatment of the real gold mining effluent, both processes showed promising performances for gold mining effluent reclamation, showing high pollutants removal rate, which is an environmental and economic interesting aspect. DCMD presented a lower flux than NF (18 kg/m^2.h and 16 kg/m^2.h for NF and DCMD, respectively, at a recovery rate of 40%) and was limited to operate up to permeate recovery rate of 40% due to severe fouling caused by to $CaSO_4$ precipitation. Although DCMD was susceptible to fouling, fouling resistance contribution to total filtration resistance is lower than observed for the NF. Furthermore, DCMD produces a permeate with a superior quality and with no restriction for reuse.

The economic analysis revealed that due to the recovery of the natural high effluent temperature, the DCMD showed low energy requirement. This increase the chances of industrial scale application of MD, usually limited by the high energy consumption. In addition, due to the high DCMD contaminant rejection, a permeate of higher quality is produced, with a low demand for pH adjustment. Thus, the application of DCMD process for

gold mining effluent reclamation could result in more significant annual cost savings if compared to NF process.

Two different configurations of MD (by vacuum, VMD; and DCMD) were tested for the treatment of a synthetic solution with similar characteristics to the gold mining effluent and both technologies had proven to be very efficient. As this effluent already present high temperature, MD could be performed with low energy consumption, favoring its application in industrial scale, as discussed before.

VMD provided an initial flux similar to that observed distillate water, showing that VMD is indeed a robust system and that it can provide high permeate fluxes. As expected, the higher the feed temperature and the vacuum pressure, higher is the permeate flux. A feed temperature of 50^{o}C and a vacuum pressure of 64 mbar were chosen as the best operational conditions, maintaining the feed flow rate at 1.25 kg/h. The pH = 5.0 was chosen as the more suitable feed pH for this treatment as it allowed for a higher and more stable permeate flux and it is less aggressive to the membrane. Recovery rate test showed that a maximum recovery rate of 30% can be achieved with high rejection efficiency (close to 100%) and also a high permeate flux. After this rate the pressure inlet starts to increase and permeate flux can decrease sharply due to the scaling caused by $CaSO_4$ precipitation. Thus, VMD is a very efficient technique that can be used for gold mining effluent reclamation.

For DCMD, as the permeate temperature remained at room temperature, costs with cooling could also be reduced. This can be applied in industrial scale, using alternative abundant industrial water sources as a permeate or even to cool down the permeate stream. When treating the synthetic solution in pH 5.0, DCMD showed great performance. Tests with different temperatures showed that the higher the feed temperature, the higher the permeate flux and the lower the membrane wetting rate. The temperature of 55^{o}C was chosen as the best feed temperature as it can provides high permeate flux and lower wetting rate and it can be maintained by a solar heating system. For the feed flow rate, it was observed that the feed flow range tested in this study didn't show very high variation, so 0.55 LPM was chosen to be the best feed flow rate as it guaranteed a transient flux without destabilizing the system of increase the pressure inlet on the membrane module.

Regarding the recovery rate, a maximum permeate recovery rate of 30% was chosen as after this, the wetting took place and the rejection efficiency of the system started to decrease. Up

to 30% of permeate recovery rate, the DCMD showed an efficiency of 96% of rejection, providing a permeate with quality enough for reuse in the industry.

For all the membrane technologies evaluated, membrane fouling was a limitating factor and its caused mostly by the $CaSO_4$. This salt is known as a potential scalant that not only ins present at high concentrations on the gold mining effluent, but has an inverse solubility in relation to temperature, which can enhance its precipitation at MD feed temperatures. The precipitation of calcium sulfate crystals can block the membrane pores, leading to a decrease on the permeate flux, or even demage the membrane. In general, the scaling found on the membranes testes was easily removed with the cleaning procedures adopted.

Solvent extraction (SX) seems to be a suitable technology for the removal of arsenic as long as the concentration os sulfate is controlled. The extractant Aliquat 336 showed the highest affinity for arsenic, extraction bot arsenite and arsenate, and removing arsenic from the synthetic solution at a rate of 80%.

The results obtained for SX showed that the application of this technology is very promising for allowing arsenic removal and recovery, extinguinshing the production of a hazardous waste and adding economical value to a metal usually seen as a toxic impurity. This is of sum importance especially considering the arsenic content of mineral ores in the state of Minas Gerais (Brazil), the health and environmental risks concerning arsenic contamination and the challenge of incrasing the ecoefficiency of the mining industry.

Thus, this work showed that membrane separation processes are suitable for gold mining effluent treatment, allowing for different configuratons and to achieve the main goals such as production of reuse water, reduce of waste production and proper treatment of an acid, complex and contaminated mining water.

CHAPTER 8:
REFERENCES

ACERO, J. L. et al. Membrane filtration technologies applied to municipal secondary effluents for potential reuse. **Journal of Hazardous Materials**, v. 177, n. 1, p. 390–398, 2010.

AGRAWAL, A.; MISHRA, D.; SAHU, K. K. Comparative performance assessment of solvents for the extraction of H2SO4 from spent electrolytic bleed stream of copper industry. **Journal of Molecular Liquids**, v. 220, p. 82–91, 2016.

AGUIAR, A. O. et al. Gold acid mine drainage treatment by membrane separation processes: An evaluation of the main operational conditions. **Separation and Purification Technology**, v. 170, p. 360–369, 2016.

AHMED, I. M. Solvent Extraction Separation Study of Fe(III) from Sulphate Medium by CYANEX 272 in kerosene. **Arab Journal of Nuclear Science and Applications**, v. 46, n. 5, p. 48–55, 2013.

AHMED, S. et al. Performance of nanofiltration membrane in a vibrating module (VSEP-NF) for arsenic removal. **Desalination**, v. 252, n. 1–3, p. 127–134, 2010.

AKBARI, H. R.; MEHRABADI, A. R.; TORABIAN, A. Determination of nanofiltration efficency in arsenic removal from drinking water. **Iranian Journal of Environmental Health Science and Engineering**, v. 7, n. 3, p. 273–278, 2010.

AL-RASHDI, B. A. M.; JOHNSON, D. J.; HILAL, N. Removal of heavy metal ions by nanofiltration. **Desalination**, v. 315, p. 2–17, 2013.

AL-ZOUBI, H. et al. Optimization Study for Treatment of Acid Mine Drainage Using Membrane Technology. **Separation Science and Technology**, v. 45, n. 14, p. 2004–2016, 15 set. 2010.

ALKHUDHIRI, A.; DARWISH, N.; HILAL, N. Membrane distillation: A comprehensive review. **Desalination**, v. 287, p. 2–18, 2012.

ANDRADE, L. H. et al. Integrated ultrafiltration-nanofiltration membrane processes applied to the treatment of gold mining effluent: Influence of feed pH and temperature. **Separation Science and Technology**, v. 52, n. 4, p. 756–766, 2017a.

ANDRADE, L. H. et al. Comprehensive bench- and pilot-scale investigation of NF for gold mining effluent treatment: Membrane performance and fouling control strategies. **Separation and Purification Technology**, v. 174, p. 44–56, 2017b.

ANDRADE, L. H. et al. Nanofiltration and reverse osmosis applied to gold mining effluent treatment and reuse. **Brazilian Journal of Chemical Engineering**, v. 34, n. 1, p. 93–107, 2017c.

ANDRADE, L. H. et al. Nanofiltration applied in gold mining effluent treatment: Evaluation of chemical cleaning and membrane stability. **Chemical Engineering Journal**, v. 323, p. 545–556, 2017d.

ANDRADE, L. H. et al. Integrated ultrafiltration-nanofiltration membrane processes applied to the treatment of gold mining effluent: Influence of feed pH and temperature. **Separation Science and Technology**, v. 52, n. 4, p. 756–766, 4 mar. 2017e.

ANDRADE, L. H. et al. Integration of two-stage nanofiltration with arsenic and calcium intermediate chemical precipitation for gold mining effluent treatment. **Environmental Technology**, p. 1–13, 7 fev. 2018.

ANTONY, A. et al. Scale formation and control in high pressure membrane water treatment systems : A review. **Journal of Membrane Science**, v. 383, n. 1–2, p. 1–16, 2011.

ASANO, T. et al. **Water Reuse: Issues, Technologies and Applications**. first ed ed. [s.l.] McGraw-Hills, 2007.

ASHAR, N. G.; GOLWALKAR, K. R. A Practical Guide to the Manufacture of Sulfuric Acid, Oleums, and Sulfonating Agents. 2013.

BADER, M. S. H. Sulfate removal technologies for oil fields seawater injection operations. **Journal of Petroleum Science and Engineering**, v. 55, n. 1, p. 93–110, 2007.

BAKER, R. **Membrane Technology and Applications, 2nd Edition**. [s.l: s.n.].

BALLINAS, M. DE L. et al. Arsenic(V) Extraction from Sulfuric Acid Media Using DBBP−D2EHPA Organic Mixtures. **Industrial & Engineering Chemistry Research**, v. 42, n. 3, p. 574–581, 1 fev. 2003.

BANAT, F.; AL-RUB, F. A.; BANI-MELHEM, K. Desalination by vacuum membrane distillation: sensitivity analysis. **Separation and Purification Technology**, v. 33, n. 1, p. 75–87, 1 set. 2003.

BARAKAT, M. A. New trends in removing heavy metals from industrial wastewater. **Arabian Journal of Chemistry**, v. 4, n. 4, p. 361–377, 2011.

BENÍTEZ, F. J.; ACERO, J. L.; LEAL, A. I. Application of microfiltration and ultrafiltration processes to cork processing wastewaters and assessment of the membrane fouling. **Separation and Purification Technology**, v. 50, n. 3, p. 354–364, jul. 2006.

BEY, S. et al. Removal of As(V) by PVDF hollow fibers membrane contactors using Aliquat-336 as extractant. **Desalination**, v. 264, n. 3, p. 193–200, 2010.

BI, F. et al. Discussion on calculation of maximum water recovery in nanofiltration system. **Desalination**, v. 332, n. 1, p. 142–146, 2014.

BORBA, R. P.; FIGUEIREDO, B. R.; MATSCHULLAT, J. Geochemical distribution of arsenic in waters, sediments and weathered gold mineralized rocks from Iron Quadrangle, Brazil. **Environmental Geology**, v. 44, p. 39–52, 2003.

BOUSSU, K. et al. Characterization of polymeric nanofiltration membranes for systematic analysis of membrane performance. **Journal of Membrane Science**, v. 278, n. 1–2, p. 418–427, 2006.

BOWELL, R. . A review of sulfate removal options for mine waters,. **Proceedings of Mine water Process**, n. September, p. 1–24, 2004.

BRANDHUBER, P.; AMY, G. Arsenic removal by a charged ultrafiltration membrane — influences of membrane operating conditions and water quality on arsenic rejection. **Desalination**, v. 140, n. 1, p. 1–14, 2001.

CABASSUD, C.; WIRTH, D. Membrane distillation for water desalination : how to chose an appropriate membrane ? v. 157, n. May, p. 307–314, 2003.

CARVALHO, A. L. et al. Separation of potassium clavulanate and potassium chloride by nanofiltration: Transport and evaluation of membranes. **Separation and Purification Technology**, v. 83, p. 23–30, 2011.

CHAN, B. K. C.; DUDENEY, A. W. L. Reverse osmosis removal of arsenic residues from bioleaching of refractory gold concentrates. **Minerals Engineering**, v. 21, n. 4, p. 272–278, 2008.

CHANG, E. E. et al. Assessing the fouling mechanisms of high-pressure nanofiltration membrane using the modified Hermia model and the resistance-in-series model. **Separation and Purification Technology**, v. 79, n. 3, p. 329–336, 2011.

CHEN, T. C. et al. Reducing industrial wastewater and recovery of gold by direct contact membrane distillation with electrolytic system. **Sustainable Environment Research**, v. 23, n. 3, p. 209–214, 2013.

CHIAM, C. K.; SARBATLY, R. **Vacuum membrane distillation processes for aqueous solution treatment-A reviewChemical Engineering and Processing: Process Intensification**Elsevier B.V., , 2014. Disponível em: <http://dx.doi.org/10.1016/j.cep.2013.10.002>

CHILDRESS, A. E.; ELIMELECH, M. Relating Nanofiltration Membrane Performance to Membrane Charge (Electrokinetic) Characteristics. 2000.

CHOONG, T. S. Y. et al. Arsenic toxicity, health hazards and removal techniques from water: an overview. **Desalination**, v. 217, n. 1–3, p. 139–166, nov. 2007.

CRISCUOLI, A.; BAFARO, P.; DRIOLI, E. Vacuum membrane distillation for purifying waters containing arsenic. **Desalination**, v. 323, p. 17–21, 2013.

DAO, T. D. et al. A new method for permeability measurement of hydrophobic membranes in Vacuum Membrane Distillation process. **Water Research**, v. 47, n. 6, p. 2096–2104, 15 abr. 2013.

DAO, T. D.; LABORIE, S.; CABASSUD, C. Direct As(III) removal from brackish groundwater by vacuum membrane distillation: Effect of organic matter and salts on membrane fouling. **Separation and Purification Technology**, v. 157, p. 35–44, 2016.

DHAR, R. K. et al. A rapid colorimetric method for measuring arsenic concentrations in groundwater. v. 526, p. 203–209, 2004.

DO, V. T. et al. Degradation of Polyamide Nanofiltration and Reverse Osmosis Membranes

by Hypochlorite. **Environmental Science & Technology**, v. 46, n. 2, p. 852–859, 17 jan. 2012.

DOLAR, D. et al. Effect of water matrices on removal of veterinary pharmaceuticals by nanofiltration and reverse osmosis membranes. **Journal of Environmental Sciences**, v. 23, n. 8, p. 1299–1307, 2011.

DRIOLI, E. et al. Integrating Membrane Contactors Technology and Pressure-Driven Membrane Operations for Seawater Desalination. **Chemical Engineering Research and Design**, v. 84, n. 3, p. 209–220, 2006.

DRIOLI, E.; ALI, A.; MACEDONIO, F. Membrane distillation: Recent developments and perspectives. **Desalination**, v. 356, p. 56–84, 2015.

DRIOLI, E.; CURCIO, E.; DI PROFIO, G. State of the Art and Recent Progresses in Membrane Contactors. **Chemical Engineering Research and Design**, v. 83, n. 3, p. 223–233, 2005.

DUONG, H. C. et al. Membrane scaling and prevention techniques during seawater desalination by air gap membrane distillation. **DES**, v. 397, p. 92–100, 2016.

FIGOLI, A. et al. Influence of operating parameters on the arsenic removal by nanofiltration. **Water Research**, v. 44, n. 1, p. 97–104, 2010.

FU, F.; WANG, Q. Removal of heavy metal ions from wastewaters: A review. **Journal of Environmental Management**, v. 92, n. 3, p. 407–418, 2011.

GABELICH, C. J. et al. High-recovery reverse osmosis desalination using intermediate chemical demineralization. **Journal of Membrane Science**, v. 301, n. 1, p. 131–141, 2007.

GOODMAN, N. B. et al. A feasibility study of municipal wastewater desalination using electrodialysis reversal to provide recycled water for horticultural irrigation. **Desalination**, v. 317, p. 77–83, 2013.

GREENLEE, L. F. et al. Reverse osmosis desalination: Water sources, technology, and today's challenges. **Water Research**, v. 43, n. 9, p. 2317–2348, 2009.

GRYTA, M. Fouling in direct contact membrane distillation process. **Journal of Membrane**

Science, v. 325, n. 1, p. 383–394, 2008.

GRYTA, M. Calcium sulphate scaling in membrane distillation process ‡. v. 63, n. May 2008, p. 146–151, 2009.

GÜELL, R. et al. Modelling of liquid-liquid extraction and liquid membrane separation of arsenic species in environmental matrices. **Separation and Purification Technology**, v. 72, n. 3, p. 319–325, 2010.

GÜELL, R. et al. Transport and separation of arsenate and arsenite from aqueous media by supported liquid and anion-exchange membranes. **Separation and Purification Technology**, v. 80, n. 3, p. 428–434, 2011.

GUILLEN-BURRIEZA, E. et al. Understanding wetting phenomena in membrane distillation and how operational parameters can affect it. **Journal of Membrane Science**, v. 515, p. 163–174, 2016.

GUPTA, B.; BEGUM, Z. Separation and removal of arsenic from metallurgical solutions using bis(2,4,4-trimethylpentyl)dithiophosphinic acid as extractant. **Separation and Purification Technology**, v. 63, n. 1, p. 77–85, 2008.

HARISHA, R. S. et al. Arsenic removal from drinking water using thin film composite nanofiltration membrane. **Desalination**, v. 252, n. 1–3, p. 75–80, 2010.

HIJI, M. F.; NTALIKWA, J. W.; VUAI, S. A. Producing sulphuric acid in Tanzania and potential sources : A review. v. 1, n. 4, p. 40–44, 2014.

HITSOV, I. et al. Economic modelling and model-based process optimization of membrane distillation. **Desalination**, v. 436, n. February, p. 125–143, 2018.

HYDRANAUTICS. **Chemical Pretreatment For RO and NF operation of the RO system. Acids Caustic Dechlorination chemicals Antiscalants and DispersantsTechnical Application Bulletin**, 2013. Disponível em: <http://www.membranes.com/docs/tab/TAB111.pdf>. Acesso em: 7 mar. 2017

IBERHAN, L.; WINIEWSKI, M. Extraction of arsenic(III) and arsenic(V) with Cyanex 925, Cyanex 301 and their mixtures. **Hydrometallurgy**, v. 63, n. 1, p. 23–30, 2002.

IBERHAN, L.; WIŚNIEWSKI, M. Removal of arsenic(III) and arsenic(V) from sulfuric acid solution by liquid-liquid extraction. **Journal of Chemical Technology and Biotechnology**, v. 78, n. 6, p. 659–665, 2003.

IHS Markit. Disponível em: <https://ihsmarkit.com/products/sulfuric-acid-chemical-economics-handbook.html>. Acesso em: 20 mar. 2017.

JACOB, P.; LABORIE, S.; CABASSUD, C. Visualizing and evaluating wetting in membrane distillation : New methodology and indicators based on Detection of Dissolved Tracer Intrusion (DDTI). **Desalination**, v. 443, n. June, p. 307–322, 2018.

JIA, Y.; DEMOPOULOS, G. P. Coprecipitation of arsenate with iron(III) in aqueous sulfate media: effect of time, lime as base and co-ions on arsenic retention. **Water research**, v. 42, n. 3, p. 661–8, fev. 2008.

JOHNSON, D. B.; HALLBERG, K. B. Acid mine drainage remediation options: A review. **Science of the Total Environment**, v. 338, n. 1–2 SPEC. ISS., p. 3–14, 2005.

KAYA, Y. et al. The effect of transmembrane pressure and pH on treatment of paper machine process waters by using a two-step nanofiltration process: Flux decline analysis. **Desalination**, v. 250, n. 1, p. 150–157, 2010.

KESIEME, U. K. Mine waste water treatment and acid recovery using membrane distillation and solvent extraction. p. 94, 2015.

KESIEME, U. K.; ARAL, H. Application of membrane distillation and solvent extraction for water and acid recovery from acidic mining waste and process solutions. **Journal of Environmental Chemical Engineering**, v. 3, n. 3, p. 2050–2056, 2015.

KHAYET, M. Solar desalination by membrane distillation : Dispersion in energy consumption analysis and water production costs (a review). **DES**, v. 308, p. 89–101, 2013.

LANGSCH, J. E. et al. New technology for arsenic removal from mining effluents. **Journal of Materials Research and Technology**, v. 1, n. 3, p. 178–181, 2012.

LOTHONGKUM, A. W. et al. Simultaneous removal of arsenic and mercury from natural-gas-co-produced water from the Gulf of Thailand using synergistic extractant via HFSLM. **Journal of Membrane Science**, v. 369, n. 1–2, p. 350–358, 2011.

LUO, H. et al. A review on the recovery methods of draw solutes in forward osmosis. **Journal of Water Process Engineering**, v. 4, p. 212–223, 2014.

MA, Q.; AHMADI, A.; CABASSUD, C. Direct integration of a vacuum membrane distillation module within a solar collector for small-scale units adapted to seawater desalination in remote places: Design, modeling & evaluation of a flat-plate equipment. **Journal of Membrane Science**, 26 jul. 2018.

MAHDI, M.; SHIRAZI, A.; KARGARI, A. A Review on Applications of Membrane Distillation (MD) Process for Wastewater Treatment. **Journal of Membrane Science and Research**, v. 1, p. 101–112, 2015.

MANAA, E.-S. A.; LASHEEN, T. A. Liquid–Liquid Extraction of Sulfuric Acid from Aqueous Sulfate Waste Solution using Alamine 336/Kerosene/TBP Solvent. **Journal of Dispersion Science and Technology**, v. 37, n. 2, p. 137–143, 1 fev. 2016.

MANDAL, B. Arsenic round the world: a review. **Talanta**, v. 58, n. 1, p. 201–235, 16 ago. 2002.

MARINO, T.; FIGOLI, A. Arsenic Removal by Liquid Membranes. **Membranes**, p. 150–167, 2015.

MERICQ, J.; LABORIE, S.; CABASSUD, C. Vacuum membrane distillation of seawater reverse osmosis brines. **Water research**, v. 44, p. 5260–5273, 2010.

MERICQ, J.; LABORIE, S.; CABASSUD, C. Evaluation of systems coupling vacuum membrane distillation and solar energy for seawater desalination. **Chemical Engineering Journal**, v. 166, n. 2, p. 596–606, 2011.

MOHAMMADI, T.; ESMAEELIFAR, A. Wastewater treatment of a vegetable oil factory by a hybrid ultrafiltration-activated carbon process. **Journal of Membrane Science**, v. 254, n. 1–2, p. 129–137, 2005.

MOHAN, D.; PITTMAN, C. U. Arsenic removal from water/wastewater using adsorbents-A critical review. **Journal of Hazardous Materials**, v. 142, n. 1–2, p. 1–53, 2007.

MONDAL, S.; WICKRAMASINGHE, S. R. Produced water treatment by nanofiltration and reverse osmosis membranes. **Journal of Membrane Science**, v. 322, n. 1, p. 162–170, 2008.

MUKHERJEE, R. et al. Application of nanofiltration membrane for treatment of chloride rich steel plant effluent. **Journal of Environmental Chemical Engineering**, v. 4, n. 1, p. 1–9, 2016.

MULLETT, M.; FORNARELLI, R.; RALPH, D. Nanofiltration of mine water: Impact of feed pH and membrane charge on resource recovery and water discharge. **Membranes**, v. 4, n. 2, p. 163–180, 2014.

NG, J. C.; WANG, J.; SHRAIM, A. A global health problem caused by arsenic from natural sources. **Chemosphere**, v. 52, n. 9, p. 1353–1359, 2003.

NGHIEM, L. D.; CATH, T. A scaling mitigation approach during direct contact membrane distillation. **Separation and Purification Technology**, v. 80, n. 2, p. 315–322, 2011.

NGUYEN, C. M. et al. Performance and mechanism of arsenic removal from water by a nanofiltration membrane. **Desalination**, v. 245, n. 1–3, p. 82–94, 2009a.

NGUYEN, C. M. et al. Performance and mechanism of arsenic removal from water by a nanofiltration membrane. **Desalination**, v. 245, n. 1, p. 82–94, 2009b.

NICOLINI, J. V.; BORGES, C. P.; FERRAZ, H. C. Selective rejection of ions and correlation with surface properties of nanofiltration membranes. **Separation and Purification Technology**, v. 171, p. 238–247, 2016.

NOBLE, R. D. (RICHARD D. .; STERN, S. A. **Membrane separations technology : principles and applications**. [s.l.] Elsevier, 1995.

PANCHAROEN, U.; POONKUM, W.; LOTHONGKUM, A. W. Treatment of arsenic ions from produced water through hollow fiber supported liquid membrane. **Journal of Alloys and Compounds**, v. 482, n. 1–2, p. 328–334, 2009.

PRAPASAWAT, T. et al. Separation of As (III) and As (V) by hollow fiber supported liquid membrane based on the mass transfer theory. v. 25, n. 1, p. 158–163, 2008.

QTAISHAT, M. R.; BANAT, F. Desalination by solar powered membrane distillation systems. **Desalination**, v. 308, p. 186–197, 2013.

QU, D. et al. Experimental study of arsenic removal by direct contact membrane distillation.

Journal of Hazardous Materials, v. 163, n. 2–3, p. 874–879, 2009.

RICCI, B. C. et al. Integration of nanofiltration and reverse osmosis for metal separation and sulfuric acid recovery from gold mining effluent. **Separation and Purification Technology**, v. 154, p. 11–21, 2015a.

RICCI, B. C. et al. Integration of nanofiltration and reverse osmosis for metal separation and sulfuric acid recovery from gold mining effluent. v. 154, p. 11–21, 2015b.

SAITUA, H.; GIL, R.; PADILLA, A. P. Experimental investigation on arsenic removal with a nanofiltration pilot plant from naturally contaminated groundwater. **Desalination**, v. 274, n. 1–3, p. 1–6, 2011.

SATO, Y. et al. Performance of nanofiltration for arsenic removal. **Water Research**, v. 36, n. 13, p. 3371–3377, 2002.

SEIDEL, A.; WAYPA, J. J.; ELIMELECH, M. Role of Charge (Donnan) Exclusion in Removal of Arsenic from Water by a Negatively Charged Porous Nanofiltration Membrane. **Environmental Engineering Science**, v. 18, n. 2, p. 105–113, mar. 2001.

SETHI, S.; WIESNER, M. R. Cost Modeling and Estimation of Crossflow Membrane Filtration Processes. **Environmental Engineering Science**, v. 17, n. 2, p. 61–79, mar. 2000.

SHEN, J. et al. Techno-economic analysis of resource recovery of glyphosate liquor by membrane technology. **Desalination**, v. 342, p. 118–125, 2014.

SHIM, W. G. et al. Solar energy assisted direct contact membrane distillation (DCMD) process for seawater desalination. **Separation and Purification Technology**, v. 143, p. 94–104, 2015.

SIERRA, C.; ÁLVAREZ SAIZ, J. R.; GALLEGO, J. L. R. Nanofiltration of Acid Mine Drainage in an Abandoned Mercury Mining Area. **Water, Air, & Soil Pollution**, v. 224, n. 10, p. 1734, 8 out. 2013.

SIVAKUMAR, M.; RAMEZANIANPOUR, M.; O'HALLORAN, G. Mine Water Treatment Using a Vacuum Membrane Distillation System. **APCBEE Procedia**, v. 5, n. February 2016, p. 157–162, 2013.

SNOW, M. J. H. et al. New techniques for extreme conditions : high temperature reverse osmosis and nanofiltration. v. 105, p. 57–61, 1996.

SRISURICHAN, S.; JIRARATANANON, R.; FANE, A. G. Mass transfer mechanisms and transport resistances in direct contact membrane distillation process. v. 277, p. 186–194, 2006.

The Essencial Chemical Industry - online. Disponível em: <http://www.essentialchemicalindustry.org/chemicals/sulfuric-acid.html>. Acesso em: 20 mar. 2017.

TOMASZEWSKA, M.; GRYTA, M.; MORAWSKI, A. W. Study on the concentration of acids by membrane distillation. **Journal of Membrane Science**, v. 102, n. C, p. 113–122, 1995.

WANG, H. et al. Permeate Flux Curve Characteristics Analysis of Cross-Flow Vacuum Membrane Distillation. **Industrial & Engineering Chemistry Research**, v. 51, n. 1, p. 487–494, 11 jan. 2012.

WANG, P.; CHUNG, T. S. Recent advances in membrane distillation processes: Membrane development, configuration design and application exploring. **Journal of Membrane Science**, v. 474, p. 39–56, 2015.

WANG, X. et al. Arsenic (V) removal from groundwater by GE-HL nanofiltration membrane: effects of arsenic concentration, pH, and co-existing ions. **Frontiers of Environmental Science & Engineering in China**, v. 3, n. 4, p. 428–433, 15 dez. 2009.

WANG, Z. et al. Experimental study on treatment of electroplating wastewater by nanofiltration. **Journal of Membrane Science**, v. 305, n. 1, p. 185–195, 2007.

WARSINGER, D. M. et al. Scaling and fouling in membrane distillation for desalination applications: A review. **Desalination**, v. 356, p. 294–313, 2015.

WISNIEWSKI, M. **Extraction of arsenic from sulphuric acid solutions by Cyanex 923Hydrometallurgy**. [s.l.] Elsevier, 1997.

XIA, S. et al. Study of arsenic removal by nanofiltration and its application in China. **Desalination**, v. 204, n. 1–3 SPEC. ISS., p. 374–379, 2007.

YAN, X.-P.; KERRICH, R.; HENDRY, M. J. Distribution of arsenic(III), arsenic(V) and total inorganic arsenic in porewaters from a thick till and clay-rich aquitard sequence, Saskatchewan, Canada. **Geochimica et Cosmochimica Acta**, v. 64, n. 15, p. 2637–2648, 2000.

YUN, Y. et al. Direct contact membrane distillation mechanism for high concentration NaCl solutions. **Desalination**, v. 188, n. 1, p. 251–262, 2006.

ZHANG, Y. et al. Electrodialysis on RO concentrate to improve water recovery in wastewater reclamation. **Journal of Membrane Science**, v. 378, n. 1, p. 101–110, 2011.

ZHAO, Z.-P. et al. Concentration of ginseng extracts aqueous solution by vacuum membrane distillation 2. Theory analysis of critical operating conditions and experimental confirmation. **Desalination**, v. 267, n. 2–3, p. 147–153, 15 fev. 2011.

ZULAIKHA, S. et al. Treatment of restaurant wastewater using ultrafiltration and nanofiltration membranes. **Journal of Water Process Engineering**, v. 2, p. 58–62, jun. 2014.

ZUO, G. et al. Energy ef fi ciency evaluation and economic analyses of direct contact membrane distillation system using Aspen Plus. **DES**, v. 283, p. 237–244, 2011.